TITLE:

SIMULATION OF INDOOR BEHAVIOR OF PESTICIDES APPLIED WITH VARIOUS METHODS BY FUGACITY MODEL(Dissertation_全文)

AUTHOR(S):

Matoba, Yoshihide

CITATION:

Matoba, Yoshihide. SIMULATION OF INDOOR BEHAVIOR OF PESTICIDES APPLIED WITH VARIOUS METHODS BY FUGACITY MODEL. 京都大学, 1995, 博士(農学)

ISSUE DATE:

1995-05-23

URL:

https://doi.org/10.11501/3102680

RIGHT:

京都大学学術情報リポジトリ
KURENAI 紅
Kyoto University Research Information Repository

(2)

SIMULATION OF INDOOR BEHAVIOR OF PESTICIDES APPLIED WITH VARIOUS METHODS BY FUGACITY MODEL

Yoshihide Matoba

TABLE OF CONTENTS

Chapter 1.

INTRODUCTION

In order to control household flies, mosquitoes and cockroaches, pesticides are usually applied in a room by various procedures. Space spraying, electric vaporizer and broadcast spraying are such popular techniques. The space spraying of aerosol is carried out with a pressurized canister. The electric vaporizer releases pesticides into a space with a new vaporizing system. The broadcast spraying is conventionally done on the surface area of a floor or carpet.

In these applications, the concentrations of the pesticides in air or floor must be adequate enough to control the insects, e.g. 0.01 mg/m^3 to 1 mg/m^3 or 1 mg/m^2 to 10 mg/m^2 on their insecticidal activities. Thus, it becomes an important matter of concern to secure human health from these pesticide spraying. Safety assessment for the human health first requires to grasp the concentrations of the pesticides in air or floor as a function of time. The concentrations become essential to estimate the intake level of the pesticides by sprayers or residents through inhalation or dermal penetration. The estimated intake level is then compared with no-observed effect level (NOEL) of the pesticides, which is determined in inhalation toxicity, dermal toxicity, skin penetration studies and etc using rats or mice. When the estimated intake level is one hundred times lower than NOEL, it is generally considered to be safe and acceptable to the sprayers or residents.

The concentrations of the pesticides that are thus the basis of safety assessment are generally measured in a room where the pesticides are applied according to description on the labels. However, the concentrations largely vary depending on the pesticide and formulation, application method, room shape, ventilation and temperature. In other words, the measuring concentrations change with a little fluctuation in room conditions and thus, the obtained data is valid only in one specific case, but invalid in the other cases. To meet the safety assessment, therefore, the concentrations in the all cases should be measured with an enormous amount of time and resources. The purpose of this study is to develop a method that can pursuit accurately the temporal pesticide behavior under various conditions excluding such

absurdity in the measurement.

A key to establish the new method is to use known or easily available physicochemical properties of the pesticide and other materials. If the method requires extremely complicated data, it is roughly the same as the real measurement of the pesticides in a room since a lot of time and resources are to be spent to obtain the data.

It is not necessarily simple, however, to describe the concentrations of the pesticide in air, floor, wall and ceiling as it stands. Firstly, for the phenomenal description, it is essential to clarify mechanisms of the behavior of the pesticides behind the measured concentrations. Thus, it becomes necessary to know generation of aerosol and vapor, rising, settling and horizontal movement of droplets, changing of droplet diameter, adsorption and desorption, volatilization, degradation and dissipation and these changes with time, and fluid dynamics and physical formula concerning droplet motion, phase change and degradation should be effectively utilized. The new method must, therefore, clarify mechanisms of indoor pesticide behavior and incorporate the results into the total description.

Secondly, for the connection of each phenomenon, it becomes essential to utilize a mathematical model, such as the Fugacity model [1)] of Mackay and Paterson (See APPENDIX). Fugacity is an escaping or migrating tendency of a chemical from one media to another depending on physicochemical properties of the both pesticide and media and thus, it seems to be useful for connecting various components in an environment.

Therefore, in this study, unsteady state fugacity models incorporated with the mechanisms of movement, phase change and degradation have been developed to simulate the pesticide behavior in a room administered by the above three application methods. The space spraying model particularly focuses on the behavior of aerosol droplets and permeation of the pesticide into the material covering the room. The electric vaporizer incorporates fluid dynamics and condensation of the evaporated pesticide in modeling. The broadcast spraying model is characterized by a drying pattern of the water-based emulsion and structure of carpet.

This paper consists of seven chapters and relates all of the endeavors in the study; Chapter

1: Introduction, Chapter 2: Space spraying model (SPRAY-MOM), Chapter 3: Electric vaporizer model by fluid dynamics, Chapter 4: Electric vaporizer model (VAPOR-MOM), Chapter 5: Broadcast spraying model (CARPET-MOM), Chapter 6: Temperature and humidity dependency and Chapter 7: Conclusion. Chapters 2 to 5 describe the development of the above three models, sensitivity analysis and validation of the models by the measured or experimental data. Chapter 6 further mentions an improvement of these models so as to trace the pesticide behavior due to room temperature and humidity changes. In Chapter 7, it is concluded that all the models established in the study can describe successfully the pesticide behavior under various conditions and can be utilized for the safety assessment of human health.

Chapter 2.

SPACE SPRAYING MODEL (SPRAY-MOM)

Introduction

Pesticide aerosol sprays are applied with a pressurized canister readily available to the public to control the household pests including flies, mosquitoes and other harmful insects. From the viewpoint of safety assessment, there have been reported up to now several experiments, where the aerial concentration of pesticide in a sprayed room was estimated [2] under various conditions such as a different air exchange rate and spraying method. However, to describe accurately the pesticide behavior on the floor, wall and ceiling as well as in air, it seems more advantageous to utilize a mathematical model such as the Fugacity model of Mackay and Paterson [1] by a modification with aerosol droplet dynamics.

In this chapter, an unsteady state model (SPRAY-MOM, Spraying Model by Matoba, Ohnishi and Matsuo) has been developed to simulate aerosol droplets, temporal variations of the aerial concentrations, amounts of pesticide on the floor, wall and ceiling in a sprayed room under various conditions. The SPRAY-MOM modeling focuses particularly on the behavior (dynamics) of aerosol droplets and a permeation of pesticide into the materials covering the room.

Theoretical

The environment to be simulated consists of five kinds of compartments: aerosol droplets (i = 1, 2, 3), air (4), floor (5), wall (6) and ceiling compartment (7) as illustrated in figure 2-1. Each compartment is treated theoretically as follows:

[1] Aerosol droplet compartment (i = 1, 2, 3)

The aerosol droplet compartments are assigned to individual particles and classified into a large (i = 1), medium (i = 2) and small particle-diameter compartments (i = 3), since the behavior of aerosol droplets mainly depends upon the diameter. Each aerosol droplet compartment is accommodated in each "spray zone".

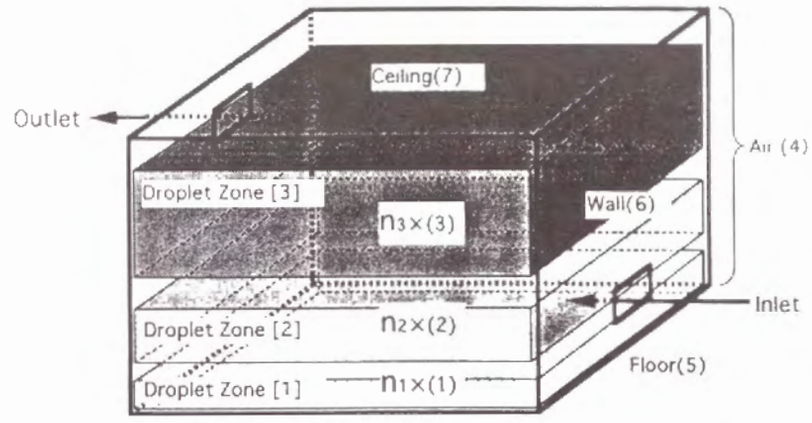

Figure 2-1. The environment to be simulated and its compartments.

Volume (V_i)

A dominant solvent of aerosol droplets will evaporate and the compartment (i) becomes smaller in volume with time. The rate of evaporation can be represented by the rate of change of particle size with time. It is controlled by the rate at which vapor can diffuse away from aerosol droplets[3], and the diameter of the compartment (i) at time t, d_{ti}, is described as follows:

$$d_{ti} = \sqrt{d_{0i}^2 - 2\ \alpha\ t} \qquad (2\text{-}1)$$

In equation 2-1, d_{0i} is the diameter of aerosol droplet compartment (i) at time 0 and α is the diameter coefficient given by:

$$\alpha = \frac{4\ D_{air}\ M\ P_d}{R\ \rho_d\ T_d}$$

where D_{air} is the diffusion coefficient of aerosol droplets in air, M molecular weight and P_d droplet surface partial pressure of the solvent, R gas constant, ρ_d droplet density and T_d droplet surface temperature (room temperature).

The vapor pressure of pesticide in aerosol droplets is usually much smaller than that of the solvent. Therefore, after the evaporation of the solvent, aerosol droplets substantially contain 100% pesticide and their ultimate diameter (d_{zi}) can be expressed as:

$$d_{zi} = \sqrt[3]{R_a}\ d_{0i} \qquad (2\text{-}2)$$

where R_a is the volume ratio of pesticide to aerosol droplets at time 0.

From equations 2-1 and 2-2, the time (t_{zi}) required for the d_{0i} to reach d_{zi} is given by:

$$t_{zi} = \frac{d_{0i}^2 - d_{zi}^2}{2\ \alpha} = \frac{1 - \sqrt[3]{R_a^2}}{2\ \alpha}\ d_{oi}^2$$

The volume (V_i) of aerosol droplet compartment (i) at time t is $(\pi/6) \cdot d_{ti}$, and the rate of the volume change until t_{zi} is as follows:

$$\frac{d\ V_{ti}}{d\ t} = -\frac{\pi}{2}\ \alpha\ d_{ti} \qquad (2\text{-}3)$$

Velocity (v_i)

A motion of aerosol droplet compartment (i) is governed by gravity and the resistance of air to particle motion. In most situations, the compartment (i) almost instantaneously comes to a constant that is terminal settling velocity (v_i) given by Stokes law[3]:

$$v_{ti} = \frac{\rho_d\ g\ S}{18\ \eta}\ d_{ti}^2 = \beta\ d_{ti}^2 = \beta\ (\ d_{0i}^2 - 2\ \alpha\ t\ ) \qquad (2\text{-}4)$$

where g is the acceleration of gravity, η viscosity of air, S slip correction factor and β velocity coefficient. According to equation 2–4, the velocity at time t (v_i) is proportional to the square of particle diameter (d_i). After the solvent evaporates from the compartment (i), the density of terminal droplets is assumed to become that of pesticide (ρ). Thus, the ultimate velocity (v_{zi}) is given by:

$$v_{zi} = (\ \rho\ /\ \rho_d\ )\ \beta\ d_{zi}^2$$

Number of aerosol droplet compartment (n_i) in each spray zone [i]

When spray is released uniformly in a space at the height h_h to h_b from the floor (i.e. $h_h - h_b$ is the thickness ($H_{[0i]}$) of spray zone at time 0), the volume of the zone ($V_{[i]}$, i = 1, 2, 3) is assumed as the product of $H_{[0i]}$ and floor area (A_5). The bottom of the spray zone [i] falls down to reach the floor after time (t_{xi}) and the spray zone is completely absorbed in the floor after time (t_{yi}). These times are calculated by the following equations:

$$h_b = \int_0^{t_{xi}} \frac{d\ v_i}{d\ t}\ dt \qquad h_h = \int_0^{t_{yi}} \frac{d\ v_i}{d\ t}\ dt$$

The number (n_{0i}) of aerosol droplet compartment (i) in each spray zone [i] is constant before the zone reaches the floor ($t < t_{xi}$). After the bottom of the zone [i] touches the floor, the number (n_i) begins to reduce according to the following equation:

$$n_i = n_{0i}\ [\ 1 - \frac{v_i}{H_{[zi]}}\ (\ t - t_{xi}\ )\ ] \qquad (2\text{-}5)$$

where $H_{[zi]}$ is an ultimate thickness of spray zone [i] defined below. When the velocity reaches the ultimate one before t_{xi} ($t_{xi} > t_{zi}$), v_i is constant and the ultimate thickness of spray zone ($H_{[zi]}$) is equal to $H_{[0i]}$. However, in a case that the spray zone is absorbed in the floor while v_i changes with time ($t_{xi} < t_{zi}$), the $H_{[zi]}$ is given by:

$$H_{[zi]} = \int_{t_{xi}}^{t_{yi}} v_i\ dt \qquad (2\text{-}6)$$

Fugacity capacity (Z_i)

The Z_i value of aerosol droplet compartment (i) is described as follows[4]:

$$Z_i = \frac{6 \times 10^6}{P_L^s\ R\ T}\ ,\quad P_L = P\ \exp^{6.79\ (\ T_M\ /\ T\ -\ 1\ )} \qquad (2\text{-}7)$$

where P_L^s is sub–cooled liquid vapor pressure, P solid (conventional) vapor pressure, T_M melting point and T room temperature.

Transference

A diffusive transfer rate of pesticide between aerosol droplet (i) and air compartment (4) can be written as:

$$\frac{d\ N_i}{d\ t} = D_{i4}\ (\ f_i - f_4\ )$$

where dN_i/dt is the flux of pesticide in aerosol droplet compartment (i), f_i and f_4 the fugacities in aerosol droplet (i) and air compartment (4), and D_{i4} a transfer parameter with an unit of mole s^{-1} Pa^{-1}. The transfer parameter (D_{i4}) can be estimated by:

$$D_{i4} = \frac{1}{1\ /\ (\ k_i\ A_i\ Z_i\ )\ +\ 1\ /\ (\ k_4\ A_i\ Z_4\ )} \qquad (2\text{-}8)$$

where A_i (surface area of aerosol droplets) is $\pi \cdot d_{ti}^2$. The velocity (k_4) of pesticide in air compartment (4) is $G/A_4 + v_i$ where G is air exchange rate and A_4 is a product of width and height of the room, and velocity k_i in aerosol droplet compartment (i) can be $k_4/100$ [5].

Photo–degradation

One of the major reactions in aerosol droplet compartment (i) is photo–degradation described by a first–order rate constant K_i. The reaction rate is written as $K_i V_i Z_i$ where K_i is $0.693/\tau_i$ and τ_i is a half–life time of photo–degradation.

Differential equation in terms of fugacity

A Level IV fugacity model describes a time-dependent chemical fate in the environment. When fugacity (f), volume (V) and chemical mass (N) for a compartment are not constant, an unsteady state behavior can be illustrated by the following equation, since N/V = Zf:

$$\frac{d f}{d t} V Z = - \frac{d V}{d t} Z f + \frac{d N}{d t}$$

where dN/dt is a movement of the chemical due to a transference and reactions etc.

Thus, the unsteady state behavior of pesticide in aerosol droplet compartment (i) is expressed by a differential equation 2–9. The volume of the compartment (i), V_i (i = 1, 2, 3), is becoming smaller with time until the ultimate diameter (d_{zi}) is attained, and the fugacity becomes increasing according to the * term in reference to equation 2–3. The pesticide in aerosol droplet compartment (i) transfers with air compartment (4) and the transference is time-dependent based on the surface area of aerosol droplets as indicated in equation 2–8. The pesticide is also photo-degraded in the compartment (i).

$$\frac{d f_i}{d t} V_i Z_i = \frac{\pi}{2} \alpha d_i Z_i f_i^* - D_{i4} (f_i - f_4) - K_i V_i Z_i f_i \qquad (2\text{-}9)$$

The fugacity (f_i, i = 1, 2, 3) is valid so long as the spray zone exists ($t < t_{yi}$). The spray zone absorption in the floor is not related to the fugacity, but the number of aerosol droplets is responsible in obedience to equation 2–5.

[2] Air compartment (4)

Volume (V_4) and Fugacity capacity (Z_4)

The volume (V_4) of air compartment (4) is equal to that of a sprayed room. The air Z value, Z_4, is 1/RT.

Air Exchange

The pesticide getting out of the environment can be calculated from an air exchange rate (G) and fugacity capacity that is $GV_4Z_4f_4$.

Transference

Transference between aerosol droplet (i) and air compartment (4) is proportional to the number of aerosol droplets n_i (i = 1, 2, 3). The number is constant until t_{xi} and begins to reduce until t_{yi} according to equation 2–5. The pesticide in air compartment (4), on the other hand, transfers with floor (5), wall (6) and ceiling compartment (7). The transfer parameter D_{4k} with floor (k = 5), ceiling (k = 6) or wall compartment (k = 7) is estimated as:

$$D_{4k} = \frac{0.693}{\tau_{4k} (1 / V_4 / Z_4 + 1 / V_k / Z_k)} \qquad (2\text{-}10)$$

where τ_{4k} is a half-life time of transference between air (4) and the k compartment.

Differential equation in terms of fugacity

The pesticide movement (dN/dt) in air compartment (4) is caused by air exchange and transference with aerosol droplet (i), floor (5), wall (6) and ceiling compartment (7) as well as photo-degradation. The number of aerosol droplets is time-dependent from t_{xi} to t_{yi} and becomes zero after t_{yi}. Thus, the unsteady state behavior of pesticide in air compartment (4) is given by equation 2–11:

$$\frac{d f_4}{d t} V_4 Z_4 = - G V_4 Z_4 f_4 - \sum_{i=1}^{3} n_i D_{i4} (f_4 - f_i) - \sum_{k=5}^{7} D_{4k} (f_4 - f_k) - K_4 V_4 Z_4 f_4 \qquad (2\text{-}11)$$

[3] Floor, wall and ceiling compartment (k = 5, 6, 7)

Volume (V_k)

A diffusion depth (e) of an organic compound in a polymer has been shown to follow a linear relationship with the square root of time (t) and diffusion constant of the pesticide (D_k)[6].

$$e = 2 \sqrt{D_k t}$$

A wooden floor is usually coated by a polymer material such as polyurethane resin and a wallpaper on the wall and ceiling is usually made of a poly(vinyl chloride) material. Thus, the volume (V_5) of floor compartment (5) as well as those (V_6 and V_7) of wall (6) and ceiling compartment (7) can be calculated by a product of e and surface area (A_k) of each compartment:

$$V_k = 2 \sqrt{D_k t} A_k \qquad (2\text{-}12)$$

The rate of change of each volume is expressed as:

$$\frac{d V_k}{d t} = \sqrt{D_k / t} A_k \qquad (2\text{-}13)$$

Fugacity capacity (Z_k)

The pesticide will be retained in the coated polymer layers and therefore, the floor Z_5 value can be calculated as $P_f \cdot C/P$, where P_f is a polymer/water partition coefficient, C water solubility and P vapor pressure of pesticide. Similarly, the wall and ceiling Z values (Z_6 and Z_7) can be calculated as $P_w \cdot C/P$, where P_w is a polymer/water partition coefficient.

Differential equation for floor compartment (5)

Differential equation 2–14 describes the unsteady state behavior of pesticide in floor compartment (5). The changing volume (V_5) of the compartment (5) with time is written by the * term according to equation 2–13.

$$\frac{d f_5}{d t} V_5 Z_5 = - \sqrt{D_k / t}\ A_5 Z_5 f_5^* + \sum_{i=1}^{3} \frac{n_{0i}}{L_{zi}} v_i V_i Z_i f_i - D_{45} (f_5 - f_4) - K_5 V_5 Z_5 f_5 \qquad (2-14)$$

The rate of fortification of pesticide from spray zone into floor is expressed as:

$$- \frac{d n}{d t} = \frac{n_{0i}}{H_{[zi]}} v_i \qquad (2-15)$$

and this is valid so long as the spray zone exists. The movement of pesticide in floor compartment (5) originates in transference with air compartment (4) and photo–degradation. The transference is time–dependent since the volume V_5 of floor compartment (5) becomes larger with time.

Differential equation for wall compartment (6)

For wall compartment (6), the time–dependent volume reduces the fugacity according to the * term and increases the transfer parameter. The pesticide transfers with air compartment (4) and photo–degrades:

$$\frac{d f_6}{d t} V_6 Z_6 = - \sqrt{D_k / t}\ A_6 Z_6 f_6^* - D_{46} (f_6 - f_4) - K_6 V_6 Z_6 f_6 \qquad (2-16)$$

Differential equation for ceiling compartment (7)

The differential equation for pesticide in ceiling compartment (7) corresponds to the wall compartment (6):

$$\frac{d f_7}{d t} V_7 Z_7 = - \sqrt{D_k / t}\ A_7 Z_7 f_7 - D_{47} (f_7 - f_4) - K_7 V_7 Z_7 f_7 \qquad (2-17)$$

Computer Programming and Data Processing

A computer program, SPRAY–MOM, was developed utilizing BASIC. IBM PS/2 was employed for the calculation and SigmaPlot was used for the graphical presentations of the results.

The program was set up in such a way that basic physicochemical data, half–life times of transference, reaction rates, spraying and room conditions were incorporated. By running, calculation of time–dependent velocity, volume and D values, resolution of unsteady state equations, and graphing of resulting amounts in each compartment versus time were performed.

[1] A Simulation of the Experiment

A spraying experiment was performed with an oil–based formulation during the summer in a typical Japanese apartment room[7].

The floor area (A_5) of 9.72 m^2 consisted of 6 mats ("tatami") and the air volume (V_4) was 23.3 m^3. The room temperature was 25°C (298 K). The spray formulation was released all at once in the center of the room during 15 sec, corresponding to the threefold amount of what is the recommended usage in the above room volume, by omnidirectional spraying so that the even spray zone was formed in a space between 2.4 m (h_a) and 1.6 m (h_b) height from the floor. During the experiment, all windows of the room remained closed against the instruction on the label, which recommends an air exchange. Under these conditions, the air exchange rate was 0.58 time h^{-1} (G).

The formulation contained 2.10 g of fenitrothion (pesticide), 168 ml of n–paraffins (Neochiozol, Chuokasei Co., Ltd., Japan) and 252 ml of propellants. The nozzle was designed to spray aerosols at a rate of 0.45 g of n–paraffins (0.27 ml) and propellants (0.41 ml) per second and thus, the sprayed volume of n–paraffins was 4.05 ml during 15 sec. The concentration of fenitrothion in aerosol droplets was 45.1 mole m^{-3}.

The released spray covered a size range of droplets from 1 to 120 μm with 30 μm on the average according to Rosin–Rammler's equation, however, it was convenient to classify the droplets into groups of 10% of 60 μm (d_{01}), 80% of 20 μm (d_{02}) and 10% of 5 μm (d_{03}) based on a particle size–distribution measured immediately after spraying by a laser diffraction droplet sizer (Malvern series 2600, Malvern Instruments Ltd., England).

The composition of Neochiozol was 8% of n–dodecane, 46% of n–tridecane, 20% of n–tetradecane, 18% of n–pentadecane, 5% of n–hexadecane and 2% of n–heptadecane[8] and thus,

an assumption was made that the component of droplet was 100% n-tridecane. The diffusion coefficient of n-tridecane (D_{air}) was estimated to be 5.17×10^{-6} ($m^2\ s^{-1}$) by a method of Wike and Lee[9]. The partial vapor pressure of n-tridecane on droplet surface (P_d) is 2.72 Pa at 20 °C, the molecular weight (M) 184.37 g $mole^{-1}$, density (ρ_d) 7.56×10^5 g m^{-3}, and diameter coefficient (α) 3.08×10^{-12} $m^2\ s^{-1}$ at 25 °C in equation 2-1.

The velocity coefficient (β) in equation 2-4 was estimated to be 2.28×10^7 ($m^{-1}\ s^{-1}$) using 1.81×10^{-2} (g $m^{-1}\ s^{-1}$) as a viscosity of air at 20 °C (η) and 1 as the slip correction factor (S) because all aerosol droplets during this simulation were larger than 1 μm in diameter.

According to equation 2-12, the volume of floor (5), wall (6) and ceiling (7) (V_k, k = 5, 6, 7) depends both on time and diffusion constant (D_k) of fenitrothion in a polymer (polyurethane and poly(vinyl chloride) in the present case). The D_k of fenitrothion was assumed to be 10^{-11} $m^2\ h^{-1}$ (2.78×10^{-15} $m^2\ s^{-1}$) since D_k in poly(vinyl chloride) was 0.96×10^{-11} $m^2\ h^{-1}$ for methyl red[10] and 1.89×10^{-11} $m^2\ h^{-1}$ for methyl palmitate[6]. The ultimate diffusion depth (a thickness of the coated polymer) for the floor was estimated to be 56 μm because the wooden floor was usually coated by a polymer at a rate of 50 g m^{-2} and the specific gravity was about 9.0×10^5 g m^{-3}. The diffusion depth for both wall and ceiling amounted to 136 μm due to the treatment of wall paper with 25% (w/w) of a polymer (specific gravities of the polymer and wall paper: 9.0×10^5 and 8.8×10^5 g m^{-3}) and the resultant whole thickness was 550 μm.

In this experiment, the floor did not consist of wood but a "tatami" made of rush. The rush was composed of 5% of ashes, 7% of crude protein, 22% of pentosan, 20% of lignin and 46% of crude fibrous lipid and gummy material[11]. To determine the "tatami" volume (V_5), 0.46 (the content of lipid and gummy material) was multiplied by the diffusion depth (e) and surface area (A_5) of a polymer-coated floor. Considering the thickness of the first surface layer of "tatami", the ultimate diffusion depth was determined to be 2.35×10^3 μm .

In defining fugacity capacities of floor (5), wall (6) and ceiling (7) (Z_k, k = 5, 6, 7), P_f and P_w values were assumed to be K_{ow} (octanol/water partition coefficient), since the solubility parameter (δ) of octanol (8.33 $cal^{0.5}\ cm^{-1.5}$) is rather close to that (9.48 ($cal^{0.5}\ cm^{-1.5}$) of poly(vinyl chloride)[12].

Other data of fenitrothion required for the simulation such as physicochemical properties, photo-degradation rate, half-life time are described in table 2-1.

Table 2-1. Primary Input Data

Input data	Fenitrothion
Physicochemical properties:	
Molecular weight (g $mole^{-1}$)	277.23
Specific gravity (g m^{-3})	1.33×10^6
Vapor pressure (Pa)	2.85×10^{-2}
Water solubility (mole m^{-3})	5.05×10^{-2}
Log K_{ow}	3.27
Melting point (K)	273.45
Photo-degradation rate (s^{-1}) in:	
Aerosol droplet (K_i, i = 1, 2, 3)	2.41×10^{-6}
Air (K_4)	1.38×10^{-7}
Floor, ceiling, wall (K_k, k = 5, 6, 7)	1.27×10^{-6}
Half-life time (s) of transference between air and:	
Floor (τ_{45})	1.30×10^5
Wall, ceiling (τ_{4k}, k = 6, 7)	1.56×10^5

[2] Sensitivity Analysis

All important parameters constituting the differential equations were varied within 2 orders (factor 0.1 and 10) of magnitude of the pesticide to test the sensitivity of the equations to the parameters.

Results and Discussion

[1] A Simulation of the Experiment

Unsteady state behavior of fenitrothion in air was simulated by the SPRAY-MOM model. The predicted time-dependent concentration, as a sequence of the total amount of fenitrothion in large- (1), medium- (2) and small-sized aerosol droplets (3) and air compartment (4) divided by indoor air volume (V_4) at a fixed time, entirely agreed with the measured one except immediately after spraying (figure 2-2). This seems to be likely that when fenitrothion was sampled by sucking the air at a flow rate of 1 ℓ min^{-1} through Tenax-GC in a glass tube, some of the aerosol droplets with a larger diameter could not be collected in the sampling tube because of their high sedimentation velocity. The SPRAY-MOM, however, can simulate undetected portions of a behavior of fenitrothion in air. The amounts of fenitrothion in concerned compartments are also shown in figure 2-2.

Soon after the release of spray, large (60 μm), medium (20 μm) and small aerosol droplets (5 μm) began to settle at each rate of falling velocity, being proportional to the square of particle size as given in equation 2–4. Their particle sizes were decreasing with time until ultimate diameters (d_{zi}, i = 1, 2, 3, respectively) were attained according to equation 2–1 (see figure 2–3) and their settling velocities were reduced with decreasing particle sizes.

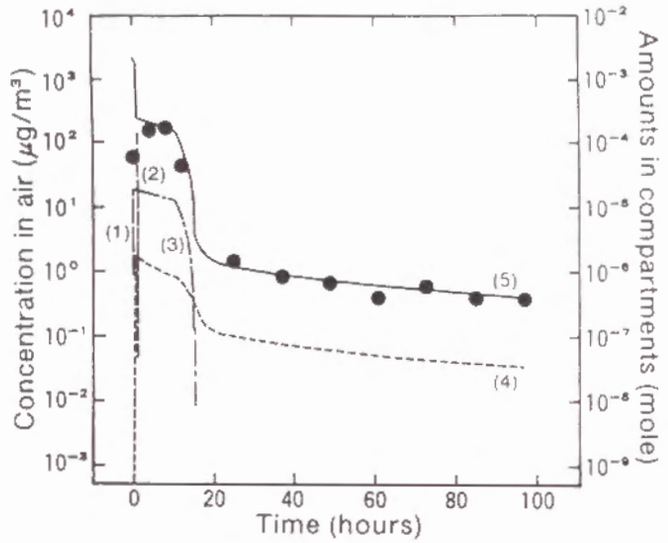

Figure 2–2. Aerial concentration of fenitrothion at an air exchange rate of 0.58 time h^{-1} as a function of time.
——: Calculation
(1) large–, (2) medium–, (3) small–sized droplets and (4) air [mole]
(5) the sum of (1)–(4) [μg m^{-3}]
●: Experiment [μg m^{-3}]

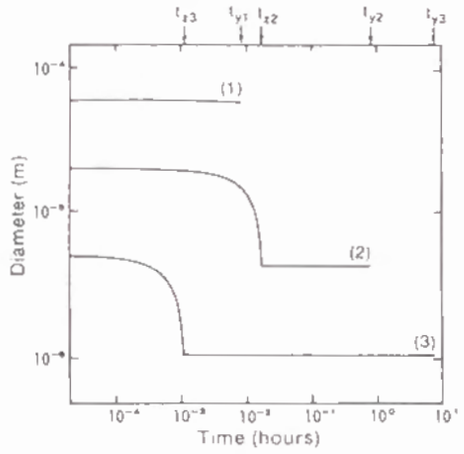

Figure 2–3. Variation of droplet diameter with time.
(1) large, (2) medium and (3) small droplets

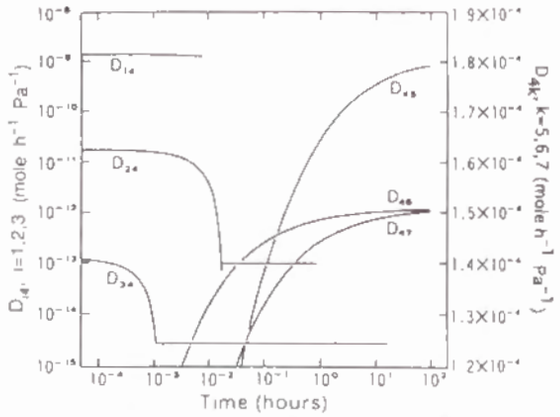

Figure 2–4. Time–dependent changes of transfer parameters between air and concerned compartments.
D_{i4}: aerosol droplets – air
D_{4k}: air – floor, wall and ceiling

Thus, the number (n_{0i}, i = 1, 2, 3) of aerosol droplets (i) in the spray zone was constant at first, but began to reduce after 20 sec, 32 min and 10 h, differently in obedience to equation 2–5. The spray zone disappeared in 30 sec, 50 min and 15 h and the ultimate width of spray zone was 83, 80 and 80 cm, respectively as calculated by equation 2–6.

The transfer parameter (D_{i4}) became smaller and constant with time according to the surface area and velocity of aerosol droplet (i) (equation 2–8 and figure 2–4). The D_{4k} (k = 5, 6 and 7) increased with time and reached plateaus. These changes were solely influenced by diffusion depth described in equation 2–10 and 2–12.

Time dependencies of fugacities in concerned compartments are given in figure 2–5. Little change of the fugacity in large droplet compartment (1) was based on the nearly constant diameter until t_{y1}. A fairly large change in the fugacities of medium (2) and small droplet compartments (3) was referred to the reduction of their diameters. Fugacity 4 (f_4) of air compartment (4) rather increased until t_{x2} mainly by a transference with aerosol droplet compartments. The f_4 did not seem to reduce largely in spite of air exchange, transference with wall and ceiling and photo–degradation. After small droplet compartment (3) started to settle onto the floor, the f_4 significantly decreased. Fugacity 5 (f_5) of floor compartment (5) very strongly increased after t_{x1}, because pesticide was fortified from large droplet compartment in accordance with equation 2–15. It then mainly reduced by transference with air, but again returned to a maximum as medium droplets (2) were absorbed on the floor. After that, f_5 constantly reduced by transference with air and photo–degradation though small droplets (3) fell onto the floor. Fugacity 6 (f_6) and 7 (f_7) in wall (6) and ceiling compartments (7) were increased with f_4 until t_{x2} and gently reduced after t_{y3}.

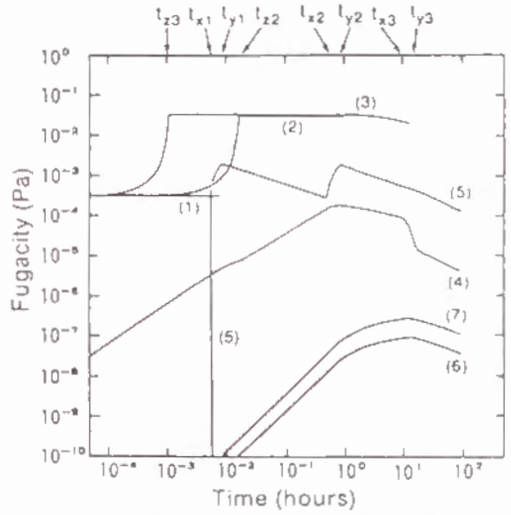

Figure 2–5. Time–dependent changes of the fugacity (fenitrothion) in compartments. (1) large, (2) medium, (3) small droplets, (4) air, (5) floor, (6) wall and (7) ceiling

[2] Sensitivity Analysis

The SPRAY-MOM model enabled to simulate the behavior of sprayed pesticide in a room under various conditions. Here, as a sensitivity analysis the pesticide behavior was examined by varying important parameters.

Influence of the Diameter of Aerosol Droplets

The air concentration on the first day is deeply influenced by the behavior of small aerosol droplet compartment (3). The diameter of aerosol droplets is destined by the nozzle type of the spraying can, the kind of formulations, the contents of the pesticide and the variation of spraying height. Figure 2–6 shows a change in total amount of the pesticide in air when the compartment (3) is of 1, 5 and 10 μm diameter, respectively. The compartment with 1 μm droplets will be completely settled after 374 h while 10 μm droplets may be settled after 4 h under the fixed slip correction factor.

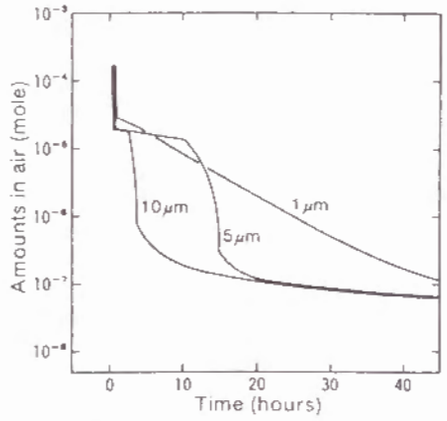

Figure 2–6. Time-dependent aerial changes of small droplets with a diameter of 1, 5 (standard) and 10 μm.

Influence of Air Exchange Rate

When all windows of the room were closed contrary to the instruction for usage, air exchange rate was 0.58 time h^{-1}. The air exchange rate is directly connected with equation 2–11 and the transfer parameter D_{i4} according to equation 2–8 and thus, its variation has a strong influence on air concentration. Figure 2–7 shows the concentrations for air exchange rates of factors 0.1, 1 and 10 (0.058, 0.58 and 5.8 time h^{-1}). The air concentration for 5.8 time h^{-1} is rapidly reduced and ten times lower than that for the experiment (0.58 time h^{-1}) after all droplet compartments have been completely absorbed in the floor. The reduction of air concentration affects the amount in the wall and ceiling although the amount on the floor is almost fixed (figure 2–7).

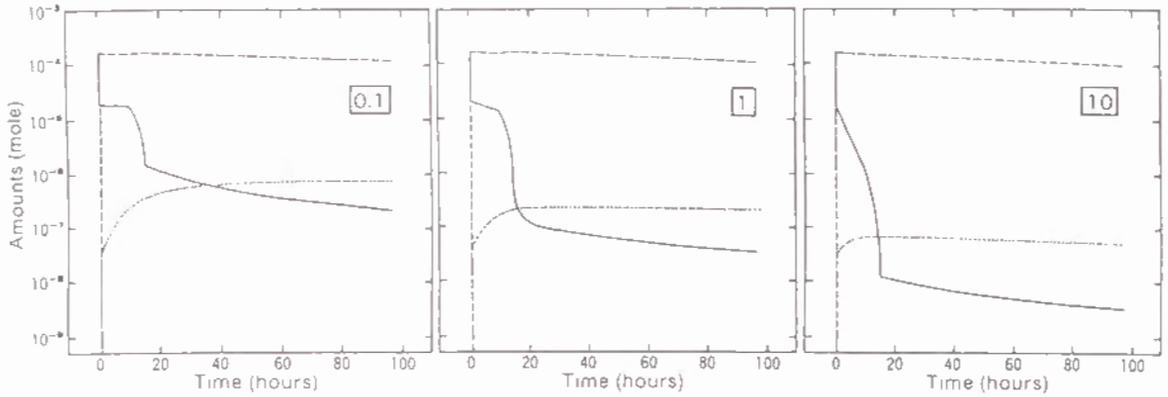

Figure 2–7. Time-dependent changes of pesticide in air, floor, wall and ceiling. A sensitivity estimate of air exchange rate (0.58 time h^{-1} × factor (0.1, 1, 10)).
——— : air, – – – – – – : floor, ····· : wall / ceiling

Influence of Floor, Wall and Ceiling Material

Two kinds of floor material were investigated in the sprayed room, i.e. "tatami" of a typical Japanese house and flooring of a typical western style. The amount in the air, wall and ceiling for the flooring at the 4th day after spraying is 52%, 77% and 77% of that for the "tatami", respectively, but no dominant differences are observed in the floor (table 2–2).

The value of diffusion constant (D_k) of compartment in the floor, wall and ceiling was 10^{-11} m^2 h^{-1} (2.78×10^{-15} m^2 s^{-1}) in the SPRAY-MOM model, however, the value should be changed owing to other materials such as carpet for the floor, non-coated wood or painted concrete for the wall and ceiling. Even though the pesticide behavior in floor compartment (5) does not differ largely from that of $D_k = 10^{12}$ and 10^{-10} m^2 h^{-1}, the amount in air, wall and ceiling after 4 days is affected as shown in table 2–2.

The transfer parameter D_{4k} was established from a half-life time (τ_{4k}) of transference between air (4) and the k compartment, where the experimental τ of fenitrothion on a leaf (for "tatami", 1.5 days) and a long chained alcohol (for wall and ceiling, 1.8 days) in dark was utilized, respectively. If τ_{4k} is 0.1 and 10 times the experimental values, an extreme variation of the pesticide in each compartment is observed as shown in table 2–2.

Table 2–2. Sensitivity to Various Factors
(Figures based on the 4th day after spraying.)

	Air (4)	Floor (5)	Wall (6)	Ceiling (7)
Experimental Simulation as Standard ("tatami")				
Mole	3.47×10^{-8}	1.10×10^{-4}	2.14×10^{-7}	2.10×10^{-7}
(ratio)	(1.00)	(1.00)	(1.00)	(1.00)
Western Style				
Mole	1.81×10^{-8}	1.12×10^{-4}	1.65×10^{-7}	1.61×10^{-7}
(ratio)	(0.52)	(1.02)	(0.77)	(0.77)
Sensitivity to Diffusion Constant (D_k)				
0.1 time				
Mole	1.01×10^{-7}	1.03×10^{-4}	3.88×10^{-7}	3.70×10^{-7}
(ratio)	(2.91)	(0.94)	(1.81)	(1.76)
10 times				
Mole	1.13×10^{-8}	1.12×10^{-4}	1.52×10^{-7}	1.51×10^{-7}
(ratio)	(0.33)	(1.02)	(0.71)	(0.72)
Sensitivity to Half-life Time with Air (τ_k, j = 5, 6, 7)				
0.1 time				
Mole	1.62×10^{-7}	8.66×10^{-5}	5.53×10^{-6}	5.23×10^{-6}
(ratio)	(4.67)	(0.79)	(25.84)	(24.90)
10 times				
Mole	3.85×10^{-9}	1.13×10^{-4}	1.40×10^{-8}	1.38×10^{-8}
(ratio)	(0.11)	(1.03)	(0.07)	(0.07)

Ratio in brackets: molar ratio of the pesticide in each compartment to the standard ("tatami")

Influence of Photo-degradation Rate

Some kinds of pesticide in a spraying formulation are known to photo-degrade more rapidly and thus, the photo-degradation rate of the pesticide was changed by a rate of 0.1 or 10 times of the standard. Small differences of the amounts of pesticide (figure 8) are observed by factors of 0.1 and 1, but there is a remarkable decrease of pesticide, if the rate is tenfold.

Influence of Vapor Pressure

Although the fugacity capacity (Z_i, i = 1, 2, 3) of aerosol droplet compartment was calculated by sub-cooled liquid vapor pressure (P_L) according to equation 2–7 and Z_k (k = 5, 6, 7) of the floor, wall and ceiling was estimated by solid vapor pressure (P), it is not clear whether the conventional (solid) or sub-cooled (liquid) vapor pressure should be used for organic substances with high molecular weight. However, in the present case, the air concentration due to Z_i from liquid vapor

pressure agrees well with that from the solid one. In the case of Z_k calculated by the liquid one, the air concentration is 58% of that by the solid one, but there are no significant differences in the other compartments (table 2–3).

The sensitivity to solid vapor pressure (P) was analyzed by using factors of 0.1 and 10 to the vapor pressure of fenitrothion. The results in figure 2–9 show the clear-cut differences in amounts of pesticide in air, wall and ceiling compartments in proportional to the P value, but there are small differences in the floor compartment.

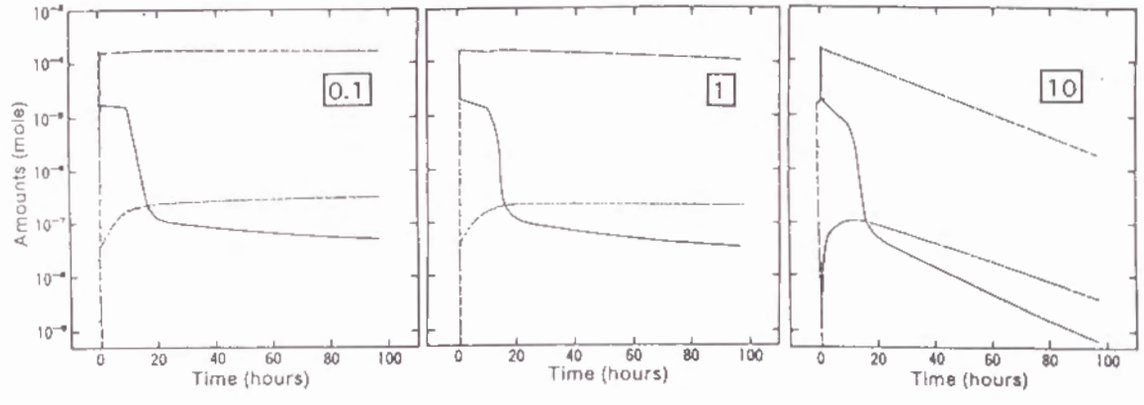

Figure 2–8. Time-dependent changes of pesticide in air, floor, wall and ceiling.
A sensitivity estimate of photo-degradation rate (standard × factor (0.1, 1, 10)).
———— : air, – – – – – – – : floor, ... : wall / ceiling

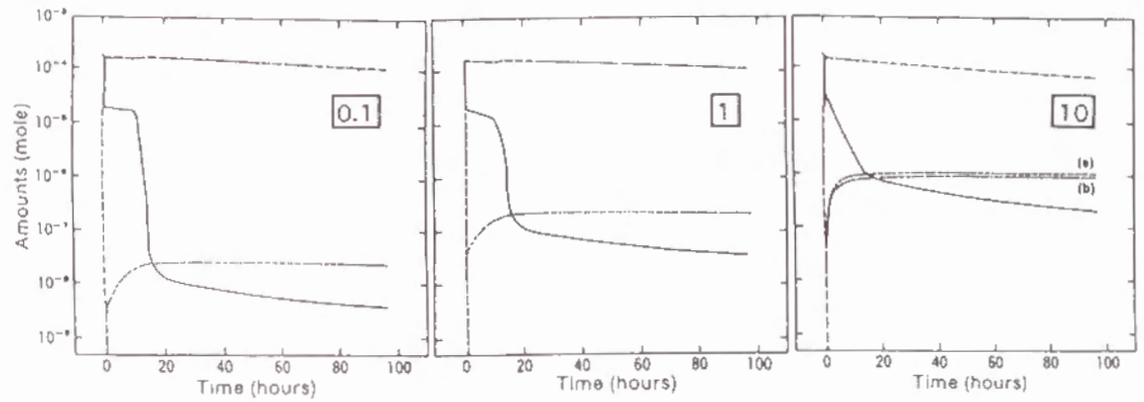

Figure 2–9. Time-dependent changes of pesticide in air, floor, wall and ceiling.
A sensitivity estimate of vapor pressure (standard × factor (0.1, 1, 10)).
———— : air, – – – – – – – : floor, ... : (a) wall / (b) ceiling

Influence of Other Physicochemical Properties of The Pesticide

Octanol/water partition coefficient (K_{ow}) and water solubility (C) are examined for 0.1 and 10 times the magnitude of fenitrothion. Both parameters directly influence fugacity capacities of the floor, wall and ceiling and the amount in air is enormously affected as shown in table 2–3.

Table 2–3. Sensitivity to Various Factors – Continuation of table 2–2 – (Figures based on the 4th day after spraying.)

	Air (4)	Floor (5)	Wall (6)	Ceiling (7)
Experimental Simulation as Standard				
(Z_i, i = 1, 2, 3 using P_L and Z_k, k = 5, 6, 7 using P)				
Mole	3.47×10^{-8}	1.10×10^{-4}	2.14×10^{-7}	2.10×10^{-7}
(ratio)	(1.00)	(1.00)	(1.00)	(1.00)
Fugacity Capacity using Solid Vapor Pressure (P)				
Mole	3.39×10^{-8}	1.07×10^{-4}	2.83×10^{-7}	2.77×10^{-7}
(ratio)	(0.98)	(0.97)	(1.32)	(1.32)
Fugacity Capacity using Liquid Vapor Pressure (P_L^s)				
Mole	2.01×10^{-8}	1.11×10^{-4}	1.75×10^{-7}	1.73×10^{-7}
(ratio)	(0.58)	(1.01)	(0.82)	(0.82)
Sensitivity to Octanol/water Partition Coefficient (K_{ow})				
0.1 time				
Mole	2.53×10^{-7}	8.67×10^{-5}	7.73×10^{-7}	6.89×10^{-7}
(ratio)	(7.29)	(0.79)	(3.61)	(3.28)
10 times				
Mole	3.60×10^{-9}	1.13×10^{-4}	1.31×10^{-7}	1.31×10^{-7}
(ratio)	(0.10)	(1.03)	(0.62)	(0.61)
Sensitivity to Water Solubility (C)				
0.1 time				
Mole	2.53×10^{-7}	8.67×10^{-5}	7.73×10^{-7}	6.89×10^{-7}
(ratio)	(7.29)	(0.79)	(3.61)	(3.28)
10 times				
Mole	3.60×10^{-9}	1.13×10^{-4}	1.31×10^{-7}	1.31×10^{-7}
(ratio)	(0.10)	(1.03)	(0.61)	(0.62)

Ratio in brackets: molar ratio of the pesticide in each compartment to the standard ("tatami")

Conclusion

The SPRAY–MOM model based on the dynamics of aerosol particles well simulated unsteady state behavior of pesticide in large, medium and small aerosol droplets, air, floor, wall and ceiling compartments inside a sprayed room under various conditions. The model predicted: the air

concentration on the first day is deeply influenced by the behavior of small droplets and air exchange rate; significant variation in all concerned compartments is expected by the variation of photo–degradation rates; and the magnitude of physicochemical properties of pesticide directly influences fugacities in each compartment and affects the total pesticide behavior. In a simulation experiment, the model described time–dependent concentrations of pesticide in air very well.

Chapter 3.

ELECTRIC VAPORIZER MODEL BY FLUID DYNAMICS

Introduction

A model of fluid dynamics enables a fairly rigorous analysis of a wide range of flow phenomena with more powerful digital computers in the last decade. The flow phenomenon is simulated by solving the basic equations of mass, momentum, energy, and a chemical species conservation.

An electric vaporizer, which heats and releases a pesticide in a vaporizer liquid, is a new delivery system for mosquito control. In order to describe accurately the behavior of pesticide released by the system into the air, in this chapter 3 the model of fluid dynamics was applied.
Thus, the pesticide behavior and air flow and temperature distribution were simulated inside a room which was supplied continuously a pesticide with the electric vaporizer and the unsteady state behavior at the moments of turning the vaporizer on and off and the simulation under the influence of varying important parameters such as the air exchange rate, locations of the air inlet and electric vaporizer and room temperature in regard to a sensitivity analysis were investigated.

Theoretical

The indoor flow is calculated as the laminar flow of a continuous fluid by using the model of fluid dynamics. Applying the model, the influences of the following boundary conditions are theoretically considered.

1. Floor, Wall and Ceiling of the Room

The boundary conditions at the floor, wall and ceiling are fixed to be independent of the inner flow. No diffusion of a chemical species from the floor, wall and ceiling to the air in the room is assumed. The chemical in the indoor flow is absorbed by bumping against the boundaries, but the surface concentration at the boundaries is set as zero. There are no photo-degradation and oxidation processes on the boundaries.

2. Air Inlet

Due to an air exchange rate (G), the air velocity at the inlet (v_{inlet}) is adopted as the following equation where V_{room} is the room volume and A_{inlet} the inlet area.

$$v_{inlet} = \frac{G\ V_{room}}{3600\ A_{inlet}}$$

3. Air Outlet

The boundary conditions of the air outlet are fixed to give a zero diffusion flux for all flow variables, but balance the exit flow with the inlet flow.

4. Electric Vaporizer

The electric vaporizer consists of three portions: (1) a wick evaporating pesticide (2) a covered heater promoting the evaporation and (3) a container for pesticide in the vaporizer liquid.

An evaporation rate (E_A') is pre-evaluated by determining the weight differences between the initial vaporizer liquid and the remaining liquid after 10 and 20 days' heating and utilized as a wick boundary condition giving an inflow velocity of pesticide (v_T) into the room by the following equation:

$$v_T = \frac{E_T\ R\ T_{wick}}{M\ P_{room}\ A_{wick}}$$

where R is the gas constant, T_{wick} the heating temperature around the wick, M the molecular weight of pesticide, P_{room} the pressure of the indoor air and A_{wick} the cross-sectional area of the wick.

A pre-calculation by the model of fluid dynamics using the boundary conditions gives a temperature (T_{cell}) of a cell of the indoor air above the wick and a mass flow rate (m_{cell}) of the indoor air into the cell.

If the sum of mass fraction of air and pesticide is assumed to be 1, the saturated mass fraction (MF_s) that is the highest limit of pesticide as complete vapor in the cell is calculated by the following equation:

$$MF_s = \frac{P_{cell}^s\ M}{P_{cell}^s\ M + (\ 101325 - P_{cell}^s\ )\ M_{air}}$$

where P_{cell}^s is the saturated vapor pressure of pesticide at T_{cell} and M_{air} the molecular weight of air.

MF_s multiplied by m_{cell} becomes a possible inflow rate of the vaporous pesticide into the cell. The evaporation rate (E_V, mole s^{-1}) of pesticide from the electric vaporizer is converted into the rate with an unit of m^3 s^{-1} by the gas law. Thus, the velocity (v_A) of pesticide obtained from the evaporation rate and A_{wick} is adopted as a wick boundary condition.

In this simulation, the complete vapor pesticide from the electric vaporizer is only calculated and the surplus pesticide incorporated into the cell above the evaporating portion is assumed to condense and not to related to the vaporous pesticide. Although the airborne chemical may be degraded by light and air–oxidation, such a change is not considered in this simulation.

5. Symmetrical Boundary

The room is completely symmetrical and half of it is calculated for the simulation. Neither there is a flux of all quantities across the symmetrical boundary nor a convective flux through the plane, and hence the normal velocity component at the symmetry plane is zero.

Data and Data Processing

The FLUENT Version 4.11 developed by Fluent Incorporated (Lebanon) was utilized as a model of fluid dynamics for the simulation and a supercomputer (CRAY–YMP 4E/132) was employed for the calculation.

[1] Simulation of the Experiment

A temporal variation in aerial concentrations of pesticide is measured during the summer in a typical Japanese apartment room being exposed to a pesticide continuously during 6 hours due to the release of pesticide from an electric vaporizer. Each formulation contains a synthetic pyrethroid (allethrin) as a pesticide. Allethrin is sampled by sucking an air volume of 20 ℓ at a flow rate of 1 ℓ min^{-1} and quantified[7]. During the experiment with an air exchange rate (G) of 0.58 h^{-1}, all windows and doors of the room remain closed.

The simulated room consists of 6 "tatami" mats (floor area, 9.72 m^2) and the air volume (V_{room}) is 23.3 m^3 (see Figure 3–1). The room temperature is 298 K. An electric vaporizer is positioned in the center of the floor and at a distance of 0.6 m from the inlet–sided front wall. The air inlet (A_{inlet}, 0.21 m × 0.30 m) is on the wall at a height of 0.15 m from the floor. An air outlet (0.25 m × 0.25 m) is on the back wall at a height of 2.05 m from the floor. All windows and doors of the room are kept closed and thus, the air inside the room moves from the air inlet to the outlet. Under these conditions, the air exchange rate is 0.57 h^{-1} (figure 3–1).

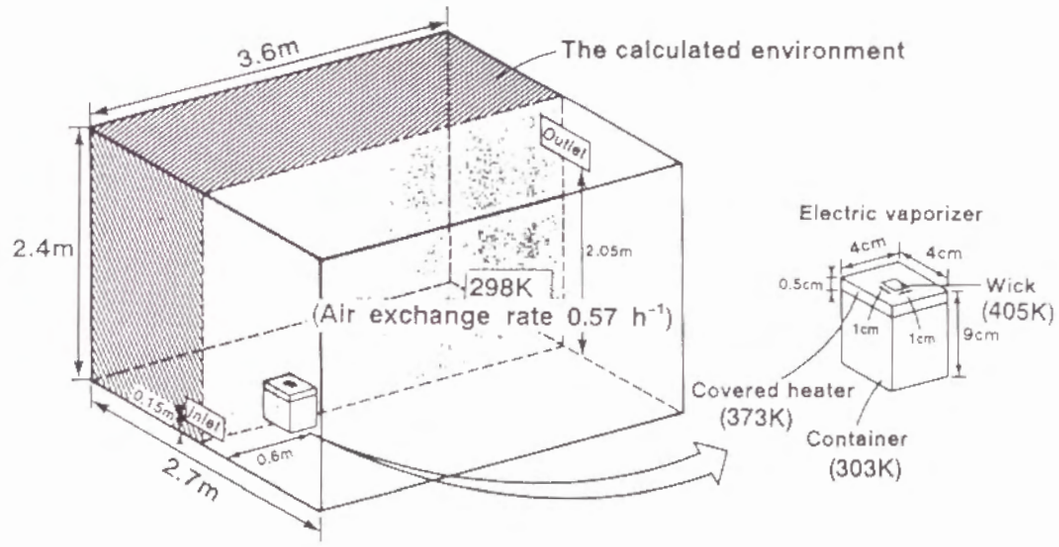

Figure 3–1. Simulation scenario with the room and electric vaporizer.

The molecular weight of allethrin (M) is 302.41 g $mole^{-1}$ and an apparent molecular weight of air (M_{air}) is 28 g $mole^{-1}$. The diffusion coefficient of allethrin is estimated to be 4.17×10^{-6} m^2 s^{-1} according to a method of Wike and Lee[9]. The specific heat capacity and heat transfer coefficient of the indoor air are considered to be 1.004×10^3 J kg^{-1} K^{-1} and $2.412.41 \times 10^{-2}$ W m^{-1} K^{-1}, respectively, as for the clean air keeping in mind that the air contains a very small amount of allethrin.

The boundary conditions at the floor, wall and ceiling are: velocities in all direction 0 m s^{-1}, temperature 298 K and the mass fraction of allethrin 0. At the air inlet, temperature is 298 K and the mass fraction 0. Under an air exchange rate of 0.57 h^{-1}, air velocity (v_{inlet}) at the air inlet is calculated to be 5.86×10^{-2} m s^{-1} in the horizontal direction from A_{inlet} and V_{room}.

The heating temperature (T_{wick}) around the wick of the electric vaporizer is 405 K and the temperatures of the cover of the heater and the container holding the vaporizer liquid are 373 K and 303 K, respectively.

The vaporizer liquid contains 2.91 % (W/V) of allethrin and a trace perfume in 45 ml of n–

paraffins. The electric vaporizer is designed to evaporate allethrin at a rate of 0.74 μg s^{-1} (E_T) by heating.

The vapor pressures (P) of allethrin at 293 K and 303 K are 5.6×10^{-3} and 1.6×10^{-2} Pa, respectively and thus, P can be expressed as a function of temperature (T) by the following equation:

$$\log P = 11.56 - \frac{4048}{T}$$

The temperature (T_{cell}) is 300 K for a cell of the indoor air above the evaporating portion by the pre-calculation. The vapor pressure (P^s_{cell}) and saturated mass fraction (MF_s) of allethrin at 300 K are calculated to be 1.18×10^{-2} Pa and 1.25×10^{-6}.

Due to the pre-calculation, the mass flow rate (m_{cell}) of the air containing allethrin flowing into the cell above the wick is 10.1 mg s^{-1}. Thus, 12.6 ng s^{-1} of allethrin (E_V) can flow into the cell as complete vapor. The evaporation rate (E_V) of allethrin from the electric vaporizer is converted to be 1.39×10^{-12} m^3 s^{-1} due to the gas law and the vertical velocity (v_A) is calculated to be 1.39×10^{-8} m s^{-1} since a cross-sectional area (A_{wick}) of the evaporating portion is 1 cm^2.

[2] Sensitivity Analysis

A sensitivity analysis was made by varying the air exchange rate, locations of the air inlet and electric vaporizer, and room temperature. Mostly however, the air exchange rate was fixed at 1.72 h^{-1} recommended for a living room[13].

Results and Discussion

[1] Simulation of the Experiment

The distribution of mass of allethrin, airflow (velocity) and temperature is calculated for a steady state (figure 3-2). The steady state airflow is deeply influenced by both the natural convection from the electric vaporizer and the forced convection from the air inlet. The main air stream bumped against the ceiling and ran to the outlet. The steep gradient at the bumping increases absorption of allethrin. Allethrin distributed toward the ceiling and entirely spread in the indoor air. The distribution of temperature within the room was rather homogeneous at roughly 298 K and hardly influenced by the heat of the electric vaporizer.

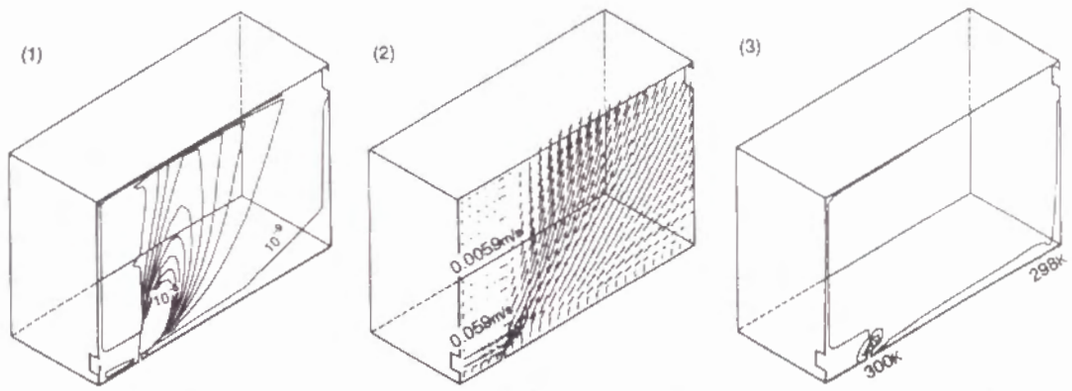

Figure 3-2. Simulation of: (1) the distribution of mass fraction of allethrin (mass fraction is divided from 0 to 1×10^{-8} by 1×10^{-9}), (2) the airflow (velocity covers the range from 2.04×10^{-3} to 5.90×10^{-2} m s^{-1}) and (3) the temperature distribution (the range is divided from 298 to 300 k by 0.2 K) at the symmetry plane of the room due to the continuous supply of allethrin by the electric vaporizer (steady state).

The aerial concentration amounts to 4.45 μg m^{-3} at the center of the room at steady state conditions, taking into account that the concentration is the product of mass of allethrin and density of air.

On the other hand, the experiment was simultaneously done with three formulations[7] and the concentration was assumed to be threefold. Thus, the concentrations at various times were divided by three (table 3-1). After 2 hours of application, the aerial concentration of allethrin seemed to approach a steady state and was 4.0 μg m^{-3} as an average of the concentrations from 2 to 6 hours.

In the simulation, the condensed portion of allethrin was neglected from the evaporation rate (E_V), although the condensed ratio amounted to 98% of allethrin evaporated from the electric vaporizer. Nevertheless, the estimated concentration of allethrin in complete vapor phase agreed well with the measured one.

Table 3-1. Aerial concentration of allethrin according to the experiment

Time after application (h)	Concentration (μg m^{-3})
0	2.5
2	4.0
4	3.4
6*	4.7
8	1.7
10	1.3
12	0.3

* Allethrin was continuously supplied for 6 hours.

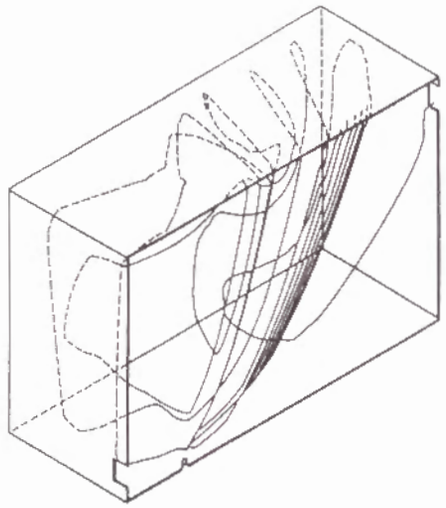

Figure 3–3. Behavior of the condensed droplets with 3.5 μm particle size and 0.23 m s^{-1} velocity at 8 cm above the electric vaporizer.

At 8 cm above the electric vaporizer, the particle size and velocity of the condensed droplets measured by a phase doppler particle analyzer (Aerometrics Inc., U.S.A.) were 3.5 μm and 0.23 m s^{-1}, respectively. The movement of the droplets above the vaporizer was simulated in a similar manner to the vapor phase by using this size and velocity and the density (756 kg m^{-3}) of n–paraffins, especially n–tetradecane, a main component of the vaporizer liquid. The condensed droplets were dispersing in the air with the rising flow immediately after evaporating from the electric vaporizer, and most droplets were then settled on the ceiling, although some droplets diffused into the indoor air (figure 3–3). Probably during the experiment the condensed droplets could not be collected in sampling tubes because the sampling flow rate was too low or allethrin disappeared by degradation.

The behavior of allethrin and airflow were additionally simulated from that moment when the electric vaporizer was turned on. After 20 sec of heating, the main flow moved near the floor to the outlet since it was influenced dominantly by the forced convection from the air inlet. Allethrin spread horizontally due to the main flow. The forced convection balanced with the rising flow from the heater after 60 sec and the distribution of allethrin extended upwards (figure 3–4). After 90 sec, the rising flow induced the main flow to bump directly to the ceiling. Both the distribution of allethrin and the airflow were close by the steady state after 180 sec, although the slope of concentration was rather higher. The concentration of allethrin at that time was 2.93 μg m^{-3} at the center of the room, while the measured one after turning on the electric vaporizer was 2.5 μg m^{-3} (table 3–1).

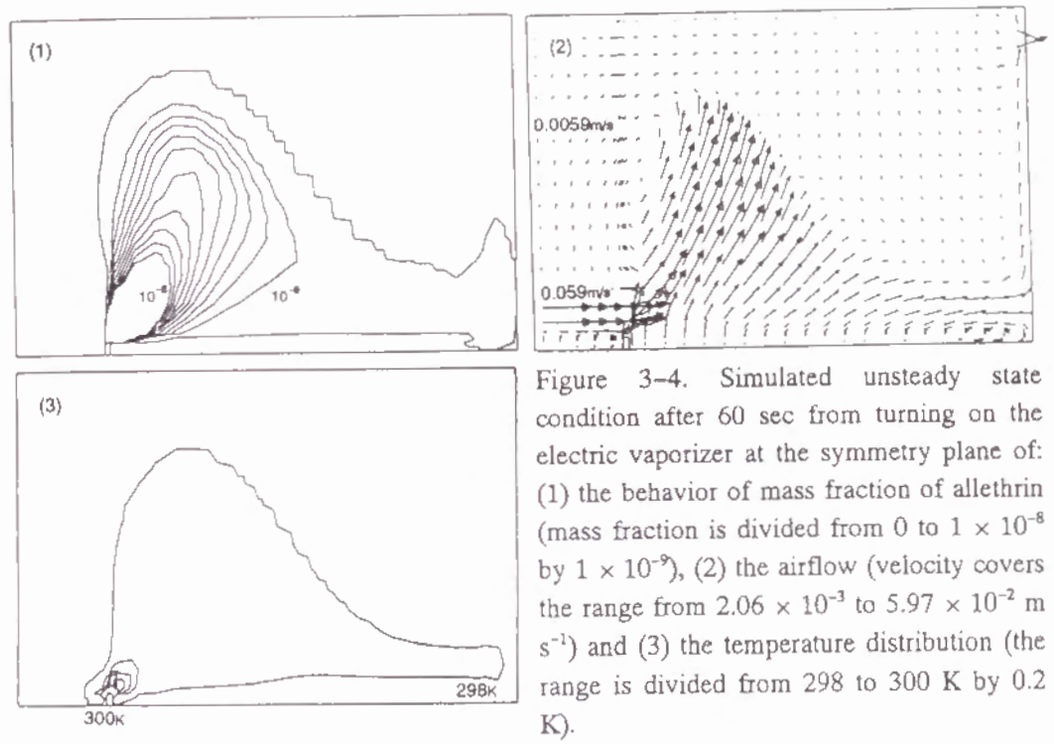

Figure 3–4. Simulated unsteady state condition after 60 sec from turning on the electric vaporizer at the symmetry plane of: (1) the behavior of mass fraction of allethrin (mass fraction is divided from 0 to 1×10^{-8} by 1×10^{-9}), (2) the airflow (velocity covers the range from 2.06×10^{-3} to 5.97×10^{-2} m s^{-1}) and (3) the temperature distribution (the range is divided from 298 to 300 K by 0.2 K).

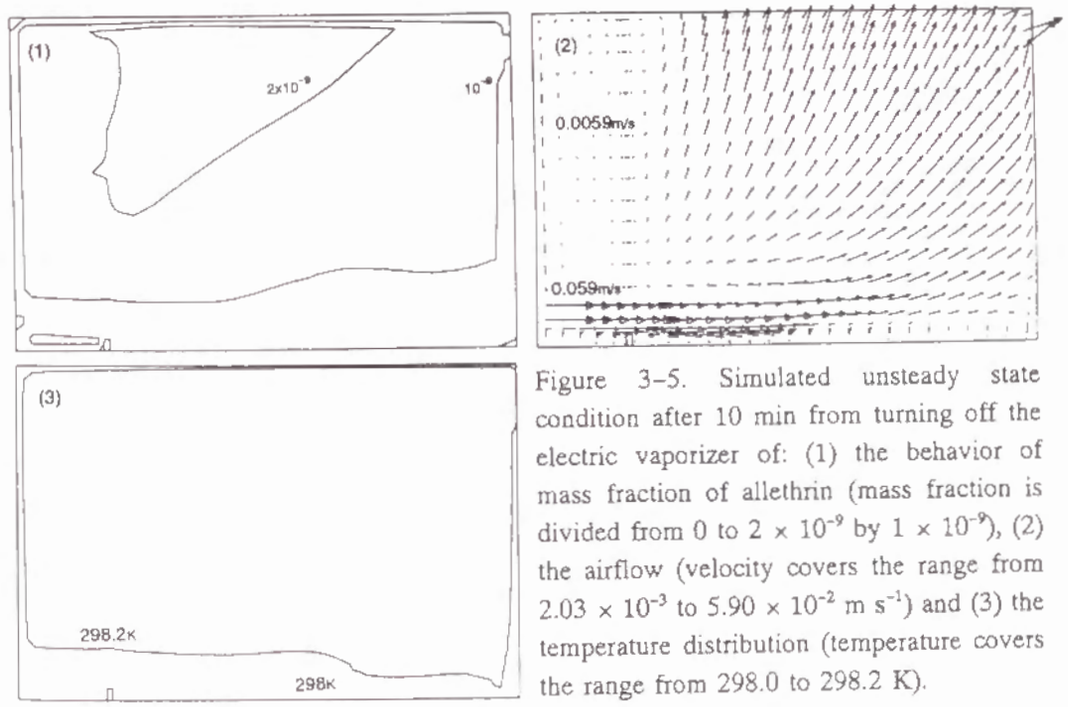

Figure 3–5. Simulated unsteady state condition after 10 min from turning off the electric vaporizer of: (1) the behavior of mass fraction of allethrin (mass fraction is divided from 0 to 2×10^{-9} by 1×10^{-9}), (2) the airflow (velocity covers the range from 2.03×10^{-3} to 5.90×10^{-2} m s^{-1}) and (3) the temperature distribution (temperature covers the range from 298.0 to 298.2 K).

Though the heating source was missing after turning off the electric vaporizer, the behavior of allethrin and the airflow were not far away from the steady state until 50 sec. From 100 sec, allethrin was slowly moving up to the ceiling and the influence of the rising flow became smaller with time. After 10 min, the concentration of allethrin was 1.97 μg m^{-3} at the center of the room (figure 3–5), while the measured one was 1.7 μg m^{-3} on 2 hours after turning off the electric vaporizer (table 3–1).

[2] Sensitivity Analysis

For a sensitivity analysis, the behavior of the pesticide at a steady state condition was examined by varying important parameters.

Influence of Air Exchange Rate

The air exchange rate of the room is directly connected with the air velocity from the air inlet and thus, its variation has a strong influence on the distribution of the pesticide. The behavior of the pesticide for air exchange rates between 0 and 1.72 h^{-1} was investigated at each steady state.

According to the non–realistic case of an air exchange rate 0, the air flow was exclusively induced by the natural convection above the electric vaporizer (figure 3–6). No forced convection from the air inlet lowered the amount of the mass flow rate (m_{cell}) into the cell above the electric vaporizer and thus, the evaporation rate (E_v) of the pesticide as complete vapor was lower than that for 0.57 and 1.72 h^{-1} (see table 3–2). The heat and the pesticide were vertically transported with an upward flow of air. A long and narrow strip of high temperature and high concentration appeared above the evaporating portion of the electric vaporizer. The steep gradient of the concentration and temperature accelerated a diffusion of the pesticide. Due to the bumping of the upward flow against the ceiling, a higher gradient of concentration near the ceiling was observed causing a higher absorption of the pesticide.

When the air exchange rate was 1.72 h^{-1} as calculated by the ASHRAE's minimum outdoor requirement for air exchange in living areas[13], the airflow was mainly influenced by the forced convection from the air inlet (figure 3–7). The main airflow containing the pesticide bumped against the outlet wall, rising along the wall and then reaching the air outlet. Another flow pattern was mixing the indoor air to some degree and the distribution of the pesticide was relatively uniform. At the floor and outlet wall, the steep gradient of concentration caused a higher absorption of the pesticide. Compared with the simulation for the experiment (0.57 h^{-1} of air exchange rate), the highest concentration was about three times lower. For the most part of the room, there was a homogeneous temperature distribution close to 298 K as for 0.57 h^{-1}.

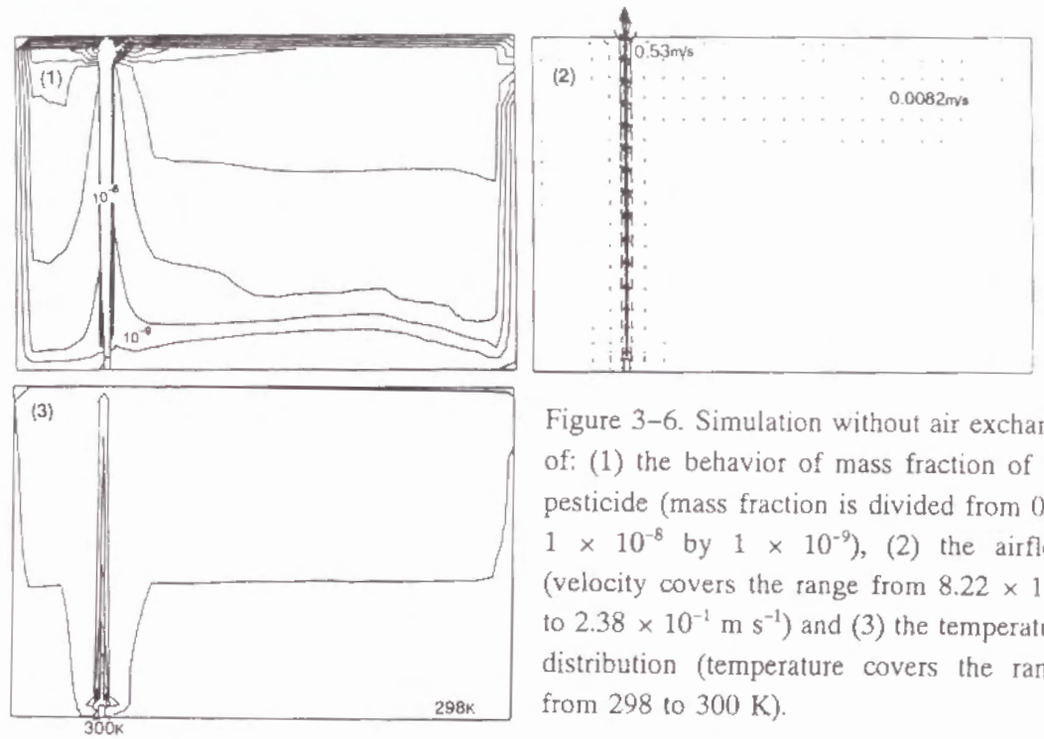

Figure 3–6. Simulation without air exchange of: (1) the behavior of mass fraction of the pesticide (mass fraction is divided from 0 to 1×10^{-8} by 1×10^{-9}), (2) the airflow (velocity covers the range from 8.22×10^{-3} to 2.38×10^{-1} m s^{-1}) and (3) the temperature distribution (temperature covers the range from 298 to 300 K).

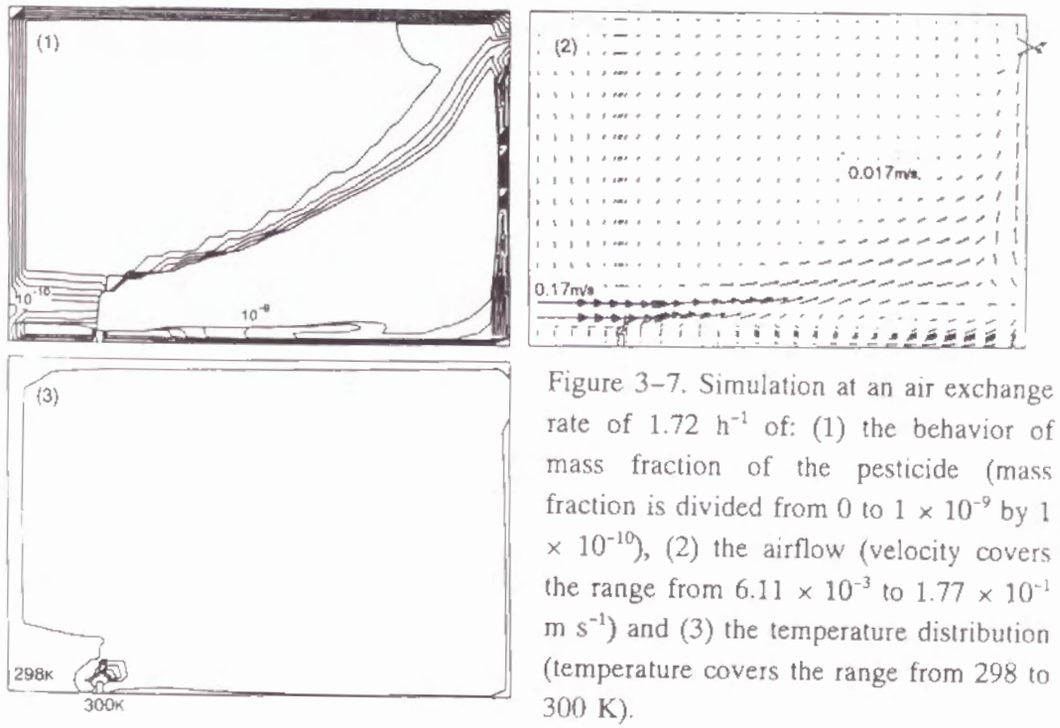

Figure 3–7. Simulation at an air exchange rate of 1.72 h^{-1} of: (1) the behavior of mass fraction of the pesticide (mass fraction is divided from 0 to 1×10^{-9} by 1×10^{-10}), (2) the airflow (velocity covers the range from 6.11×10^{-3} to 1.77×10^{-1} m s^{-1}) and (3) the temperature distribution (temperature covers the range from 298 to 300 K).

A mass fraction of the pesticide (MF) at the center of the room for an air exchange rate of 1.72 h^{-1} was lower than for 0 and 0.57 h^{-1}, but no substantial differences between 0 and 0.57 h^{-1} were observed. Although MF at the center of the room was strongly affected by the flow pattern of the pesticide, it was influenced at the outlet by the balance of air influx, evaporation and boundary absorption rates. The velocity of the mainstream from the air inlet to the outlet, moreover, affected the stagnation time in the room and the diffusion of the pesticide, and the concentration of the pesticide at the outlet was inversely proportional to the inlet flow. The highest vertical velocity component, v above the electric vaporizer for 0 h^{-1} meant that missing forced convection from the air inlet graduated a steep gradient of the temperature or promoted the natural convection. The vertical v was also strongly affected by the balance of the forced and natural convection and decreased with increasing air exchange rate. Sensitivities toward air exchange rate are summarized in table 3–2.

Table 3–2. Sensitivities toward air exchange rate

Air exchange rate		**0 h^{-1}**	**0.57 h^{-1}**	**1.72 h^{-1}**
Calculation conditions	T_{cell}	301	300	300
	m_{cell}	4.78×10^{-3}	1.01×10^{-2}	9.37×10^{-3}
	E_V	6.63×10^{-9}	1.26×10^{-8}	1.17×10^{-8}
	v	7.29×10^{-9}	1.39×10^{-8}	1.29×10^{-8}
MF at the center of the room		3.66×10^{-9}	3.89×10^{-9}	5.73×10^{-10}
MF at the air outlet		4.33×10^{-9}	1.47×10^{-9}	8.19×10^{-10}
v above the electric vaporizer (vertical v)		1.14×10^{-1} (1.14×10^{-1})	4.85×10^{-2} (1.38×10^{-2})	1.67×10^{-2} (5.95×10^{-4})

Influence of the Location of Air Inlet

The influence of changing the air inlet height from 0.15 m (lower site) to 1.10 m (middle site) and 2.04 m (upper site) from the floor was studied.

When the air inlet was at middle position, the mainstream of the air was directed away from the electric vaporizer and the evaporated the pesticide with the rising flow was transferred by the forced convection from the air inlet (figure 3–8). The main flow bumped against the ceiling just before arriving at the outlet. The steep gradient of the pesticide at the ceiling caused its high absorption.

When the air inlet was at upper position, the forced convection from the inlet hardly influenced the flow of the indoor air below the inlet, where the airflow was stagnated and dominated by diffusion. The pesticide was initially transported to the mainstream by the natural convection and then to the air outlet by the forced convection. Additionally observed were the higher concentration of the pesticide around the ceiling above the electric vaporizer and the steep gradient of concentrations below the ceiling and above the floor. Sensitivities toward the air inlet position are summarized in table 3–3.

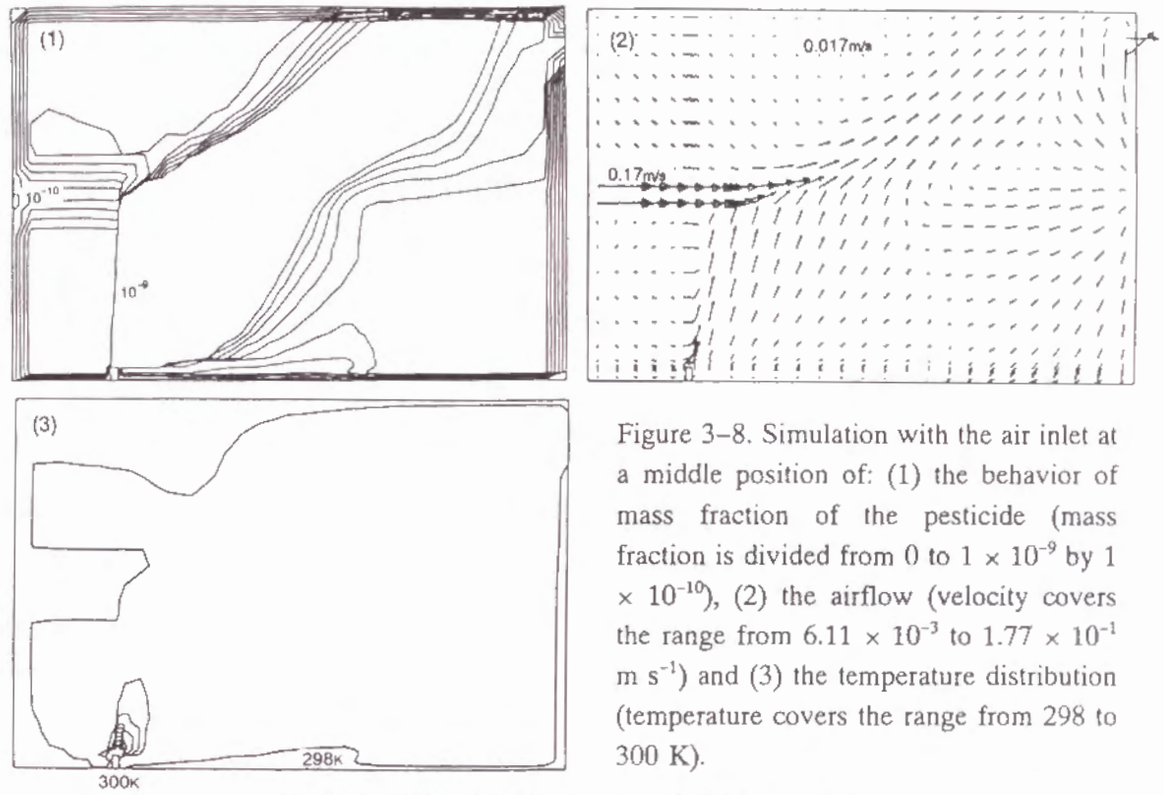

Figure 3–8. Simulation with the air inlet at a middle position of: (1) the behavior of mass fraction of the pesticide (mass fraction is divided from 0 to 1×10^{-9} by 1×10^{-10}), (2) the airflow (velocity covers the range from 6.11×10^{-3} to 1.77×10^{-1} m s^{-1}) and (3) the temperature distribution (temperature covers the range from 298 to 300 K).

Table 3–3. Sensitivities toward air inlet position

Air inlet position		**Lower**	**Middle**	**Upper**
Calculation conditions	T_{cell}	300	300	300
	m_{cell}	9.37×10^{-3}	1.10×10^{-2}	7.54×10^{-3}
	E_V	1.17×10^{-8}	1.37×10^{-8}	9.44×10^{-9}
	v	1.29×10^{-8}	1.06×10^{-8}	1.04×10^{-8}
MF at the center of the room		5.73×10^{-10}	1.44×10^{-9}	7.14×10^{-10}
MF at the air outlet		8.19×10^{-10}	7.87×10^{-10}	7.14×10^{-10}

Influence of the Location of Electric Vaporizer

When an electric vaporizer fixed at the center of the floor, 0.60 m apart from the inlet wall was elevated from the floor to middle (1 m) and upper (2 m) heights of the room by putting it on e.g. a furniture, the airflow became complicated because the air from the inlet escaped or bumped the electric vaporizer and got out of the outlet.

When the electric vaporizer was positioned at the middle position, the main flow moved near the floor and then to the outlet wall (figure 3–9). The position of the electric vaporizer was away from the mainstream in the stagnated range of the flow. The pesticide was transported almost by the rising flow, stagnated around the ceiling and hardly moved to the outlet. A fairly large amount of the evaporated the pesticide was supposed to be absorbed by the ceiling above the electric vaporizer. The most part of the room was almost at 298 K and the portion above the electric vaporizer had a short and narrow strip of higher temperature zone.

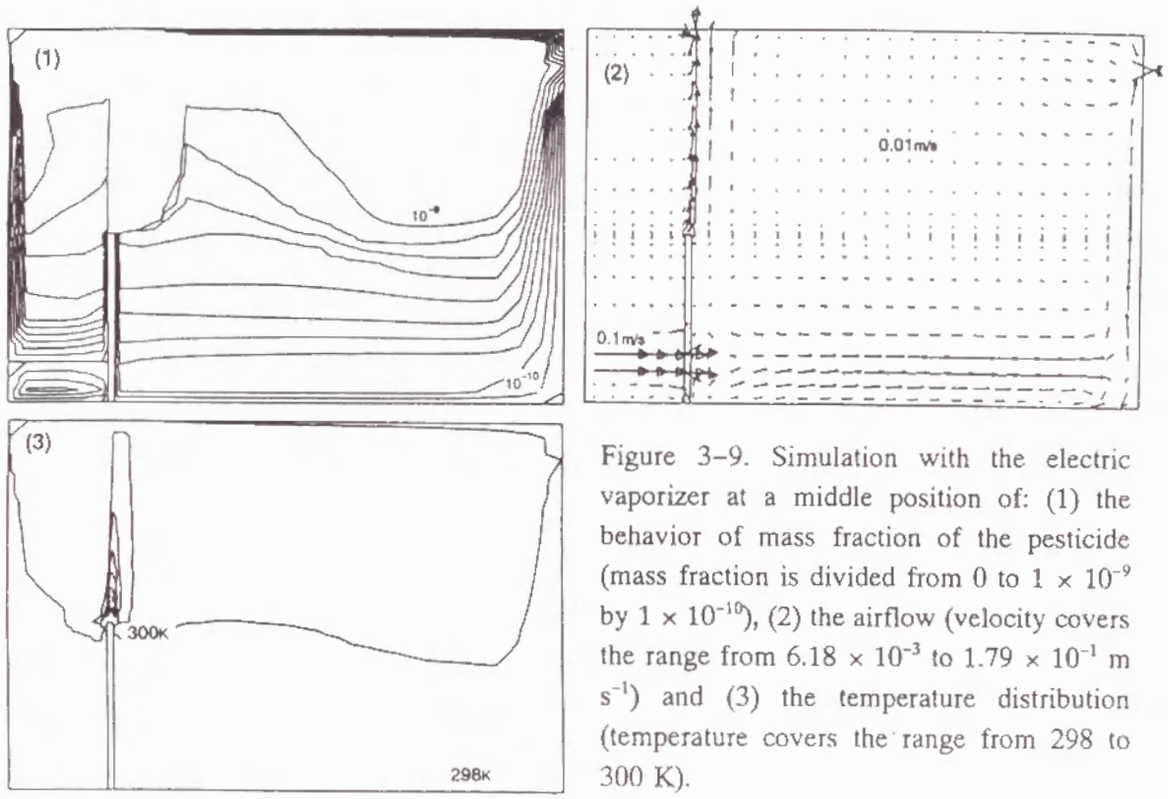

Figure 3–9. Simulation with the electric vaporizer at a middle position of: (1) the behavior of mass fraction of the pesticide (mass fraction is divided from 0 to 1×10^{-9} by 1×10^{-10}), (2) the airflow (velocity covers the range from 6.18×10^{-3} to 1.79×10^{-1} m s^{-1}) and (3) the temperature distribution (temperature covers the range from 298 to 300 K).

When the electric vaporizer was positioned at the upper position, the flow from the air inlet did not influence the distribution of the pesticide. The main airflow moved on the floor and then to outlet wall away from the electric vaporizer. The pesticide was stagnated above the evaporating portion and diffused nearby the electric vaporizer. Sensitivities toward the location of electric vaporizer are summarized in table 3–4.

Table 3–4. Sensitivities toward the location of electric vaporizer

Electric vaporizer position		Lower	Middle	Upper
Calculation conditions	T_{cell}	300	300	300
	m_{cell}	9.37×10^{-3}	9.08×10^{-3}	8.63×10^{-3}
	E_V	1.17×10^{-8}	1.14×10^{-8}	1.08×10^{-8}
	v	1.29×10^{-8}	1.25×10^{-8}	1.19×10^{-8}
MF at the center of the room		5.73×10^{-10}	8.65×10^{-10}	6.58×10^{-10}
MF at the air outlet		8.19×10^{-10}	8.82×10^{-10}	3.81×10^{-10}

Influence of Room Temperature

The temperature of a living room in Japanese summer is usually from 293 K to 303 K. Thus, the temperature of a living room covered a range from 293 and 303 K. The airflow and the distribution of the pesticide were almost the same as at 298 K although the distribution of the temperature was only changed around the electric vaporizer. The evaporation rate (E_V) for 303 K was, however, more than twice that for 293 K due to the differences of the vapor pressure of the pesticide at each temperature (T_{cell}). Thus, the mass fractions (MF) of the pesticide at the center of the room and at the outlet at 303 K exceeded those at 298 K. Sensitivities toward the room temperature are summarized in table 3–5.

Table 3–5. Sensitivities toward room temperature

Temperature of the room		293 K	298 K	303 K
Calculation conditions	T_{cell}	296	300	305
	m_{cell}	9.70×10^{-3}	9.37×10^{-3}	9.04×10^{-3}
	E_V	7.98×10^{-9}	1.17×10^{-8}	1.88×10^{-8}
	v	8.77×10^{-9}	1.29×10^{-8}	2.07×10^{-8}
MF at the center of the room		3.83×10^{-10}	5.73×10^{-10}	6.80×10^{-10}
MF at the air outlet		5.09×10^{-10}	8.19×10^{-10}	9.89×10^{-10}
v above the electric vaporizer (vertical v)		1.67×10^{-2} (4.95×10^{-4})	1.67×10^{-2} (5.95×10^{-4})	1.68×10^{-2} (7.13×10^{-4})

Conclusion

A computer program of fluid dynamics calculating the laminar flow of a continuous fluid was successfully used for the simulation of an active ingredient being released with an electric vaporizer to a room during summer. Although the complete vapor of pesticide from the electric

vaporizer was only calculated, i.e. the surplus of pesticide which condenses to form droplets was excluded, the aerial concentration at the center of the room agreed well with the measured one in the experiment.

As in a simulation, it was most likely that the condensed droplets above the electric vaporizer were moving in the air with the rising flow immediately after evaporation and most droplets then deposited on the ceiling, which in the experiment could not be collected in sampling tubes. Disappearance of pesticide by degradation would be also another possibility.

By a sensitivity analysis, the model predicted successfully the dependencies of pesticide concentration, airflow and temperature distribution on changes in the air exchange rate, locations of the air inlet and electric vaporizer, and room temperature.

Chapter 4.

ELECTRIC VAPORIZER MODEL (VAPOR-MOM)

Introduction

In chapter 3 [14], a room which was supplied continuously a pesticide with the electric vaporizer was simulated by a fluid dynamics model solving the basic equations of mass, momentum, energy and chemical species conservation. In the simulation, however, complete vapor-phase pesticide from the electric vaporizer only was calculated, and surplus pesticide was assumed to condense and not to be related to the vaporous pesticide. Degradation of the airborne chemical by light and air-oxidation also was not considered.

In this chapter, a mathematical model such as the Fugacity model of Mackay and Paterson[1] was utilized incorporating the results of the fluid dynamics [14], droplet dynamics [15], transference and degradation processes to describe the pesticide behavior more accurately. Thus, unsteady state model (VAPOR-MOM, the electric vaporizer model by Matoba, Ohnishi and Matsuo) was developed along this line.

Theoretical

The simulating environment consists of five kinds of compartments: condensed droplets (i = 1, 2, 3), airs (j = 4, 5, 6), floor (7), wall (8) and ceilings (k = 9, 10, 11) as illustrated in figure 4-1. The condensed droplets are divided into three compartments (i = 1, 2, 3) by generation and disappearance times. The air is classified into three compartments: vapor- (j = 4), droplet-supplying (j = 5) and breathing air (j = 6). The ceiling is classified into three compartments: the first compartment is absorbing the droplets (k = 9), the second connecting the droplet-supplying air compartment (k = 10) and the third covering the above two (k = 11). Each compartment is treated theoretically as follows:

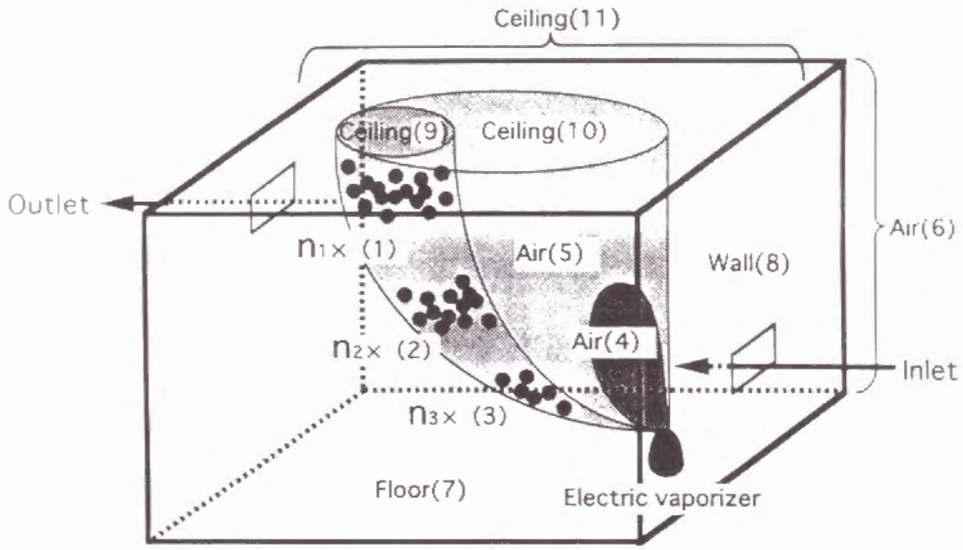

Figure 4-1. Simulation scenario with the room and compartments.
Condensed droplet (1, 2 and 3), airs (4, 5 and 6),
floor (7), wall (8) and ceiling compartments (9, 10 and 11)

[1] Condensed Droplet Compartment (i = 1, 2, 3)

All pesticide is initially evaporated as complete vapor from an electric vaporizer but some pesticide condenses to yield droplets since the evaporating rate (E_T) exceeds an upper limit of pesticide existing as complete vapor. In chapter 3, a pre-calculation using a fluid dynamics program gives temperature (T_{cell}) of a cell of the indoor air above wick of the electric vaporizer and a mass flow rate (m_{cell}) of the indoor air into the cell [14]. If sum of mass fraction of air and pesticide is assumed to be 1, saturated mass fraction or upper limit of vaporous pesticide (MF_s) in the cell is calculated by the following equation:

$$MF_s = \frac{P^s_{cell}\, M}{P^s_{cell}\, M + (101325 - P^s_{cell})\, M_{air}}$$

where P^s_{cell} is saturated vapor pressure of pesticide at T_{cell}, and M and M_{air} molecular weight of pesticide and air. MF_s multiplied by m_{cell} becomes a possible inflow rate of the vaporous pesticide into the room. Therefore, condensed ratio (C_r) to the evaporated pesticide is described as:

$$C_r = 1 - MF_s\, m_{cell} / E_T$$

Volume (V_i)

The condensed droplets contain pesticide and a dominant solvent of the vaporizer liquid. The dominant solvent will evaporate and the compartment (i = 1, 2, 3) becomes smaller in volume with time. According to chapter 2 [15], the volume (V_i) at time t_i after evaporation is $(\pi/6) \cdot d_i^3$ and the rate of change of the volume until t_z is as follows:

$$\frac{d\, V_i}{d\, t} = - \frac{\pi}{2}\, \alpha\, d_i \qquad (4\text{-}1)$$

where t_z is time until the solvent completely evaporates, α diameter coefficient depending on kinds of the droplet solvent and d_i time-dependent diameter.

Velocity (v_i)

A motion of the condensed droplet compartment is governed by a rising current caused by heat of the electric vaporizer, gravity and resistance of air to particle motion. The movement of the droplets with time can be simulated by the fluid dynamics program [14] shown in figure 3-3 in chapter 3.

Number of Condensed Droplet Compartment (n_i)

The total number of the condensed droplets generated per second (dn_T/dt) is calculated as the following equation where d_0 is an initial size of condensed droplets, R_a volume ratio of pesticide in condensed droplets immediately after condensation and ρ pesticide density to the vaporizer liquid.

$$\frac{d\, n_T}{d\, t} = E_T\, C_r / (\frac{\pi}{6}\, d_0^3\, R_a\, \rho)$$

The condensed droplets are continuously generated and absorbed into the ceiling within a life time (t_ℓ). For simplicity, the released droplets are separated into three compartments: the first one (i = 1) is intermittently introduced into the room for one-third of t_ℓ and the number (n_i) of the droplets is $(dn_T/dt) \cdot t_\ell/3$. The second (i = 2) generates at $t_\ell/3$ later with the same number and the third (i = 3) generates at $2 \cdot t_\ell/3$ (i = 3) later. Thus, three compartments continuously generate above the electric vaporizer, rise up and are absorbed by the ceiling in the life time (t_ℓ).

Fugacity Capacity (Z_i)

Z_i value of the condensed droplet compartment (i) is described as the following equation [15] where P_L is sub-cooled liquid vapor pressure, R the gas constant and T room temperature.

$$Z_i = \frac{6 \times 10^6}{P_L R T}$$

Transference

The moving course of the droplet compartments is within the droplet-supplying air compartment (j = 5). A diffusive transfer rate of pesticide between condensed droplets (i = 1, 2, 3) and air compartment (5) can be written as:

$$\frac{d N_i}{d t} = D_{i5} (f_i - f_5)$$

where dN_i/dt is a flux of pesticide in condensed droplet compartment (i), f_i and f_5 fugacities in condensed droplet (i) and air compartment (5), and D_{i5} a transfer parameter. The transfer parameter (D_{i5}) can be estimated by:

$$D_{i5} = \frac{1}{1 / (k_i A_i Z_i) + 1 / (k_5 A_i Z_5)} \qquad (4\text{-}2)$$

where A_i is surface area of condensed droplets $\pi \cdot d_{ti}^2$. The velocity (k_5) of pesticide in air compartment (5) is $G \cdot V_{room}/A_{room} + v_i$ where G is air exchange rate of the room, V_{room} volume of the room and A_{room} cross-sectional area (product of width and height) of the room, and velocity k_i is $k_5/100$.

Photo-degradation and Oxidation

The major reactions in condensed droplet compartment (i) are photo-degradation and oxidation described by a combined first-order rate constant K_i. The reaction rate is written as $K_i V_i Z_i$ where K_i is $0.693/\tau_i$ and τ_i is a half-life time of photo-degradation and oxidation.

Differential Equation in Terms of Fugacity

On a Level IV fugacity model, the unsteady state behavior of pesticide in condensed droplet compartment (i) is expressed by a differential equation 4-3.

$$\frac{d f_i}{d t} V_i Z_i = \frac{\pi}{2} \alpha d_i Z_i f_i - D_{i5} (f_i - f_5) - K_i V_i Z_i f_i \qquad (4\text{-}3)$$

An initial fugacity of the droplet compartment (i) is $R_a \cdot \rho/M/Z_i$. The volume (V_i) of the compartment is becoming smaller with time until an ultimate diameter (d_z) is attained and the fugacity increases according to the first term in the right side in reference to equation 4-1.

The pesticide in condensed droplet compartment (i) transfers with air compartment (5) and the transference is time-dependent based on the surface area of condensed droplets as indicated in equation 4-2. The pesticide is also photo-degraded and oxidized in the compartment (i). The absorption by the ceiling does not change the droplet fugacity (f_i), but the absorbing ceiling fugacity (f_9) varies.

[2] Air Compartment (j = 4, 5, 6)

From results of pesticide distribution by the fluid dynamics program, the air can be divided into three compartments i.e. vapor- (j = 4), droplet-supplying (j = 5) and breathing air compartment (j = 6). The vaporous pesticide is introduced into the vapor-supplying air compartment (4) and the condensed droplets generate and rise up within the droplet-supplying air compartment (5).

Volume (V_j) and Fugacity Capacity (Z_j)

Each volume of air compartments is V_j (j = 4, 5, 6) and sum of each compartment is equal to that of the room supplied with pesticide. An air fugacity capacity, Z_j, is 1/RT.

Evaporation Rate (E_v)

The vaporous pesticide is introduced into air compartment (4) at a rate of E_v:

$$E_v = E_T (1 - C_r) / M$$

Air Exchange

The pesticide in each air compartment is transferred by a fluid movement caused by air exchange from one to another compartment. A velocity (v_f) of the fluid is $G \cdot V_{room}/A_{room}$ and the carried air mass among air compartments (j = 4, 5, 6) is $v_f \cdot A_j$ where A_j is cross-sectional area of each air compartment.

Transference

Transference between condensed droplet (i = 1, 2 or 3) and droplet-supplying air compartment (j = 5) is proportional to the number (n_i) of condensed droplets. The n_i is constant from generation to absorption. The pesticide in air compartment (5) transfers with droplet (i) and ceiling compartments (k = 9, 10), while that in breathing air compartment (j = 6) transfers with floor (7), wall (8) and ceiling compartment (11). The transfer parameter D_{jk} of air (j = 5, 6) with floor (k = 7), wall (k = 8) or ceiling compartment (k = 9, 10, 11) is estimated as the following equation where τ_{jk} is a half-life time of transference between air (j) and each compartment k.

$$D_{jk} = \frac{0.693}{\tau_{jk} (1 / V_j / Z_j + 1 / V_k / Z_k)}$$

Differential Equation for Air Compartment (j = 4)

Movement of pesticide in vapor-supplying air compartment (j = 4) is caused by emission of pesticide as complete vapor, transference with droplet-supplying air compartment (j = 5) and photo-degradation and oxidation. Thus, the unsteady state behavior of pesticide in vapor-supplying air compartment (j = 4) is given by equation 4-4:

$$\frac{d f_4}{d t} V_4 Z_4 = E_v + v_f A_4 (Z_5 f_5 - Z_4 f_4) - K_4 V_4 Z_4 f_4 \quad (4\text{-}4)$$

Differential Equations for Air Compartments (j = 5 and 6)

The unsteady state behaviors of pesticide in droplet-supplying and breathing air compartments (j = 5 and 6) are given by equations 4-5 and 4-6 since the pesticide of the air compartments transfers with floor, wall or ceilings:

$$\frac{d f_5}{d t} V_5 Z_5 = v_f \{ A_4 Z_4 f_4 - (A_4 + A_5) Z_5 f_5 + A_5 Z_6 f_6 \} - \sum_{i=1}^{3} n_i D_{i5} (f_5 - f_i) - \sum_{k=9}^{10} D_{5k} (f_5 - f_k) - K_5 V_5 Z_5 f_5 \quad (4\text{-}5)$$

$$\frac{d f_6}{d t} V_6 Z_6 = v_f \{ A_5 Z_5 f_5 - (A_5 + A_{room}) Z_6 f_6 \} - \sum_{k=7}^{8} D_{6k} (f_6 - f_k) - D_{6,11} (f_6 - f_{11}) - K_6 V_6 Z_6 f_6 \quad (4\text{-}6)$$

[3] Floor, Wall and Ceiling Compartment (k = 7, 8, 9, 10, 11)

Volume (V_k)

Volumes (V_k, k = 7,8,9,10,11) of floor, wall and ceiling compartments can be calculated by:

$$V_k = 2 \sqrt{D_k t} A_k$$

where D_K is a diffusion constant of pesticide and A_k surface area of each compartment. The rate of change of each volume is expressed as [15]:

$$\frac{d V_k}{d t} = - \sqrt{D_k / t} A_k$$

Fugacity Capacity (Z_k)

A floor Z_7 value can be calculated as $P_f \cdot C/P$, where P_f is a polymer/water partition coefficient, C water solubility and P solid (conventional) vapor pressure. Similarly, wall and ceiling Z values (Z_k, k=8,9,10,11) can be calculated as $P_w \cdot C/P$, where P_w is a polymer/water partition coefficient.

Differential Equations for Floor and Wall Compartments (k = 7 and 8)

Differential equations 4-7 and 4-8 describe the unsteady state behaviors of pesticide in floor and wall compartments. The changing volume (V_7 and V_8) of the compartments (7 and 8) with time

is written by the first term in the right side.

$$\frac{d f_7}{d t} V_7 Z_7 = - \sqrt{D_k / t} A_7 Z_7 f_7 - D_{6\,7} (f_7 - f_6) - K_7 V_7 Z_7 f_7 \quad (4\text{-}7)$$

$$\frac{d f_8}{d t} V_8 Z_8 = - \sqrt{D / t} A_8 Z_8 f_8 - D_{6\,8} (f_8 - f_6) - K_8 V_8 Z_8 f_8 \quad (4\text{-}8)$$

Differential Equation for Ceiling Compartment (9)

For ceiling compartment (9), the following fugacity (f_a) is added every time when the condensed droplets touch the ceiling:

$$f_a = n_i V_{ia} Z_i f_{ia} / (V_9 Z_9) \quad (4\text{-}9)$$

where V_{ia} and f_{ia} are volume and fugacity of droplet compartment (i) just before absorption.

The time-dependent volume (V_9) reduces the fugacity according to the first term in the right side and increases the transfer parameter. The pesticide also transfers with air compartment (j = 5):

$$\frac{d f_9}{d t} V_9 Z_9 = - \sqrt{D_k / t} A_9 Z_9 f_9 - D_{5\,9} (f_9 - f_5) - K_9 V_9 Z_9 f_9$$

Differential Equations for Ceiling Compartments (10 and 11)

The differential equations for pesticide in ceiling compartments (10 and 11) connecting the air compartments (5 or 6) are:

$$\frac{d f_{10}}{d t} V_{10} Z_{10} = - \sqrt{D_k / t} A_{10} Z_{10} f_{10} - D_{5,\,10} (f_{10} - f_5) - K_{10} V_{10} Z_{10} f_{10} \quad (4\text{-}10)$$

$$\frac{d f_{11}}{d t} V_{11} Z_{11} = - \sqrt{D / t} A_{11} Z_{11} f_{11} - D_{6,\,11} (f_{11} - f_6) - K_{11} V_{11} Z_{11} f_{11} \quad (4\text{-}11)$$

Computer Programming and Data Processing

For pre-calculation, FLUENT Version 4.11 (Fluent Incorporated, Lebanon) was utilized as a fluid dynamics program and a supercomputer, CRAY-YMP 4E/132, was employed for the calculation. A computer program, VAPOR-MOM, was developed by utilizing BASIC. IBM PS/2 was employed for the programming and calculation.

The program was set up in such a way that basic physicochemical data, half-life times of transference, photo-degradation and oxidation rate, supplying quantity of the chemical and room conditions were incorporated. By running, calculation of time-dependent velocity, volume and D values, resolution of unsteady state equations, and graphing of resulting amounts in each compartment versus time were performed.

[1] Simulation of an Experiment

A temporal variation in aerial concentration of pesticide was measured during the summer in a typical Japanese apartment room, where an electric vaporizer was used continuously for 6 hours per day [7]. The formulation contains a synthetic pyrethroid (allethrin) as a pesticide.

According to the experiment, a simulated room consists of 6 "tatami" mats (floor area, 9.7 m^2), air volume (V_{room}) of 23.3 m^3 and air exchange rate of 0.58 time h^{-1}. The room temperature is 298 K. The location of the electric vaporizer, air inlet and outlet and boundary conditions for the calculation by the fluid dynamics program are the same as in chapter 3 [14].

The vaporizer liquid contains 1.94×10^{-2} (R_a, V/V) of allethrin and a trace perfume in 45 ml of n-paraffins. The electric vaporizer is designed to evaporate allethrin at a rate of 7.36×10^{-7} g s^{-1} (E_r) by heating.

The composition of n-paraffins is 0.5% of n-tridecane, 69.8% of n-tetradecane, 23.8% of n-pentadecane, 3.4% of n-hexadecane and 0.7% of n-heptadecane and thus, an assumption is made as that the component of the condensed droplets is 100% n-tetradecane. The diffusion coefficient of n-tetradecane is estimated to be 4.91×10^{-6} (m^2 s^{-1}) according to a method of Wike and Lee [9]. The partial vapor pressure of n-tetradecane on droplet surface is 1.77 Pa at 298 K, the molecular weight 198.39 g $mole^{-1}$, density 7.59×10^5 g m^{-3}, and diameter coefficient (α) 2.38×10^{12} m^2 s^{-1} at 289 K.

As for volumes (V_k, k = 7, 8, 9, 10, 11) of floor (7), wall (8) and ceiling (9, 10, 11), D_K of allethrin is set to be 2.78×10^{-15} m^2 s^{-1} and the ultimate diffusion depth is to be 2.35×10^3 μm

for floor made of "tatami" and 136 μm for the wall and ceiling [15]. As for the fugacity capacities of floor (7), wall (8) and ceiling (9, 10, 11) (Z_k, k = 7, 8, 9, 10, 11), P_f and P_w values are set to be K_{ow} (octanol/water partition coefficient).

The transfer parameter D_{jk} (j=5,6, k=7,8,9,10,11) is established from a half-life time (τ_{jk}) of transference between the air (j) and the floor, wall and ceiling (k) compartment. A experimental τ of fenitrothion on a leaf (for "tatami") and a long chained alcohol (for wall and ceiling) is 1.5 and 1.8 days, respectively. Since the vapor pressure of allethrin is 3-fold lower than that of fenitrothion, the vaporization of allethrin from the k compartment is likely to be lower than that of fenitrothion. The rate of loss of a compound will be proportional to the product of vapor pressure and the square root of molecular weight[16]. Thus, in the case of allethrin the half-life time (τ_{jk}) for the "tatami" and the wall and ceiling is estimated to be 4.3 and 5.1 days, respectively.

The half-life time of photo-degradation and oxidation in the condensed droplet (i = 1, 2, 3) and air compartment (j = 4, 5, 6) is adopted to be 3 hours from an experiment where allethrin on silica gel was irradiated by sunlight as well as by a 360 nM lamp [17]. Due to our experiment, only 27% and 23% of phenothrin and tetramethrin was respectively degraded in a coated polymer layer of a floor with a daily sunshine period of 4 days. Thus, the half-life time of allethrin as a kind of pyrethroid is amounted to be 10 days in the floor, wall and ceiling compartment (k = 7, 8, 9, 10, 11). These data of allethrin required for the simulation are summarized in table 4-1.

Table 4-1. Primary Input Data

Input data	Allethrin
Physicochemical properties:	
Molecular weight (g mole^{-1})	302.41
Specific gravity (g m^{-3})	1.5×10^{6}
Solid vapor pressure (Pa)	9.53×10^{-3}
Liquid vapor pressure (Pa)	1.68×10^{-2}
Water solubility (mole m^{-3})	1.42×10^{-2}
Log K_{ow}	4.78
Melting point (K)	323
Diffusion coefficient (m^2 s^{-1})	4.17×10^{-6}
Half-life time (s) of transference between air and:	
Floor (τ_{67})	3.71×10^{5}
Ceiling (τ_{jk}, j=5,6, k=9,10,11)	4.45×10^{5}
Half-life time (s) of photo-degradation and oxidation in:	
Condensed droplet (K_i, i = 1, 2, 3)	1.08×10^{4}
Air (K_j, j = 4, 5, 6)	1.08×10^{4}
Floor, wall, ceiling (K_k,k=7,8,9,10,11)	8.64×10^{5}

[2] Sensitivity Analysis

All important parameters constituting the differential equations are varied within 2 orders (factor 0.1 and 10) of magnitude to test the sensitivity of the equations to the parameters.

Results and Discussion

[1] Simulation of the Experiment

Pre-simulation by the Fluid Dynamics Program

A fluid dynamics program was employed in order to determine the condensed ratio to the evaporated allethrin (C_r), the distribution of allethrin in air and the movement of the condensed droplets.

Table 4-2. Summary of the calculated values

T_{cell}	300 K
P^s_{cell}	1.18×10^{-2} Pa
MF_s	1.25×10^{-6}
m_{cell}	1.01×10^{-2} g s^{-1}

The condensed ratio (C_r) to the evaporated allethrin amounted to 0.98 by a calculation as described in chapter 3 [14]. Table 4-2 is a summary of the calculated values. From the result of the distribution of the allethrin in air, the air and ceiling compartments can be respectively divided into three compartments. The volumes and cross-sectional areas of the air compartments and surface areas of the ceiling compartments are shown in tables 4-3 and 4-4.

Table 4-3. Volume and cross-sectional area of each air compartment

Air compartments	Volume (m^3)	Cross-sectional area (m^2)
Vapor-supplying air (4)	$V_4 = 2$	$A_4 = 1.20$
Droplet-supplying air (5)	$V_5 = 3$	$A_5 = 0.96$
Breathing air (6)	$V_6 = 18.3$	$A_{room} = 7.48$

Table 4-4. The surface area of each ceiling compartment

Ceiling compartments	Surface area (m^2)
Ceiling absorbing the droplets (9)	$A_9 = 0.8$
Ceiling connecting the droplet-supplying air (10)	$A_{10} = 2$
Ceiling connecting the breathing air (11)	$A_{11} = 6.9$

An initial size of the condensed droplets (d_0) was 3.5 μm when measured by a phase doppler particle analyzer (Aerometrics Inc., U.S.A.). From the size of the droplets, its movement was simulated by the fluid dynamics program. The life time (t_ℓ) of the droplets from generation to absorption on the ceiling was 49.3 sec. The simulated velocity (v_i) with time after evaporation (t_i) was expressed by the following equation where the R value (square root of the coefficient of determination) is 0.92.

$$v_t = 3.44\times10^{-2} + 1.74\times10^{-4}\, t_i + 2.25\times10^{-4}\, t_i^2 - 2.03\times10^{-5}\, t_i^3 + 7.12\times10^{-7}\, t_i^4 - 1.06\times10^{-8}\, t_i^5 + 5.07\times10^{-11}\, t_i^6 \qquad (4\text{-}12)$$

Simulation by the Fugacity Model (VAPOR-MOM)

The unsteady state behavior of allethrin in air, floor, wall and ceiling was simulated by the VAPOR-MOM model. The predicted time-dependent concentration in the breathing air compartment (6) entirely agreed with the measured one, where the room was exposed to allethrin continuously during 6 hours (figure 4-2). The temporal concentrations in the vapor- (4) and droplet-supplying air compartment (5) are also shown in figure 4-2.

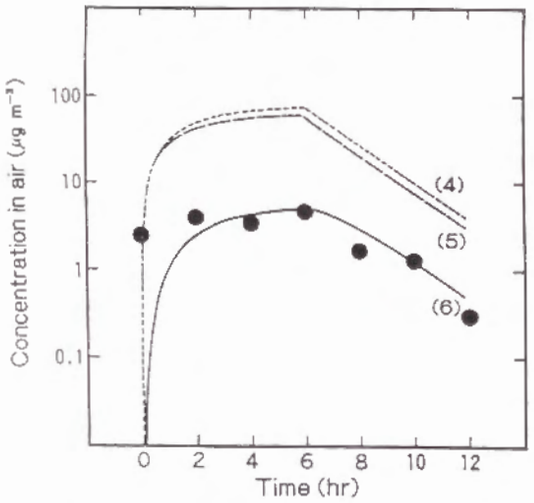

Figure 4-2. Aerial concentration of allethrin as a function of time.
Closed circles: experiment
Lines: calculation;
(4) vapor-, (5) droplet-supplying and (6) breathing air compartment

The condensed droplets were intermittently generated and changed in diameter and velocity during the life time (t_ℓ) (equation 4-1, 4-12 and figure 4-3). Due to equation 4-2, the transfer parameter ($D_{i,5}$) between droplet (i = 1, 2, 3) and droplet-supplying compartment (j = 5) was also time-dependent as shown in figure 4-4.

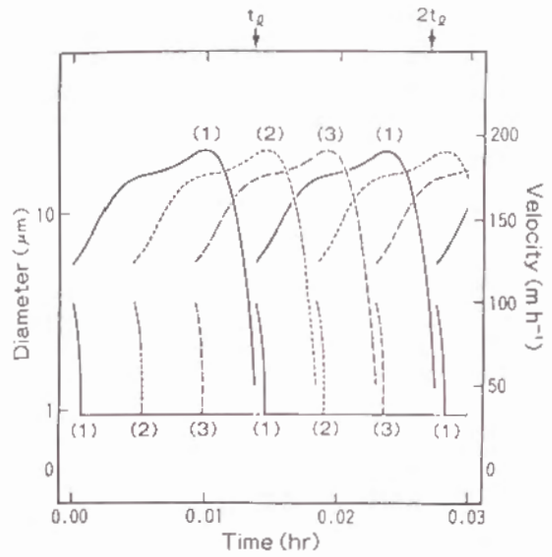

Figure 4-3. Time-dependent changes of the diameter (d_i) and velocity (v_i) of condensed droplets (i=1,2,3).

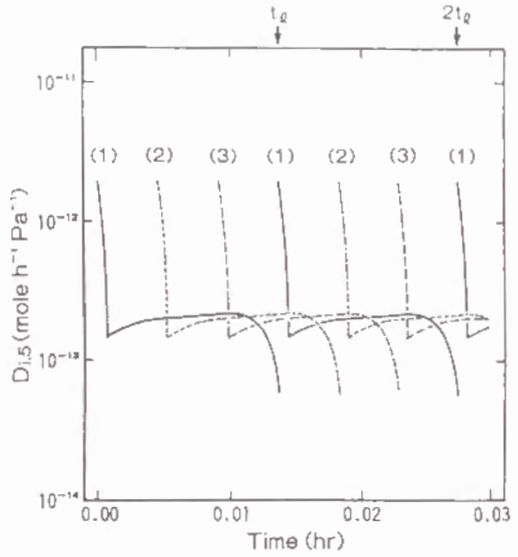

Figure 4-4. Time-dependent changes of the transfer parameters ($D_{i,5}$) between droplets (i=1,2,3) and air compartment (5).

Variation of fugacities in concerned compartments with time are given in figure 4-5. The fugacities in the droplets (i = 1, 2, 3) rapidly increased after generation from the electric vaporizer due to the decrease in volume of droplets (equation 4-3). After the solvent constituting the droplet completely evaporated (t_z), a little change of the fugacity was caused by transference with air (5), photo-degradation and oxidation. When the first droplet compartment (i = 1) was absorbed into the ceiling (9), a fairly large change of fugacity in the ceiling was observed according to equation 4-9. There was a little difference in fugacities between vapor- (4) and droplet-supplying air compartment (5) although the ratio of allethrin supplied from the electric vaporizer was 2 for (4)- to 98 for (5)-compartment. An increase of fugacity in the breathing air (6) was caused by the air exchange (equation 4-6). These changes in the air compartments (j = 5, 6) elevated fugacities in floor (7), wall (8) and ceiling (k = 10, 11) (equation 4-7, 4-8, 4-10 and 4-11).

Temporal variations of amounts of allethrin in concerned compartments are shown in figure 4-6 and 4-7. A fairly large decrease of allethrin in droplet compartments (i = 1, 2, 3) was observed until t_z (figure 4-6). The ceiling intermittently increased in amounts of allethrin by every droplet-absorption from t_ℓ after emission of allethrin to turning off the electric evaporator. Amounts of allethrin in the airs (j = 4, 5, 6) decreased after cease of emission (6 hours) due to the air exchange, transference and the photo-degradation and oxidation (figure 4-7). In spite of photo-degradation and oxidation, amounts of allethrin in floor (7), wall (8) and ceiling (k = 10, 11) slightly increased even after cease of emission from the electric vaporizer. This is because the air

compartments (j = 4, 5, 6) transferred allethrin to the floor (7), wall (8) and ceiling (k = 10, 11) since the fugacities in the air compartments were larger than those in the concerned compartments.

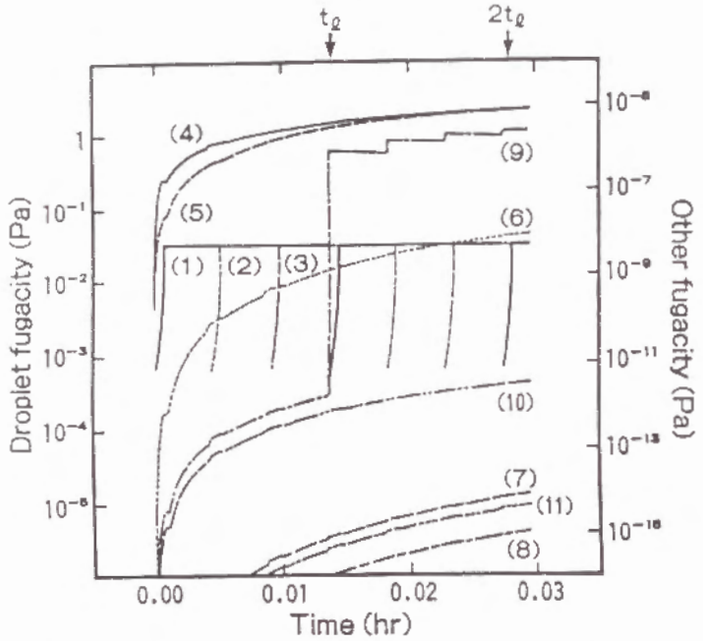

Figure 4–5. Time–dependent changes of fugacities in concerned compartments. Droplets (i=1,2,3), airs (j=4,5,6), floor (7), wall (8) and ceilings (k=9,10,11)

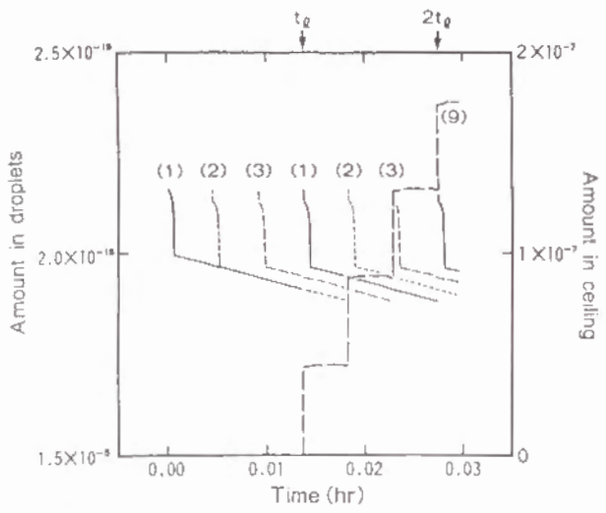

Figure 4–6. Time–dependent changes of pesticide amounts in droplet compartments (i=1,2,3) and ceiling (9).

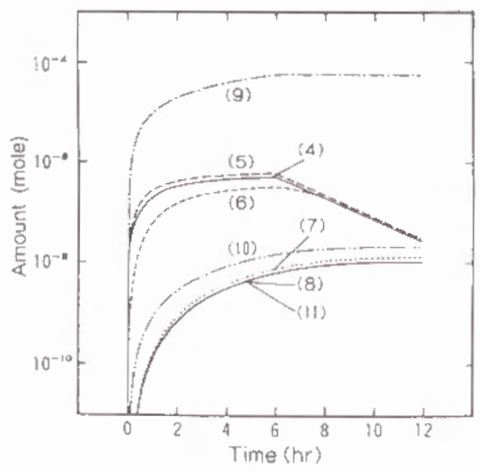

Figure 4–7. Time–dependent changes of pesticide amounts in airs (j=4,5,6), floor (7), wall (8) and ceilings (k=9,10,11).

[2] Sensitivity Analysis

The VAPOR–MOM model enabled to simulate the pesticide behavior supplied with the electric vaporizer in a room under various conditions. Here, as a sensitivity analysis the pesticide behavior was examined by varying important parameters.

Influence of Air Exchange Rate

When all windows of the room were closed, air exchange rate was 0.58 time h^{-1}. The air exchange rate is directly connected with the transfer parameter between the droplets and air compartment, D_{i5}, according to equation 4–2 and the fluid velocity determining air mass among air compartments (equation 4–4, 4–5 and 4–6). Figure 4–8 shows time–dependent changes of pesticide amounts in concerned compartments at air exchange rates of factors 0.1, 1 and 10 (0.058, 0.58 and 5.8 time h^{-1}). Although the transfer rate from the droplets to air compartment (D_{i5}) is proportional to the air exchange rate (equation 4–2), the air concentration for 5.8 time h^{-1} is much lower than that for 0.58 time h^{-1} due to outflow of the pesticide to outdoor and decreases rapidly after cease of emission from the electric vaporizer. The concentration for 0.058 time h^{-1} is higher than 0.58 time h^{-1}. These changes in the air concentration affect the amount in the floor although that on the ceilings is fixed.

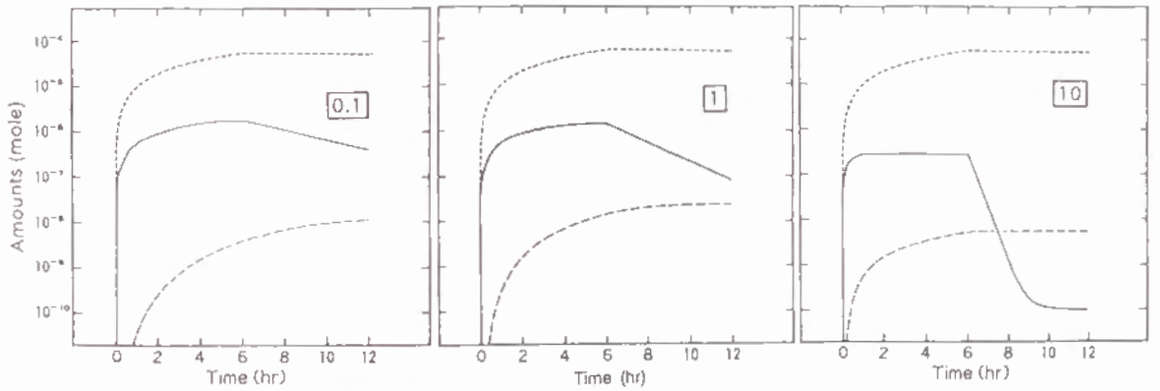

Figure 4–8. Simulation for a sensitivity estimate of the air exchange rate (0.58 h^{-1} × factor 0.1, 1 or 10). ————: Sum of airs (j = 4, 5 and 6), – – – – –: Sum of floor and wall, ·····: Sum of ceilings (k = 9, 10 and 11)

Influence of Photo–degradation and Oxidation Rate

Pyrethroids used in vaporizer liquid formulations are known to be photo–degraded and oxidized rapidly. In the simulation, however, the half–life times of degradation in floor, wall and ceiling are considered to be rather longer because coated wooden floor and wall paper usually contain some antioxidants. The degradation rate, off course, should be changed owing to the kinds of pyrethroids and materials, e.g. carpet, non–coated wood or painted concrete for the floor and/or

wall. Figure 4–9 shows the temporal amounts of the pesticide in concerned compartments for the degradation rates of factors 0.1, 1 and 10. Small differences of the pesticide in the ceiling compartments (k = 9, 10 and 11) are observed by factors of 0.1 and 10, but there is especially a remarkable decrease of the pesticide in the air compartments (j = 4, 5 and 6) if the rate is tenfold.

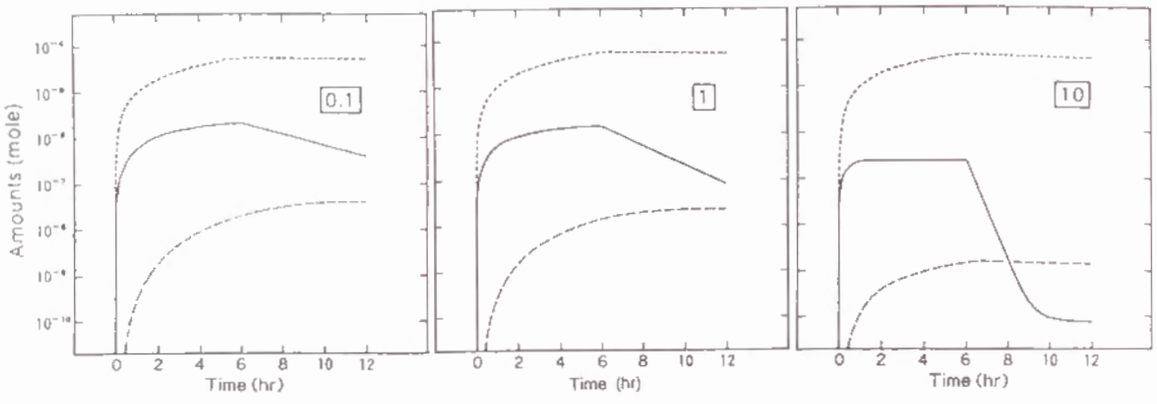

Figure 4–9. Simulation for a sensitivity estimate of the degradation rate (standard × factor 0.1, 1 or 10). ————: Sum of airs (j = 4, 5 and 6), - - - - - - -: Sum of floor and wall, ·····: Sum of ceilings (k = 9, 10 and 11)

Influence of Transfer Rate

The transfer parameter D_{jk} (j=5,6 and k=7,8,9,10,11) is based on a half–life time (τ_{jk}) of transference between the air (j) and the floor, wall and ceiling (k). Simulation for a sensitivity estimate of the half–life time by factors 0.1, 1 and 10 is shown in figure 4–10. If τ_{jk} is 10 times of the standard, a larger amount of the pesticide remains in the floor and wall and the aerial concentration slightly decreases.

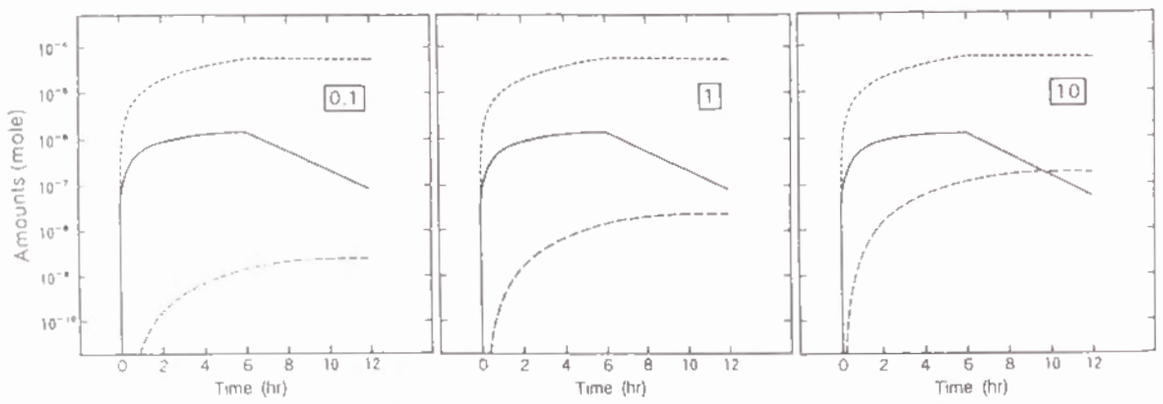

Figure 4–10. Simulation for a sensitivity estimate of the half–life time of transference (standard × factor 0.1, 1 or 10). ————: Sum of airs (j = 4, 5 and 6) - - - - - - -: Sum of floor and wall, ·····: Sum of ceilings (k = 9, 10 and 11)

Influence of Vapor Pressure

The sensitivity of solid vapor pressure (P) is analyzed by using factors of 0.1 and 10 to the vapor pressure of allethrin. The results in figure 4–11 show the clear–cut differences in amounts of the pesticide in air, floor and wall compartments in proportional to the P value, but there is small decrease of the pesticide in ceiling compartments even if the rate is tenfold.

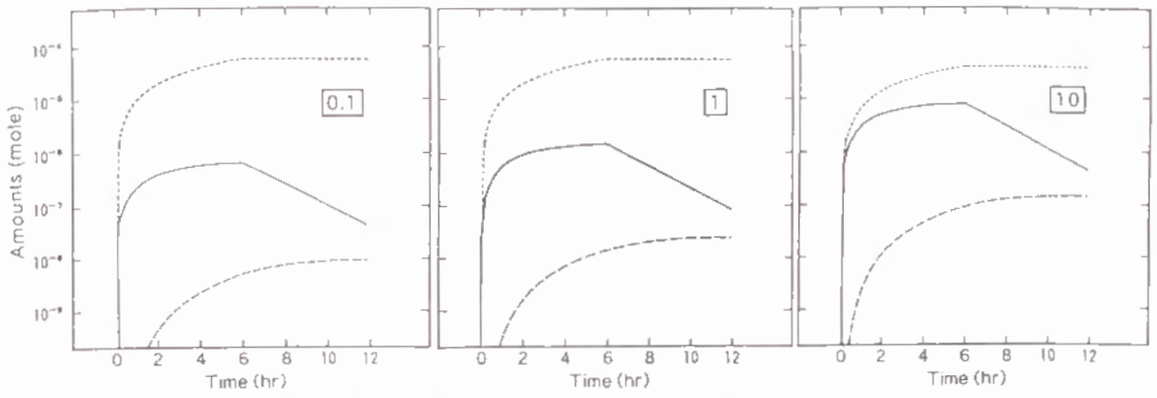

Figure 4–11. Simulation for a sensitivity estimate of the vapor pressure (standard × factor 0.1, 1 or 10). ————: Sum of airs (j = 4, 5 and 6) - - - - - - -: Sum of floor and wall, ·····: Sum of ceilings (k = 9, 10 and 11)

Influence of Other Physicochemical Properties of the Pesticide

Octanol/water partition coefficient (K_{ow}) and water solubility (C) are examined for 0.1 and 10 times the magnitude of allethrin. Both parameters directly influence fugacity capacities of the floor, wall and ceiling, but there are little differences in amounts of the pesticide in the concerned compartments by factors of both 0.1 and 10.

Conclusion

A new Fugacity model VAPOR–MOM was established for an electric vaporizer delivery system in a room. The model incorporating the fluid and droplet dynamics and the transference and degradation processes well simulated an unsteady state behavior of pesticide in air, floor, wall and ceiling inside a room supplied by the electric vaporizer under various conditions. In sensitivity analysis, it was turned out that both air exchange rate and degradation rate influence remarkably the air concentration of pesticide.

In a simulation experiment, the model enabled to describe time-dependent concentrations of the aerial pesticide in good accordance with measured ones.

Chapter 5.

BROADCAST SPRAYING MODEL (CARPET-MOM)

Introduction

A broadcast pesticide emulsion based on water or oil is conventionally sprayed on the surface area of a floor or carpet within the room, where the pests habitat. From the viewpoint of safety assessment, amounts of pesticide in air and on floor become particularly important in this procedure. To describe accurately the pesticide behavior in the procedure, it seems more sophisticated to use a Fugacity model by incorporating droplet dynamics [15], fluid dynamics [19] and evaporating phenomenon of the emulsion from the carpet.

Thus, in this chapter, a new room carpet application model (CARPET-MOM) was developed along this line.

Theoretical

When a broadcast pesticide emulsion based on water is sprayed on the floor, some portion sticks on the floor and the other flies as flying droplets in air. Simulating environment thus has six kinds of compartments appearing on the application. These compartments are water pool (1), flying droplets (i = 2 and 3 for a large and small-diameter particle), air (4), floor (k = 5), wall (k = 6) and ceiling (k = 7) as illustrated in figure 5-1. Each compartment is treated theoretically as follows:

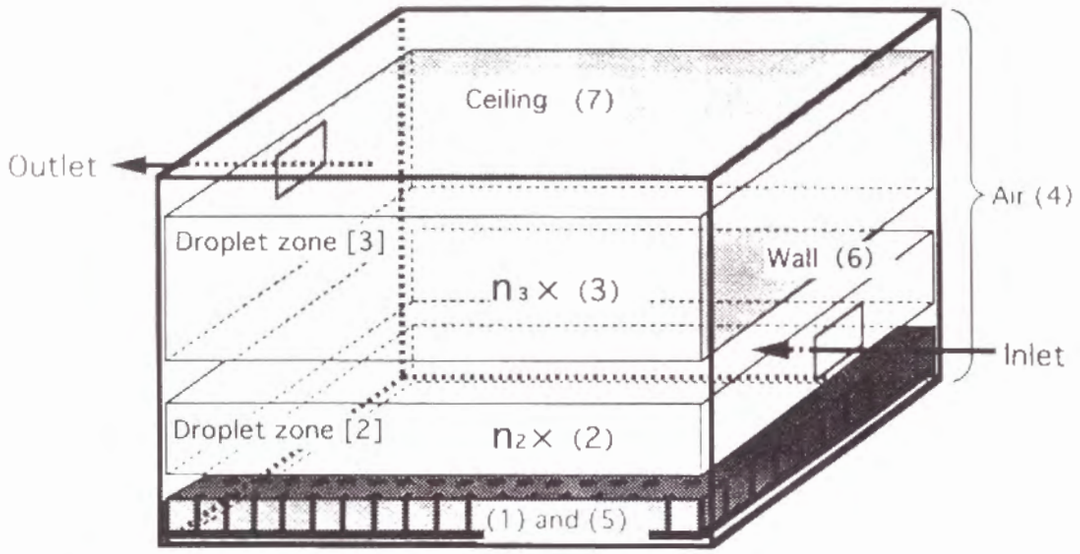

Figure 5-1. Simulation scenario with the room and compartments. Water pool (1), flying droplets (2 and 3), air (4), floor (5), wall (6) and ceiling compartment (7).

[1] Water Pool Compartment (1)

Volume (V_1)

A floor is covered with a carpet. The carpet is made of a polymer textile which has air capillaries and a bottom space. When a broadcast emulsion is sprayed on the carpet, the emulsion fills the air capillaries and the surplus pools in the bottom space. Thus the water pool compartment (1) forms among and under the textile. The polymer textile is the floor compartment (5).

The water pool compartment consists of a large amount of water as a diluent, small amount of organic solvent as an emulsifiable aid and pesticide. The emulsion decreases in volume by evaporation or drying and finally disappears. The drying rate of emulsion is almost as the same as that of water. When the temperature of the compartment is constant (T_w), the drying rate (R_d) per m^2 of the floor follows the Lewis relation [20]:

$$R_d = A_1 \, h \, (\, H_w - H \,) \, / \, C_H$$

where A_1 is a ratio of air-faced surface area of the capillaries to that of the floor, H_w humidity at T_w, H humidity at room temperature. The humid heat (C_H) reads:

$$C_H = 0.24 + 0.46 \, H$$

When a natural convection transfers heat under a small difference in temperatures of the water pool (T_w) and indoor air (T), the film coefficient of heat transfer (h) is as follows by neglecting radiation [21]:

$$h = 3.06 \times 10^{-4} \, (\, T - T_w \,)^{1/3}$$

Although the volume decreases with time, the surface area ratio (A_1) of the water pool compartment to the floor keeps a constant. When water completely evaporates, the water compartment (1) disappears and the remaining pesticide transfers to the floor compartment (5).

Fugacity Capacity (Z_1)

In the water pool compartment, pesticide resides in the organic solvent layer of emulsion. Thus, initial fugacity capacity (Z_1) of the compartment is K_{ow} C / P, where K_{ow} is octanol/water partition coefficient, C water solubility and P solid (conventional) vapor pressure of pesticide. Once the organic solvent begins to evaporate, the Z_1 gradually nears a fugacity capacity of water (C / P). Therefore, the Z_1 is assumed to change with evaporation of the solvent:

$$Z_1 = (\, e^{-at} \, K_{ow} + 1 - e^{-at} \,) \, C \, / \, P$$

where a is a constant for the solvent and t time after application.

Connection with flying droplets (i = 2, 3)

The flying droplets are classified and assigned as a large (i = 2) and small-diameter particle compartment (i = 3).

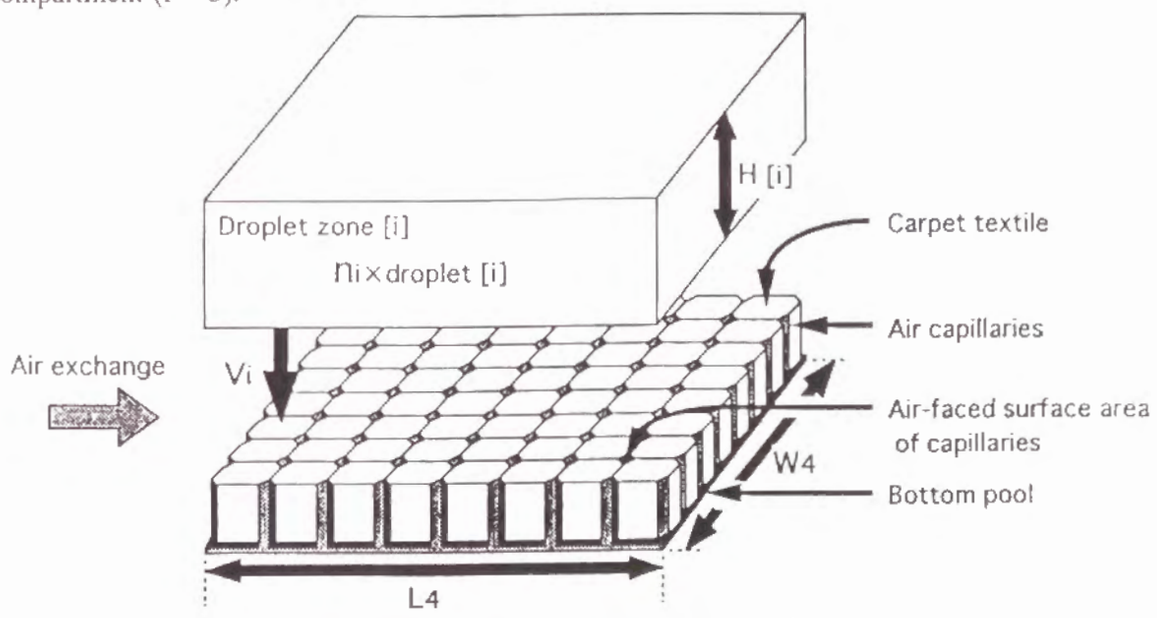

Figure 5-2. Simulation scenario with the floor and droplet compartments.

Number n_i of flying droplets (i = 2, 3) exists in each droplet zone ([i] = 2, 3) with a thickness ($H_{[i]}$). The droplet zone falls down to the floor according to a terminal settling velocity v_i. Atmosphere in the sprayed room faces the surface area (A_1) of water pool compartment and that (A_5) of carpet textile. After the bottom of zone [i] touches both the water pool (1) and floor compartment (5), pesticide in the flying droplets (i = 2, 3) transfers to both compartments. The increasing rate of pesticide in the compartment (1) is $n_i\ v_i\ A_1\ /\ H_{[i]}$ and that in the floor compartment is $n_i\ v_i\ A_5\ /\ H_{[i]}$.

Transference with air (4) and floor (5)

Pesticide in the water pool (1) transfers with air (4) and floor compartment (5). Diffusive transfer rate of pesticide between the water pool (1) and air compartment (4) can be written as:

$$\frac{d f_1}{d t} V_1 Z_1 = - D_{1,4} (f_1 - f_4)$$

where f_1 and f_4 are fugacities in the compartments (1 and 4), the $D_{1,4}$ a transfer parameter estimated by:

$$D_{1,4} = \frac{1}{1 / (k_1 A_1 L_4 W_4 Z_1) + 1 / (k_4 A_1 L_4 W_4 Z_4)}$$

where Z_4 is fugacity capacity of the air compartment (4) and k_1 and k_4 are pesticide velocities in the water pool (1) and air compartment (4), respectively. The velocity k_4 is G L_4 where G is air exchange rate and L_4 room length along the velocity vector. The pesticide velocities on the water surface (k_1) reads k_4 / 100 [15].

Transfer parameter $D_{1,5}$ between the water pool (1) and floor compartment (5) is:

$$D_{1,5} = \frac{1}{1 / (k_1 A_{15} L_4 W_4 Z_1) + 1 / (k_5 A_{15} L_4 W_4 Z_5)}$$

where Z_5 is fugacity capacity of the floor compartment (5) and A_{15} L_4 W_4 a contacting area between the air capillaries and carpet textile. Since pesticide penetrates into the carpet textile, depth of the floor compartment (5) is time-dependent as expressed by 2 $(D_k\ t)^{0.5}$ where D_k is pesticide diffusion constant in the floor [3]. Thus, the velocity of pesticide in the floor (k_5) reads $(D_k / t)^{0.5}$.

Photo-degradation and Oxidation

Major reactions in the water pool compartment (1) are photo-degradation and oxidation described by a combined first-order rate constant K_1. The reaction rate reads K_1 V_1 Z_1 where K_1 is 0.693 τ_1^{-1} and τ_1 is a half-life time of photo-degradation and oxidation.

Differential Equation for Water Pool Compartment (1)

Every time a flying droplet falls down to the water pool compartment, the compartment accepts pesticide in the droplet. The volume of the water pool compartment (V_1) is becoming smaller with time until the water completely evaporate. While the organic solvent in the compartment evaporates, the fugacity capacity (Z_1) decreases toward the water capacity (C/P). The pesticide in the water pool (1) transfers with the air (4) and floor compartment (5) and degrades by oxidation and photolysis. Thus, the unsteady state behavior of pesticide in the water pool compartment (1) is:

$$\frac{d f_1}{d t} V_1 Z_1 = \sum_{i=2}^{3} n_i v_i A_1 V_i Z_i f_i / H_{[i]} + R_d L_4 W_4 Z_1 f_1 - \sum_{k=4}^{5} D_{1,k} (f_1 - f_k) - K_1 V_1 Z_1 f_1$$

[2] Flying Droplet Compartment (i = 2, 3)

The droplet zone [2] accommodating large droplets (i = 2) initially forms in the lower space of the room. That [3] for small droplets (i = 3) does in the higher one.

Volume (V_i)

A dominant solvent (water) of the droplets will evaporate and the compartments (i = 2, 3) become smaller in volume with time. Until water completely evaporates, the volume decreases as follows [15].

$$\frac{d V_i}{d t} = - \frac{\pi}{2} \alpha d_i$$

where d_i is a time dependent diameter and α diameter coefficient expressed by the following equation:

$$\alpha = \frac{4 D_{air} M}{R \rho_d} \left(\frac{P_w}{T_w} - \frac{P_\infty}{T_\infty} \right)$$

where D_{air} is a diffusion coefficient of water in air, M the molecular weight, ρ_d the droplet density, T_w the droplet surface temperature and R the gas constant. P_d and T_d are a partial pressure and temperature on the droplet surface. P_∞ and T_∞ are a partial pressure and temperature well away from the droplets and T_∞ is virtually equivalent to room temperature (T).

Velocity (v_i)

Gravity and air resistance to particle motion decide a perpendicular motion of the droplet compartment. The velocity of the compartment (i) almost instantaneously comes to a constant that is the terminal settling velocity (v_i) given by Stokes law:

$$v_i = \frac{\rho\ g}{18\ \eta}\ S\ d_i^2 = \beta\ S\ (\ d_{0i}^2 - 2\ \alpha\ t\ )$$

where g is gravity acceleration, η air viscosity, β velocity coefficient and d_{0i} is initial diameter. S is slip correction factor derived from Cunningham correction factor [3]:

$$S = 1 + \frac{2}{7.6\times10^7\ d_i}\ [\ 6.32 + 2.01\ \exp\ (\ -8.322\times10^6\ d_i\ )\ ]$$

After water completely evaporates, each droplet becomes a terminal settling droplet of a constant diameter, which only contains pesticide.

Number of Flying Droplet Compartment (n_i)

At time 0, each droplet zone ([i] = 2, 3) forms a space with a thickness ($H_{[i]}$), width (W_4) and length (L_4) at a certain height from the floor. The droplet zone begins to fall down according to the perpendicular velocity of droplets (v_i). The bottom of the zone ([i] = 2, 3) then touches the water pool and/or floor compartment. The n_i begins to reduce at a rate of $n_i\ v_i\ /\ H_{[i]}$ on assuming the droplets spread uniformly in the zone.

Some number of droplets also disappears through the windows by air exchange. Small particles (i = 3) with negligible inertia will follow the indoor flow lines perfectly. Large particles (i = 2) may continue to move in a straight line to the floor despite the indoor flow. However, since the large particles (i = 2) decrease in volume and become small in diameter, this compartment (i = 2) is also assumed to follow the velocity of indoor flow.

The following equation shows the decreasing rate of the compartments caused by adsorption to the water pool and/or floor compartment and air exchange. Before the zone ([i] = 2, 3) reaches the floor, the droplet number (n_i) decreases only by air exchange.

$$\frac{d\ n_i}{d\ t} = -\frac{n_i}{H_{[i]}}\ v_i - \frac{n_i}{L_4}\ k_4$$

Fugacity Capacity (Z_i)

The flying droplet compartment (i = 2, 3) has fugacity capacity (Z_i) of 6×10^6 / (P R T_d) according to chapter 2 [15].

Transference

Transfer parameter between the flying droplets (i = 2, 3) and air compartment (4) can be written as:

$$D_{i,4} = \frac{1}{1\ /\ (\ k_i\ A_i\ Z_i\ )\ +\ 1\ /\ (\ v_i\ A_i\ Z_4\ )}$$

where A_i is surface area of each flying droplet ($\pi\ d_i^2$). Pesticide velocity from air (4) to the droplets (i = 2, 3) is equivalent to the terminal settling velocity (v_i) of the droplet since the horizonal movement of the droplets follows the air flow. The pesticide velocity on the droplet surface (k_i) reads v_i / 100 [15].

Differential Equation for Flying Droplet Compartment (i = 2, 3)

On a Level IV fugacity model, an unsteady state behavior of pesticide in the flying droplet compartment (i) is:

$$\frac{d\ f_i}{d\ t}\ V_i\ Z_i = \frac{\pi}{2}\ \alpha\ d_i\ Z_i\ f_i - D_{i,4}\ (\ f_i - f_4\ ) - K_i\ V_i\ Z_i\ f_i$$

The flying droplet compartment decreases in volume with time, while the fugacity increases. The pesticide in the droplet transfers with the air compartment (4). The transference is time-dependent on the surface area and velocity changes of flying droplets. The pesticide in the compartment (i) is also photo-degraded and oxidized. Every time the water pool and/or floor adsorb a droplet, the droplet loses fugacity (f_i) and the water pool (1) and/or floor (5) compartment gain the pesticide.

[3] Air Compartment (4)

Volume (V_4) and Fugacity Capacity (Z_4)

The volume of the air compartment, V_4, is equal to that of the room supplied with pesticide. An air fugacity capacity, Z_4, is 1 / (R T).

Air Exchange

Air exchange expels some pesticide in the air compartment (4) out of the environment at a rate of G V_4 Z_4 f_4.

Transference

Transference between the flying droplet (i = 2, 3) and air compartment (4) is proportional to the droplet number (n_i). The n_i varies due to adsorption to the water pool and/or floor compartment and air exchange. The pesticide in the air compartment (4), on the other hand, transfers with the

water pool (1), floor (5), wall (6) and ceiling (7). The air transfer parameter $D_{4,j}$ with the floor (k = 5), wall (k = 6) or ceiling compartment (k = 7) is:

$$D_{4,k} = \frac{1}{1 / (k_4 A_k Z_4) + 1 / (k_k A_k Z_k)}$$

where A_k is surface area of the wall (k = 6) and ceiling compartment (k = 7). The surface area of floor is $A_5 L_4 W_4$. The pesticide velocity k_k in compartment j is $(D_k / t)^{0.5}$ as described in [1].

Differential Equation for Air Compartment (4)

Air flux in the air compartment (4) is caused by air exchange and transference with the water pool (1), flying droplets (i = 2, 3), floor (5), wall (6) and ceiling (7) as well as photo-degradation and oxidation. Thus, the unsteady state behavior of pesticide in the air compartment (4) is:

$$\frac{d f_4}{d t} V_4 Z_4 = - G V_4 Z_4 f_4 - D_{1,4} (f_4 - f_1) - \sum_{i=2}^{3} n_i D_{i,4} (f_4 - f_i) - \sum_{k=5}^{7} D_{4,k} (f_4 - f_k) - K_4 V_4 Z_4 f_4$$

[4] Floor, Wall and Ceiling Compartment (k = 5, 6, 7)

Volume (V_k)

The floor compartment is a polymer textile. Since pesticide penetrates into the polymer textile at a depth of 2 $(D_k t)^{0.5}$, a product of the depth and pesticide-faced surface area (A_{a5}) affords the volume of the floor (V_5). Until pesticide in the floor compartment (5) reaches an ultimate diffusion depth, the rate of volume change is:

$$\frac{d V_5}{d t} = \sqrt{D_k / t}\ A_{a5}$$

The volume of wall (6) and ceiling compartment (7) is similarly 2 $(D_k t)^{0.5} A_k$ (j = 6, 7).

Fugacity Capacity (Z_k)

The floor compartment is the carpet textile. Wall paper covers the wall and ceiling. The carpet textile and wall paper consist of a polymer. Thus, Z_k value (k = 5, 6, 7) can be calculated as K_{ow} C / P.

Differential Equation for Floor Compartment (5)

The following differential equation describes the unsteady state behavior of pesticide in the floor. The equation incorporates fortification of pesticide from the droplet zones and changing volume (V_5). The pesticide movement in the floor compartment (5) originates in transference with the water pool (1) and air compartment (4), photo-degradation and oxidation.

$$\frac{d f_5}{d t} V_5 Z_5 = \sum_{i=2}^{3} n_i v_i A_5 V_i Z_i f_i / H_{[i]} - \sqrt{D_k / t}\ A_{a5} Z_5 f_5 - D_{1,5} (f_5 - f_1) - D_{4,5} (f_5 - f_4) - K_5 V_5 Z_5 f_5$$

Differential Equation for Wall and Ceiling Compartment (k = 6, 7)

A differential equation for the wall (k = 6) and ceiling compartments (k = 7) includes the transference ($D_{4,k}$), photo-degradation and oxidation as well as the influence from time-dependent volume.

$$\frac{d f_k}{d t} V_k Z_k = - \sqrt{D_k / t}\ A_k Z_k f_k - D_{4,k} (f_k - f_4) - K_k V_k Z_k f_k$$

Computer Programming and Data Processing

A computer program, CARPET-MOM, was developed by using BASIC. IBM PS/2 was employed for the programming and calculation.

The program incorporated basic physicochemical data, photo-degradation and oxidation rate, supplying quantity of the chemical and room conditions. By running, performed were calculation of time-dependent fugacity capacity, volumes, velocities, and transfer parameters, resolution of unsteady state equations, and graphing of resulting pesticide behaviors in each compartment versus time.

[1] Simulation of an Experiment

[Outline of the Experiment]

An emulsifiable concentrate was diluted with water to prepare 0.5% of chlorpyrifos emulsion and applied to a typical American apartment room. Chlorpyrifos as pesticide controls a wide range of household pests. The treatment rate was one gallon per 1,600 ft^2 following the label. A pressure regulator promoted an uniform application. The room lacked furniture during application and

testing. A period of two hours was allowed for drying by opening windows and then all windows were kept closed.

A temporal variation of concentration of chlorpyrifos in air and amount on floor was measured [18]. Immediately after the application, about 60% of the treated chlorpyrifos existed on the floor and about 0.006% was estimated to be in air by sucking air method.

[Simulating the Experiment]

A simulated room has carpet (4.6 m × 3.2 m) and wall paper (room height, 3 m). The room temperature and humidity are 298 K (T) and 1.19×10^{-2} kg-H_2O / kg-dry air (H) equivalent to 60% relative humidity. An air exchange rate of the room (G) is 5 time h^{-1} during the drying time and 0.5 time h^{-1} after all windows are closed.

When 0.5% emulsion of chlorpyrifos is applied to the floor at the rate of 25.4 ml m^{-2}, 60% of the emulsion forms a water pool compartment and 40% flies as the flying droplets. Only small droplets with less than 1 μm diameter in air were collected in the experiment and its amount was 0.006% of the treated chlorpyrifos. Thus, this figure is used for the small droplets (i = 3) and the rest (almost 40%) is for the large droplets (i = 2).

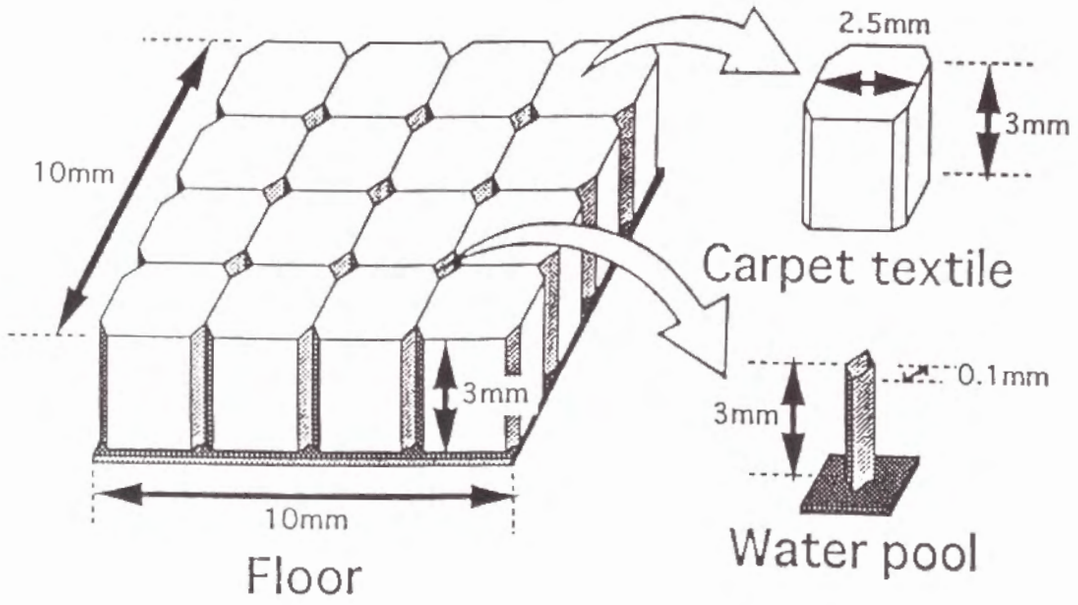

Figure 5-3. Simulation scenario with sizes of the water pool and floor compartment.

Water Pool Compartment (1)

The treated floor is a textile carpet and has air capillaries. The sprayed emulsion fills the air capillaries and the surplus forms a thin pool under the textile (figure 5-3). Thus, the sum of cross sectional or air-faced area (A_1) of air capillaries is 1.6×10^{-3} m^2 per m^2 of the floor and the rest is that of floor compartment (A_5). The contacting surface area (A_{15}) between the water pool (1) and floor compartment (5) is 0.192 m^2 per m^2 of the floor. Since the floor compartment accepts chlorpyrifos from the water pool and droplet compartments, the area (A_{a5}) connecting with chlorpyrifos is 1.19 m^2 per m^2 of the floor.

When heat transfer between the air and water pool compartment gets in a dynamic equilibrium, surface temperature (T_d) of water pool compartment is equal to a wet-bulb temperature (T_w : 292.5 K) of the room. According to humidity chart, humidity H_w at T_w is 1.50×10^{-2} kg-H_2O / kg-dry air. Film coefficient of heat transfer (h) is 5.40×10^{-4} kcal s^{-1} m^{-2} K^{-1} at T_w and T. Humid heat (C_H) at H is 0.245 kcal (K kg-dry air)$^{-1}$. Thus, constant rate of drying (R_d) of the broadcast emulsion is calculated to be 1.09×10^{-8} kg-H_2O s^{-1} per m^2 of the floor.

The broadcast emulsion (25.4 × 0.6 ml per m^2 of the floor) has 0.5% of chlorpyrifos as pesticide and 8.26×10^{-2} g of xylene as organic solvent. Since evaporation rates of xylene and water are in a ratio of 0.56 g to 0.44 g [16], the R_d of xylene reads 6.10×10^{-9} kg-xylene s^{-1} m^{-2}. Thus, 99% of the xylene evaporates at 3.72 hr after the application.

The fugacity capacity (Z_1) is K_{ow} C / P at 0 hr, but reaches (0.01 K_{ow} + 0.99) C / P at 3.72 hr after the application. Therefore, the Z_1 can be expressed as follows:

$$Z_1 = (e^{-1.24\,t} K_{ow} + 1 - e^{-1.24\,t}) C / P$$

Flying Droplet Compartment (i = 2, 3)

The large droplet zone ([i] = 2) for large droplets (i = 2) forms a 2 m thick space ($H_{[2]}$) on the floor. The small zone ([i] = 3) does a 1 m thick space ($H_{[3]}$) on the zone [2] to the ceiling. These zone lengths and widths are the same as the room length and width (L_4 and W_4).

Immediately after a broadcast spraying to a floor, an average diameter of flying droplets near the floor is 10 μm when measured by a phase doppler particle analyzer (Aerometrics Inc., U.S.A.). Therefore, the size of flying large droplets (d_{02}) is adopted to be 10 μm. That of small droplets (d_{03}) is assumed to be 1 μm that is conventionally quantified by sucking air.

The treated rate and the floor area decide a total necessary volume (374 ml) of chlorpyrifos emulsion. Since allotment for the droplet compartments is 40% (i = 2) and 0.006% (i = 3), each

volume of the compartments is 150 ml for i = 2 and 2.24×10^{-2} ml for i = 3. Each volume divided by a droplet volume ($\pi\ d_{0i}^3\ /\ 6$) gives the number of the droplets. Thus, n_2 and n_3 immediately after the application read 2.87×10^{11} and 4.28×10^{10}, respectively.

The component of the flying droplets is assumed to be 100% water. The diffusion coefficient of water (D_{air}) is 2.4×10^{-5} m^2 s^{-1} at T_d [3]. The partial vapor pressure on droplet surface (P_d) at T_d reads 2.26×10^3 Pa according to the following equation [3]:

$$\log_{10} P = 10.23 - \frac{1750}{T - 38}$$

The partial pressure of water vapor well away from the droplets (P_∞) is calculated to be 1.90×10^3 Pa by the above equation (3.16×10^3 Pa at T_∞) and room humidity (60% relative humidity). Thus, the diameter coefficient (α) is 2.81×10^{-10} m^2 s^{-1} as the droplet density (ρ_d) is 1.0×10^6 g m^{-3}. The velocity coefficient (β) becomes 2.94×10^7 m^{-1} s^{-1} as air viscosity (η) at 298 K [3] is 1.85×10^{-2} g m^{-1} s^{-1}.

Compartment k (k = 5, 6, 7)

The diffusion constant (D_k) in poly(vinyl chloride) is 2.67×10^{-15} m^2 s^{-1} for methyl red and 5.25×10^{-15} m^2 s^{-1} for methyl palmitate [6]. Wike and Lee and Lydersen-Forman-Thodos methods [22] give diffusion coefficient (D_{air}) in air of 4.27×10^{-6} m^2 s^{-1} for methyl red and 4.54×10^{-6} m^2 s^{-1} for methyl palmitate. Since the $D_k\ /\ D_{air}$ ratio is almost 10^9, the D_k of chlorpyrifos in floor, wall and ceiling becomes 4.52×10^{-15} m^2 s^{-1} based on D_{air} value (4.52×10^{-6} m^2 s^{-1}) of chlorpyrifos estimated by Wike and Lee method.

Ultimate diffusion depth for the floor is to be 1.25 mm due to the width (2.5 mm) of the carpet textile and 136 μm for the wall and ceiling [15].

Chemical Data

Half-life time (τ) of photo-degradation and oxidation of chlorpyrifos in each compartment is 52.45 hr based on an experiment where chlorpyrifos on a thin film was exposed to a 300 Nm lamp [23]. Data of chlorpyrifos required for the simulation are summarized in table 5-1.

[2] Sensitivity Analysis

All important parameters constituting the differential equations are varied to test the sensitivity of the equations to the parameters.

Table 5-1. Primary Input Data

Physicochemical properties	Chlorpyrifos
Molecular weight	350.62 g mole^{-1}
Solid vapor pressure (P)	6.7×10^{-3} Pa
Water solubility (C)	1.1×10^{-3} mole m^{-3}
Octanol/water partition coefficient (K_{ow})	$10^{5.1}$
Half-life time of photo-degradation and oxidation (τ)	1.89×10^5 s
Diffusion constant in a polymer (D_k)	4.52×10^{-15} m^2 s^{-1}

Results and Discussion

[1] Simulation of the Experiment

The CARPET-MOM model was run to simulate an unsteady state behavior of chlorpyrifos in air, floor, wall and ceiling. The results show that the predicted time-dependent concentration in air and amount on floor entirely agreed with the measured ones (figure 5-4 and 5). In the model, chlorpyrifos in air was designed to exist in the droplets (i = 2, 3) and air compartment (4) and chlorpyrifos on floor was in the water pool (1) and floor compartment (5). Aerial concentration of chlorpyrifos estimated by the sucking air method seems to be equivalent to a sequence of the total amount of chlorpyrifos in the small-sized flying droplets (3) and air compartment (4) divided by room volume (V_4). Measured amounts on floor should be also equivalent to a sequence of the total amount of chlorpyrifos in the water pool (1) and floor compartment (5) divided by the floor area ($L_4\ W_4$).

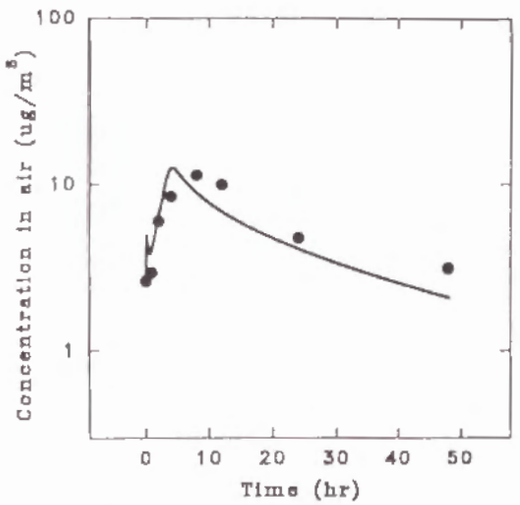

Figure 5-4. Aerial concentrations of chlorpyrifos as a function of time. Closed circles: experiment, Solid line: calculation

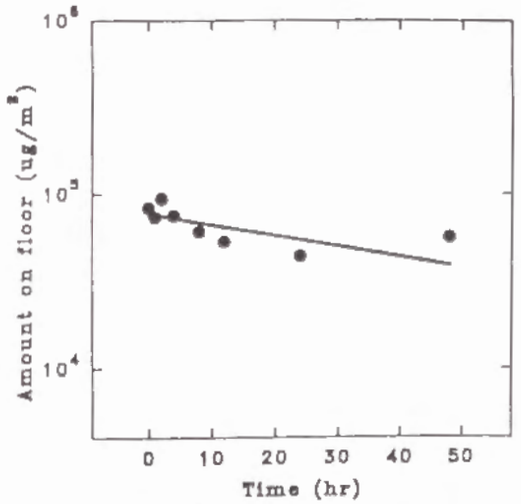

Figure 5-5. Chlorpyrifos amounts on floor as a function of time. Closed circles: experiment, Solid line: calculation

Volume (V_1) of the water pool compartment (1) decreased with time. Xylene in the compartment completely evaporated at 3.76 hr post application and the compartment disappeared at 387 hr. Diameter (d_i, i = 2, 3) of the flying droplet compartment (i) also decreased and reached an ultimate diameter. Initial diameter (d_{02}, 10 μm) of the large-sized droplets (2) reached 1.71 μm at 0.169 sec. Diameter (d_{03}, 1 μm) of the small-sized droplets (3) became 0.171 μm at 1.69×10^{-3} sec. Volume (V_k, k = 5, 6, 7) of the floor (5), wall (6) and ceiling compartment (7) increased with time due to penetration of chlorpyrifos into the polymer. Chlorpyrifos in each compartment (k = 5, 6, 7) reached to an ultimate depth of the floor (5), wall (6) and ceiling compartment (7) at 2.40×10^4, 284 and 284 hr, respectively.

Large-sized droplets (i = 2) initially settled at a velocity (v_2) of 10.8 m h^{-1} with 1.02 of Cunningham correction factor (S). When diameter of the droplets reached a constant, the v_2 became 0.340 m h^{-1} where the S was 1.10. Velocity (v_3) of the small-sized droplets (3) similarly changed from 0.124 m h^{-1} (S = 1.17) to 6.35×10^{-3} m h^{-1} (S = 2.05).

Number (n_2) of the large-sized droplets (2) decreased with time due to the air exchange and adsorption on the compartment 1 and/or 5 (figure 5-6). The n_3 of the small-sized droplets (3) similarly, but rather slowly decreased due to only the air exchange until its droplet zone [3] touched the compartment 1 and/or 5 at 315 hr. Decreasing rate of the n_3 is, however, almost as the same as that of n_2 under the higher air exchange rate (5 time h^{-1}) of the initial 2 hr. Thus, the air exchange affected the decreasing rate of n_i. The n_2 disappeared at 5.88 hr and the n_3 did at 473 hr.

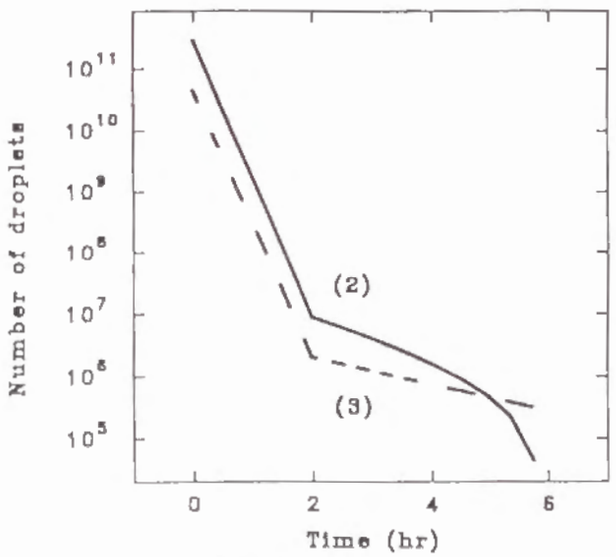

Figure 5-6. Numbers of droplet compartments as a function of time.
Large-sized droplets (2) and small-sized droplets (3)

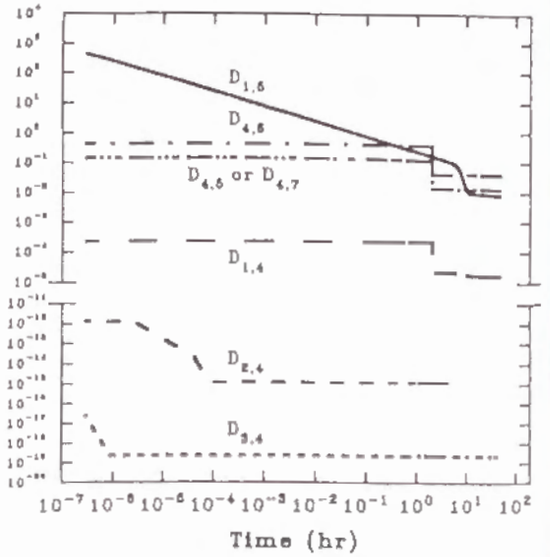

Figure 5-7. Transfer parameters as a function of time.
Transfer parameter ($D_{x,y}$) between compartment x and y.

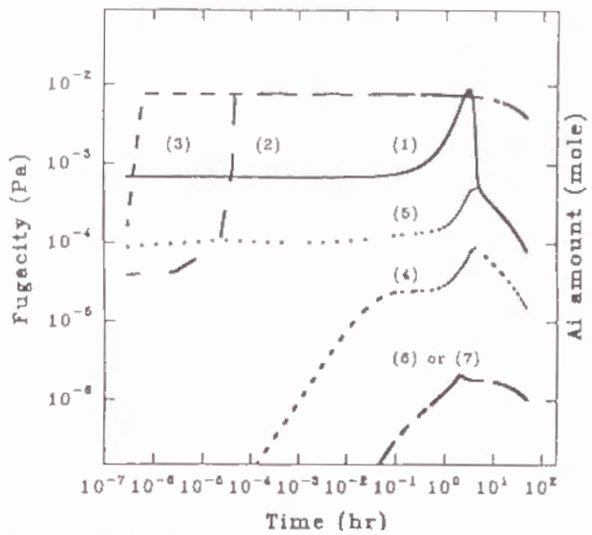

Figure 5-8. Fugacities of concerned compartment as a function of time.
Water (1), droplets (i = 2, 3), air (4), floor (5), wall (6) and ceiling (7).

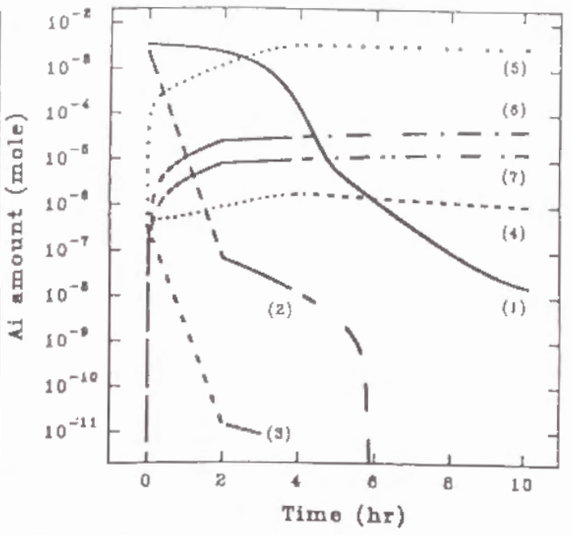

Figure 5-9. Amounts of chlorpyrifos in concerned compartments as a function of time.
Water (1), droplets (i = 2, 3), air (4), floor (5), wall (6) and ceiling (7).

Transfer parameter ($D_{1,4}$) between the water pool (1) and air compartment (4) as well as $D_{4,k}$ (k = 5, 6, 7) changed due to velocity (k_4) of chlorpyrifos in the air compartment (4) at 2 hr post application (figure 5-7). $D_{1,5}$ between the water pool (1) and floor compartment (5) decreased with time mainly affected by the time-dependent fugacity capacity (Z_1). $D_{i,4}$ (i = 2, 3) between the droplet (i) and air compartment (4) also decreased according to the diameter (d_i, i = 2, 3) of the droplets.

The CARPET-MOM model successfully described the temporal fugacities in concerned compartments as shown in figure 5-8. A fairly large change in the fugacities (f_i, i = 2, 3) of the large (2) and small-sized droplet compartment (3) was referred to the reduction of their diameters. Fugacity (f_1) of the water pool compartment (1) attained a maximum at 3.06 hr post application. Fugacities of the air (4) and floor compartment (5) similarly reached maximum points at 4.15 hr. Fugacities f_6 and f_7 initially increased, but slowly decreased after the turning point (2 hr) of the air exchange.

Amounts of chlorpyrifos in concerned compartments read a sequence of the fugacity multiplied by the fugacity capacity and volume (figure 5-9). According to the time-dependent fugacity capacity (Z_1) of the water pool compartment (1), amount of chlorpyrifos in the compartment transferred to the air (4) and in particular, to the floor compartment (5) and fairly rapidly decreased with time. Amounts of chlorpyrifos in the droplet compartments (i = 2, 3) were affected

by the air exchange rate and the amount of the droplets (2) was completely adsorbed on the compartment 1 and/or 5 at 5.88 hr. Amount of chlorpyrifos in the wall (6) and ceiling compartment (7) similarly attained turning points (2 hr) due to the change of air exchange rate. When a transferred amount of chlorpyrifos from the water pool compartment (1) became smaller, the amount in the floor compartment (5) neared a plateau. Time-dependent change in amount of the air compartment (4) followed that of floor compartment (5).

Transfer rate of chlorpyrifos through a contacting area of two concerned compartments was expressed as a sequence of transfer parameter multiplied with the difference in fugacities between the compartments and divided by their contacting area. Transferred chlorpyrifos from the water pool (1) and floor (5) to air compartment (4) peaked at 2 hr (figure 5-10). It then returned to a maximum point at 3.05 hr for the water (1) and 3.95 hr for the floor compartment (5). Chlorpyrifos in the air compartment (4), on the other hand, moved to the wall (6) and ceiling compartments (7). The transfer rate became a maximum at 2 hr and again returned to a higher point at 4.15 hr.

Aerial transfer rate from both the droplets (i = 2, 3) to air compartment (4) was expressed as a sequence of transfer parameter multiplied with the fugacity-difference and divided by the room volume (V_4) as shown in figure 5-11. Total chlorpyrifos in the large (2) and small-sized droplets (3) fairly largely transferred to air compartment (4) until the large droplets attained the ultimate diameter (0.169 sec). The transfer rate then changed around 2 hr when the air exchange rate varied and 5.88 hr when the droplets (2) completely disappeared.

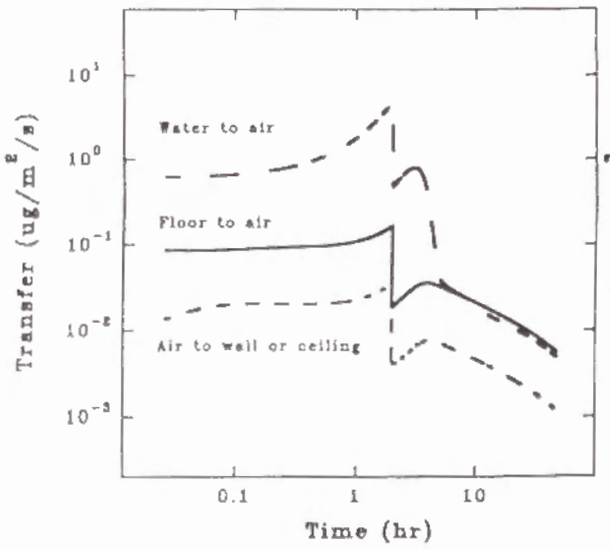

Figure 5-10. Transfer rate of chlorpyrifos per contacting area as a function of time.

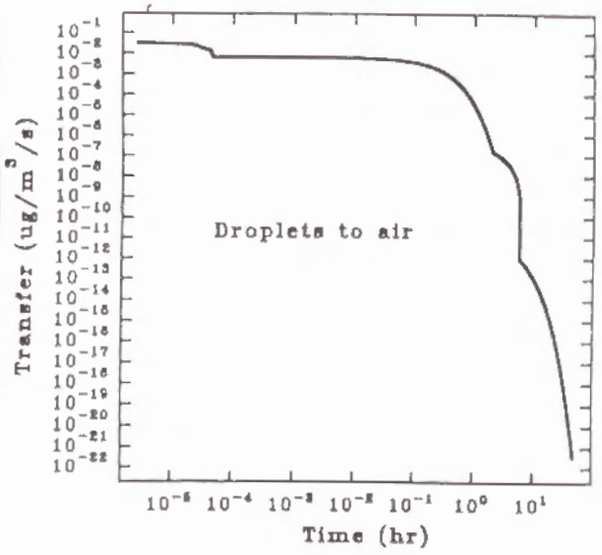

Figure 5-11. Aerial transfer rate of chlorpyrifos as a function of time.

[2] Sensitivity Analysis

The CARPET-MOM model enabled to simulate the pesticide behavior in broadcast spraying to a room carpet under various conditions. Here, as a sensitivity analysis the pesticide behavior was examined by varying important parameters with the pesticide as a reference or standard.

Influence of Air Exchange Rate

When all windows were opened, air exchange rate was 5 time h^{-1}. The rate under the closed conditions was usually 0.5 time h^{-1}. The air exchange rate directly affects the transfer parameters such as $D_{1,4}$, $D_{1,5}$ and $D_{4,j}$ (k = 5, 6, 7), decreasing rates of number (n_i) of the droplet compartments (i = 2, 3) and fluid velocity carrying air mass in the simulating environment. Figure 5-12 shows time-dependent changes of amounts of the pesticide in concerned compartments at air exchange rates of factors 0.1, 1 and 10.

Under the factor 0.1, the exchange rate was 0.5 time h^{-1} during the application and 0.05 time h^{-1} after 2 hr. Amounts of the pesticide in the air (4) and floor compartment (5) were slightly higher than those in a standard condition (factor 1). But, total amount of the pesticide in the wall (6) and ceiling compartment (7) was much lower than the standard due to a lower transference between the air (4) and these compartments (6 and 7).

When the air exchange rates set 50 time h^{-1} during the treatment and 5 time h^{-1} after 2 hr (factor 10), no dominant differences are observed in the air (4) and floor compartment (5). But, the increase of the transference between the air (4) and compartments of 6 and 7 causes a higher amount of the pesticide in these compartments (6 and 7).

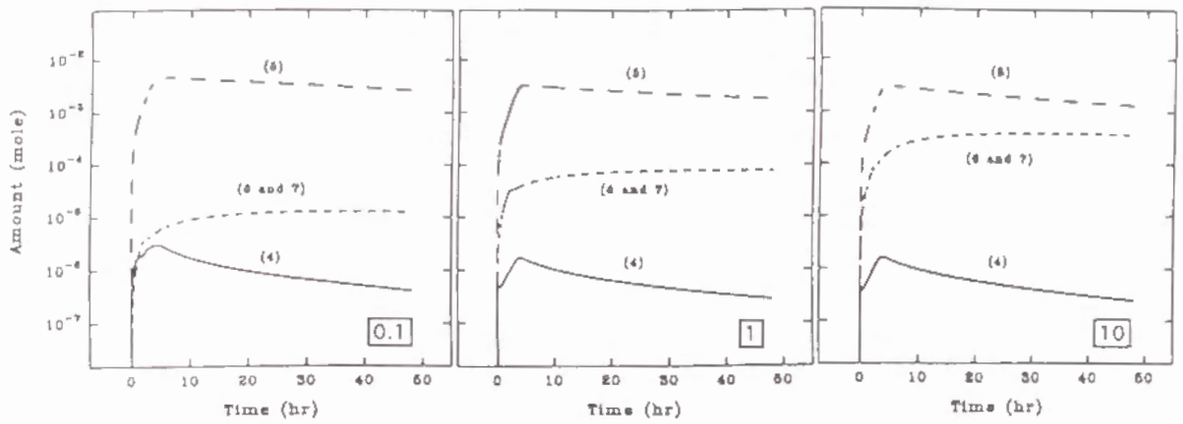

Figure 5-12. Simulation for a sensitivity estimate of the air exchange rate. Amounts of the pesticide in the air (4), floor (5) and sum (6 and 7) of wall and ceiling compartment.

Influence of Physicochemical Properties of the Pesticide

Sensitivity to the photo-degradation and oxidation rate (K) is analyzed by using factors of 0.1 and 10. Results as in figure 5-13 show clear-cut differences in amounts of the pesticide in the air (4), floor (5) and sum (6 and 7) of wall and ceiling compartment when the rate is tenfold.

Vapor pressure (P) of the pesticide affects all fugacity capacities except the air compartment (4) and all transfer parameters. Amounts of the pesticide in the air (4) and sum (6 and 7) of wall and ceiling compartment vary in proportional to the P value as shown in figure 5-14.

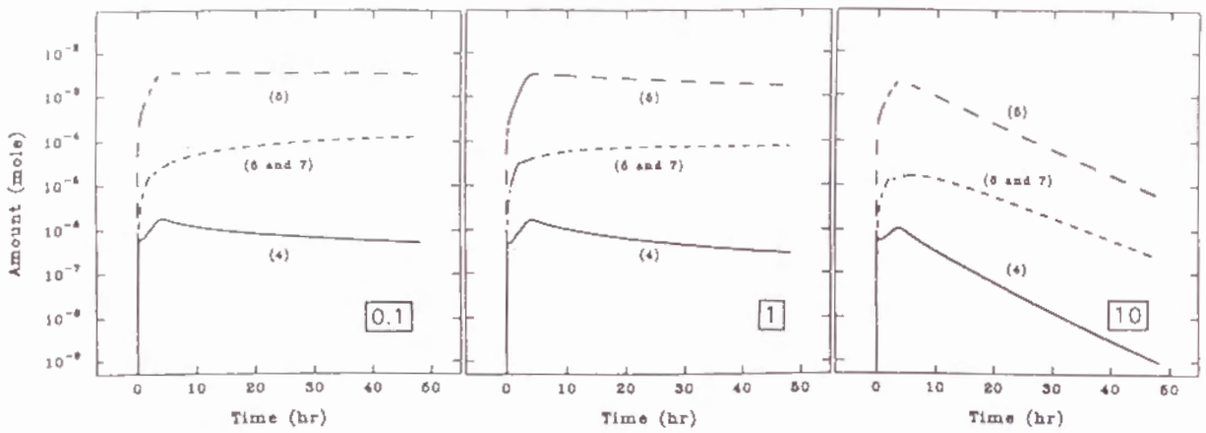

Figure 5-13. Simulation for a sensitivity estimate of the photo-degradation and oxidation rate of the pesticide. Amounts the pesticide in the air (4), floor (5) and sum (6 and 7) of wall and ceiling compartment.

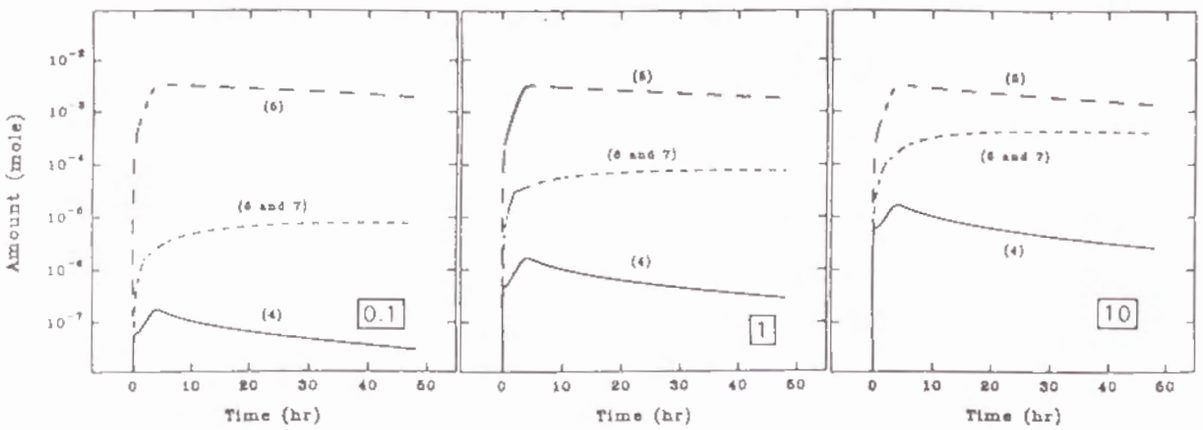

Figure 5-14. Simulation for a sensitivity estimate of the vapor pressure of the pesticide. Amounts of the pesticide in the air (4), floor (5) and sum (6 and 7) of wall and ceiling compartment.

Octanol/water partition coefficient (K_{ow}) also affects fugacity capacities of the water pool (1), floor (5), wall (6) and ceiling compartment (7) and transfer parameters of the concerned compartments. Thus, Amounts of the pesticide in the air (4) and sum (6 and 7) of wall and ceiling compartment vary according to the K_{ow} change. Although the factors for K_{ow} are of an opposite sense to those for P, the changes are almost same in magnitude as the fluctuation by the P change.

Conclusion

A new Fugacity model CARPET-MOM was established for a broadcast spraying to a room carpet. The model incorporating droplet and fluid dynamics, water evaporation, transference and degradation processes well simulated unsteady state behaviors of pesticide in air and on floor, wall and ceiling under various conditions. In sensitivity analysis, it was turned out that physicochemical properties of the pesticide influence remarkably the aerial concentrations and amounts of the pesticide on wall and ceiling.

In a simulation experiment, the model described time-dependent aerial concentrations and amounts of the pesticide on floor in good accordance with measured ones.

Chapter 6.

TEMPERATURE- AND HUMIDITY- DEPENDENCY

Introduction

To simulate indoor behavior of applied pesticides, three Fugacity models are described in the previous chapters: SPRAY-MOM[15], VAPOR-MOM[19] and CARPET-MOM [24].

(1) SPRAY-MOM can describe the pesticide behavior in a room where pesticide aerosols are sprayed.

(2) VAPOR-MOM can analyze the pesticide behavior when an electric vaporizer, a new delivery system for mosquito control, is used.

(3) CARPET-MOM can simulate the pesticide behavior when a broad cast treatment is done on the surface area of a floor or carpet.

The established models successfully described temporal variations of concentrations or amounts of a pesticide under various conditions, but only at a fixed room temperature and humidity. Thus, in chapter 6 these models were improved so as to trace the pesticide behavior when room temperature and humidity are varied[25].

Theoretical

[1] Space Spraying (SPRAY-MOM)

When an aerosol is sprayed in indoor air, the simulating environment has five kinds of compartments appearing on the application. These compartments are aerosol droplets (i =1, 2 and 3), air (4), floor (k = 5), wall (k = 6) and ceiling (k = 7) as illustrated in figure 6-1. The aerosol droplets are divided into three compartments: large- (i = 1), medium- (i = 2) and small-diameter particles (i = 3).

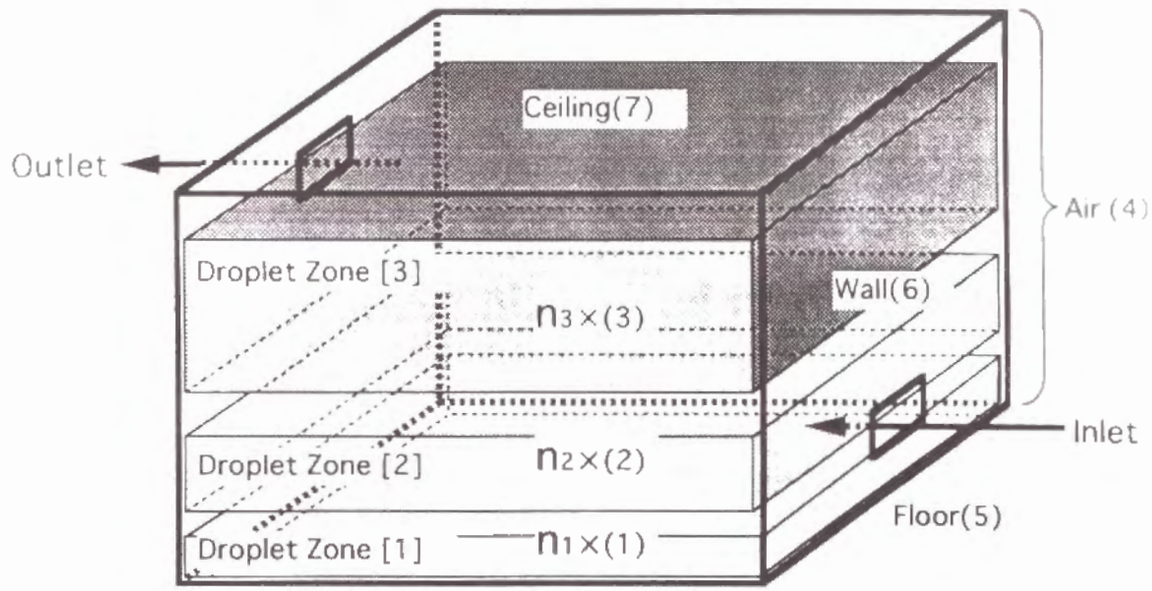

Figure 6-1. Simulation scenario with the room and compartments. Droplets (1, 2 and 3), air (4), floor (5), wall (6) and ceiling compartment (7).

Behavior of the aerosol droplets compartment (i)

In spraying, a dominant solvent of droplets evaporates and volume (V_i) of the compartments (i) decreases with time according to the following equation [24]:

$$-\frac{d V_i}{d t} = -\frac{2 \pi D_{air} M}{R \rho_d}\left(\frac{P_d}{T_d} - \frac{P_\infty}{T_\infty}\right) d_i = \alpha d_i \qquad (6\text{-}1)$$

where d_i is a diameter of the compartment i, D_{air} diffusion coefficient of the solvent in air, M molecular weight, ρ_d droplet density, R gas constant and α volume coefficient. P_d and T_d are partial pressure and temperature on the droplet surface. P_∞ and T_∞ are partial pressure and temperature well away from the droplets and T_∞ is virtually equivalent to room temperature (T). Thus, the decreasing rate in volume depends on temperature and humidity and affects fugacity (f_i) of the droplets compartment.

The settling velocity (v_i) of the compartment (i) is given by Stokes law [24]:

$$v_i = \frac{\rho_d g}{18 \eta} S d_i^2 = \beta S d_i^2 \qquad (6\text{-}2)$$

where β is velocity coefficient, g gravity acceleration, S slip correction factor and η air viscosity that depends on temperature.

Volume of the floor, wall and ceiling compartment (k)

The floor, wall and ceiling compartments (k) increase in volume with time as expressed by the following equation[15]:

$$\frac{d\,V_k}{d\,t} = A_k \sqrt{D_k / t} \qquad (6\text{-}3)$$

where A_k is surface area of the compartment k and D_k diffusion coefficient of the pesticide in compartment k that is changeable with temperature, Thus, the volume of the compartment k depends on temperature and affects fugacity (f_k) of the compartment k.

Physicochemical properties of the pesticide

Water solubility (C) and vapor pressure (P) of the pesticide depend on temperature and are expressed by the following equations:

$$\log C = a_c - b_c / T$$
$$\log P = a_p - b_p / T$$

where a_c, b_c, a_p and b_p are constants and dependent on kinds of the pesticide. The constants of fenitrothion are defined as in table 6–1.

Table 6–1. Constants for water solubility and vapor pressure of fenitrothion

Constant	Value
a_c	4.671
b_c	1813
a_p	11.32
b_p	3825

Fugacity capacity of each compartment consists of physicochemical properties such as water solubility and vapor pressure (See table 6–2). Thus, room temperature affects all fugacity capacities.

Table 6–2. Fugacity capacity of each compartment

Compartment	Fugacity Capacity
Droplets (i)	6×10^6 / (P R T)
Air (j)	1 / (R T)
Floor, wall and ceiling (k)	K_{ow} C / P

K_{ow}: octanol/water partition coefficient

Transfer parameter ($D_{x,y}$) of the pesticide between compartment x and y is estimated by using the fugacity capacities (Z_x and Z_y) as follows:

$$D_{x,y} = \frac{1}{1 / (k_x A_{x,y} Z_x) + 1 / (k_y A_{x,y} Z_y)}$$

where k_x or k_y is velocity of the pesticide in the compartment x or y and $A_{x,y}$ is contact area

between the compartments x and y. The velocity k_i includes the settling velocity (v_i) and k_k equals $(D_k/t)^{0.5}$. Thus, transfer parameters involving the velocities and fugacity capacities also depend on temperature.

[2] Electric Vaporizer (VAPOR–MOM)

An electric vaporizer, which heats and releases a pesticide in a vaporizer liquid, is a new delivery system for mosquito control. When the electric vaporizer is used in a room, the simulating environment has five kinds of compartments: condensed droplets (i = 1, 2, 3), airs (j = 4, 5, 6), floor (7), wall (8) and ceilings (k = 9, 10, 11) as illustrated in figure 6–2.

The condensed droplets are divided into three compartments (i = 1, 2 and 3) by generation and disappearance times. The air is classified into three compartments: vapor– (j = 4), droplet–supplying (j = 5) and breathing air (j = 6). The ceiling is classified into three compartments: the first compartment absorbs the droplets (k = 9), the second connects the droplet–supplying air compartment (k = 10) and the third covers the above two compartments (k = 11).

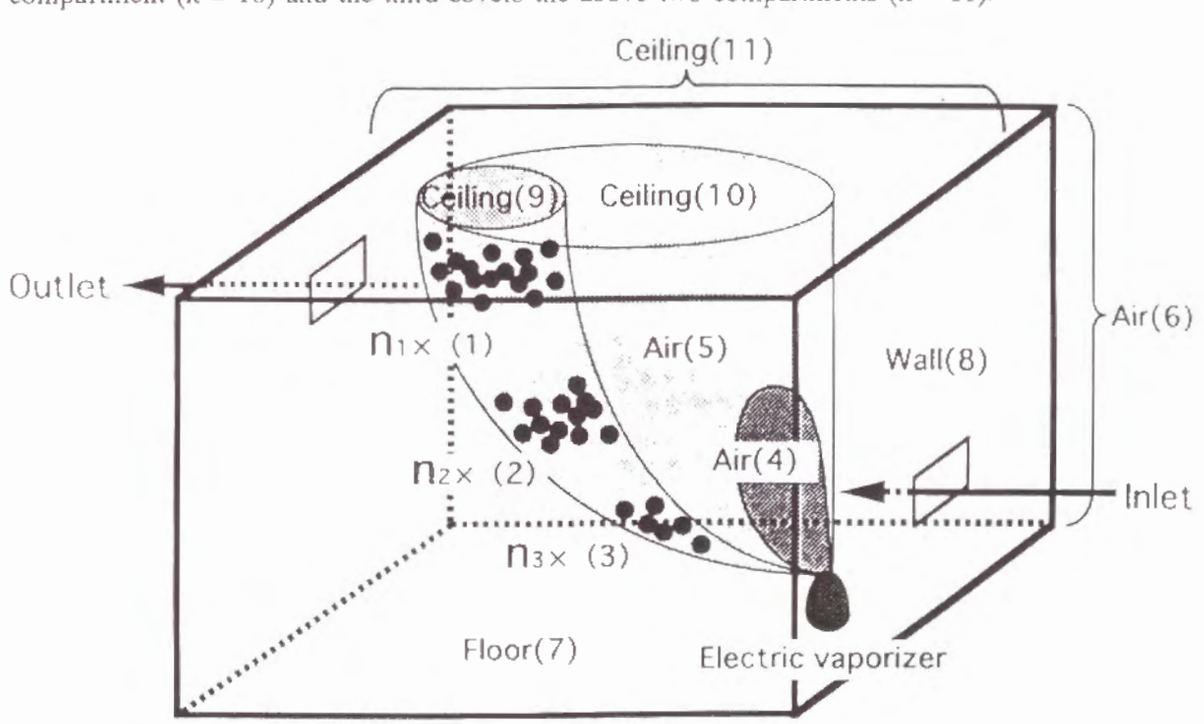

Figure 6–2. Simulation scenario with the room and compartments. Condensed droplets (1, 2 and 3), airs (4, 5 and 6), floor (7), wall (8) and ceiling compartments (9, 10 and 11).

Behavior of the condensed droplet compartment (i)

All of the pesticide is initially evaporated as complete vapor from the electric vaporizer, but some of the pesticide condenses to yield droplets. Temperature (T_{cell}) of a cell just above the wick of the electric vaporizer and a mass flow rate (m_{cell}) of the indoor air into the cell depend on room temperature (T) as described by the following equations [14]:

$$T_{cell} = 1808 - 11.02\ T + 0.02\ T^2$$

$$m_{cell} = 0.029 - 6.6\times10^{-5}\ T - 6.183\times10^{-19}\ T^2$$

Saturated mass fraction or upper limit (MF_s) of vaporous pesticide entering into the cell is calculated by the following equation [19]:

$$MF_s = \frac{P^s_{cell}\ M}{P^s_{cell}\ M + (\ 101325 - P^s_{cell}\ )\ M_{air}}$$

where P^s_{cell} is saturated vapor pressure of the pesticide at T_{cell} and M and M_{air} molecular weight of the pesticide and air. MF_s multiplied by m_{cell} becomes a possible inflow rate of the vaporous pesticide into the room. Therefore, condensed ratio (C_r) to the evaporated pesticide is described as (E_T, evaporating rate):

$$C_r = 1 - MF_s\ m_{cell} / E_T$$

The condensed droplets become smaller in volume with time since a solvent of the droplets evaporates. The rate of change of the volume is expressed in equation 6–1 and dependent on temperature.

Volume of the floor, wall and ceiling compartment (k)

Volumes (V_k) of the floor, wall and ceiling compartment can be calculated by the equation 6–3.

Physicochemical properties of the pesticide

Table 6–3 gives the constants for water solubility and vapor pressure of allethrin. Temperature affects all fugacity capacities and transfer parameters.

Table 6–3. Constants for water solubility and vapor pressure of allethrin

Constant	Value
a_c	27.92
b_c	8870
a_p	11.56
b_p	4048

[3] Broadcast Spraying (CARPET–MOM)

When a broadcast emulsion based on water is sprayed on a carpet, some portion sticks on the carpet and the other flies as flying droplets in air. Simulating environment thus has six kinds of compartments appearing on the application. These compartments are water pool (1), flying droplets (i = 2 and 3 for a large and small–diameter particle), air (4), floor (k = 5), wall (k = 6) and ceiling (k = 7) as illustrated in figure 6–3.

Behavior of the flying droplets compartment (i)

Equations 6–1 and 6–2 describe behavior of the flying droplets.

Volume of the water pool compartment

Water pool compartment formed among and under the carpet textile decreases in volume by evaporation or drying at a following rate (R_d) and finally disappears [24]:

$$R_d = \frac{3.06\times10^{-4}\ \sqrt[3]{T - T_w}\ A_1}{0.24 + 0.46\ H}\ (\ H_w - H\ )$$

where A_1 is a ratio of air–faced surface area of the compartment to that of the carpet, T room temperature, T_w wet–bulb temperature in the room, H room humidity and H_w saturated humidity at T_w.

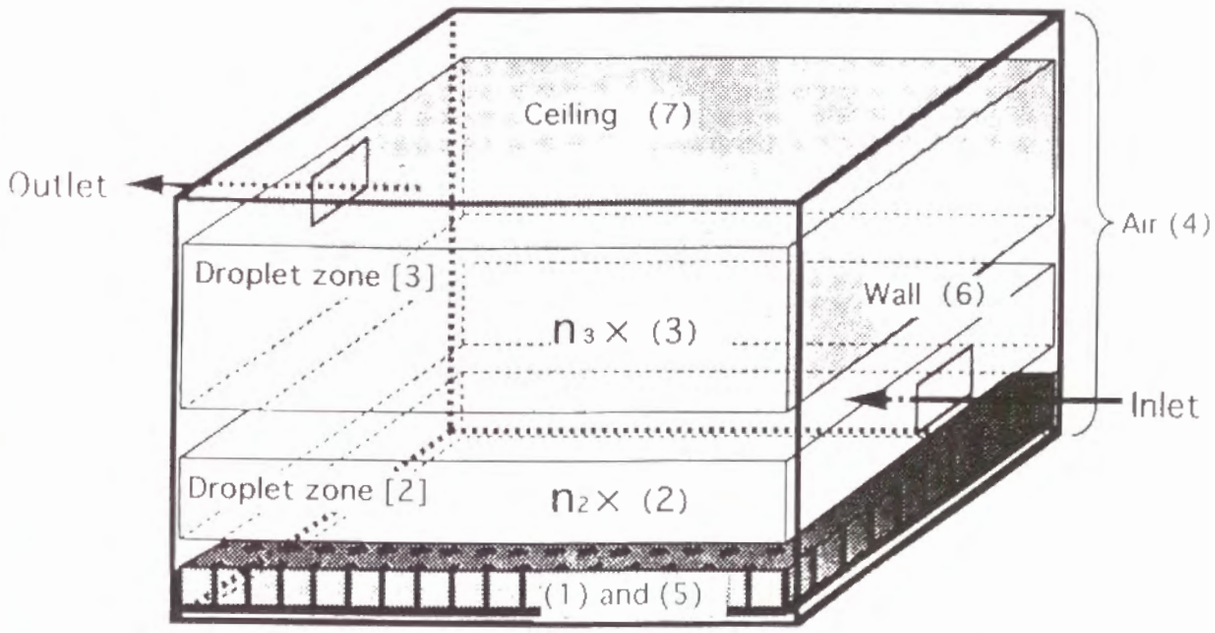

Figure 6–3. Simulation scenario with the room and compartments. Water pool (1), flying droplets (2 and 3), air (4), floor (5), wall (6) and ceiling compartment (7).

When a room is at a relative humidity (φ), room humidity (H) is calculated by the following equation where p_s is saturated vapor pressure of water at room temperature (T).

$$H = \frac{0.621\ \varphi\ p_s}{1.01\times10^7\ -\ \varphi\ p_s}$$

Thus, the dying rate (R_d) of the water pool compartment changes with temperature and humidity.

Volume of the floor, wall and ceiling compartment

Equation 6–3 describes volumes (V_k) of the floor, wall and ceiling compartment.

Physicochemical properties of the pesticide

Table 6–4 shows the constants for water solubility and vapor pressure of chlorpyrifos.

Table 6–4. Constants for water solubility and vapor pressure of chlorpyrifos

Constant	Value
a_c	19.05
b_c	6558
a_p	5.621
b_p	2323

Fugacity capacity (Z_1) of the water pool compartment is expressed by the following equation where a is a constant obtained from an evaporation rate (R_d) of the water pool compartment.

$$Z_1 = (e^{-at} K_{ow} + 1 - e^{-at}) C / P$$

Thus, room temperature affects all fugacity capacities while room humidity does the fugacity capacity of the water pool compartment. Related transfer parameters also depend on temperature and/or humidity.

Computer Programming and Data Processing

Computer programs for the space spraying, electric vaporizer and broadcast spraying were developed with BASIC. IBM PS/2 was employed for the programming and calculation. For estimation of the condensed ratio, FLUENT Version 4.11 (Fluent Incorporated, Lebanon) was utilized and a supercomputer, CRAY–YMP 4E/132, was run.

[1] Space Spraying (SPRAY–MOM)

The component of the aerosol droplets was assumed to be 100% n–tridecane and volume coefficient (α) was estimated using molecular weight (M, 184.37 g $mole^{-1}$) and partial pressures P_d (table 6–5) and P_∞ (0 Pa) of n–tridecane.

The droplet density (ρ_d, 7.56×10^5 g m^{-3}) afforded the velocity coefficient (β). Room humidity did not affect the parameters, but temperature did as in the following table.

Table 6–5. Temperature dependency of parameters

Temperature	288 K	298 K	308 K
D_{air}	5.08×10^{-6}	5.15×10^{-6}	5.23×10^{-6}
P_d	3.21	7.41	16.2
α	7.88×10^{-12}	1.78×10^{-11}	3.83×10^{-11}
η	1.80×10^{-2}	1.85×10^{-2}	1.90×10^{-2}
β	2.29×10^{7}	2.23×10^{7}	2.17×10^{7}
D_k	4.97×10^{-15}	5.03×10^{-15}	5.11×10^{-15}
C	2.38×10^{-2}	3.86×10^{-2}	6.09×10^{-2}
P	1.09×10^{-2}	3.05×10^{-2}	7.96×10^{-2}

[2] Electric Vaporizer (VAPOR–MOM)

To get a condensed ratio (C_r) to the evaporated pesticide, the upper limit (MF_s) of vaporous pesticide and mass flow rate (m_{cell}) of the indoor air into the cell were estimated by the pre–calculation and saturated vapor pressure (P^s_{cell}), evaporating rate (E_T, 7.4×10^{-7} g s^{-1}), M 302.41 g $mole^{-1}$ of allethrin and M_{air} 28.97 g $mole^{-1}$ of air.

The component of the condensed droplets (i = 1, 2, 3) was assumed to be 100% n–tetradecane (M 198.36 g $mole^{-1}$) and volume coefficient (α) was estimated as in space spraying (n–tridecane). Temperature–dependent parameters were as in table 6–6.

[3] Broadcast Spraying (CARPET–MOM)

To get a drying rate (R_d) of the water pool compartment, the web–bulb temperature (T_w) was taken from a humidity chart and saturated vapor pressure (p_s) of water was used for the calculation of room humidity (H) and saturated humidity (H_w). The ratio (A_1) was 1.6×10^{-3} m^2 per m^2 of the floor.

Table 6–6. Temperature dependency of parameters

Temperature	288 K	298 K	308 K
T_{cell}	293	300	311
P^s_{cell}	5.55×10^{-3}	1.17×10^{-2}	3.50×10^{-2}
MF_s	5.72×10^{-7}	1.21×10^{-6}	3.61×10^{-6}
m_{cell}	1.08×10^{-2}	1.01×10^{-2}	9.35×10^{-3}
C_r	0.992	0.983	0.954
D_{air}	4.83×10^{-6}	4.91×10^{-6}	4.98×10^{-6}
P_d	0.594	1.78	5.00
P_∞	0	0	0
α	1.49×10^{-12}	4.39×10^{-12}	1.21×10^{-11}
D_k	4.11×10^{-15}	4.17×10^{-15}	4.25×10^{-15}
C	1.32×10^{-3}	1.43×10^{-2}	1.32×10^{-1}
P	3.19×10^{-3}	1.59×10^{-2}	2.61×10^{-2}

The component of the flying droplets was assumed to be 100% water and volume coefficient (α) was estimated by diffusion coefficient (D_{air}) of water in air, partial pressures (P_d and P_∞), temperatures (T_w and T_∞) and molecular weight (M, 18 g mole^{-1}) of water. The air viscosity (η) afforded velocity coefficient (β) as droplet density (ρ_d) was 1×10^6 g m^{-3}.

Temperature dependency

When room relative humidity was fixed at 60%, temperature–dependent parameters were as in table 6–7.

Table 6–7. Temperature dependency at 60% relative humidity

Temperature	288 K	298 K	308 K
T_w	284	292.5	301
H	6.32×10^{-3}	1.19×10^{-2}	2.14×10^{-2}
H_w	8.40×10^{-3}	1.50×10^{-2}	2.44×10^{-2}
R_d	6.44×10^{-9}	1.09×10^{-8}	1.12×10^{-8}
D_{air}	2.29×10^{-5}	2.40×10^{-5}	2.52×10^{-5}
P_d	1.31×10^{3}	2.26×10^{3}	3.77×10^{3}
P_∞	1.02×10^{3}	1.89×10^{3}	3.36×10^{3}
α	3.33×10^{-10}	4.52×10^{-10}	5.54×10^{-10}
η	1.80×10^{-2}	1.85×10^{-2}	1.90×10^{-2}
β	3.03×10^{7}	2.95×10^{7}	2.87×10^{7}
D_k	4.44×10^{-15}	4.53×10^{-15}	4.58×10^{-15}
C	1.90×10^{-4}	1.10×10^{-3}	5.73×10^{-3}
P	3.59×10^{-3}	6.69×10^{-3}	1.20×10^{-2}

Humidity dependency

The following table lists humidity–dependent parameters at a fixed room temperature (298 K).

Table 6–8. Humidity dependency at 298 K

Relative Humidity	40%	60%	80%
T_w	289	292.5	295.5
H	7.85×10^{-3}	1.19×10^{-2}	1.52×10^{-2}
H_w	1.19×10^{-2}	1.50×10^{-2}	1.72×10^{-2}
R_d	1.69×10^{-8}	1.09×10^{-8}	5.38×10^{-9}
D_{air}	2.35×10^{-5}	2.40×10^{-5}	2.43×10^{-5}
P_d	1.81×10^{3}	2.26×10^{3}	2.72×10^{3}
P_∞	1.26×10^{3}	1.89×10^{3}	2.53×10^{3}
α	6.50×10^{-10}	4.52×10^{-10}	2.36×10^{-10}

Results and Discussion

[1] Space Spraying (SPRAY–MOM)

Temperature dependency

Temperature–dependent behavior of fenitrothion was examined for 288 K, 298 K and 308 K. Room temperature directly influenced all fugacity capacities as shown in the following table.

Table 6–9. Temperature–dependent fugacity capacity (* K_{ow}: $10^{3.27}$)

Temperature	288 K	298 K	308 K
Aerosol droplets (i)	2.30×10^{5}	7.94×10^{4}	2.94×10^{4}
Air (j)	4.18×10^{-4}	4.04×10^{-4}	3.90×10^{-4}
Floor, wall and ceiling (k)*	4.07×10^{3}	2.36×10^{3}	1.42×10^{3}

The fugacity capacities decreased with temperature and there was a remarkable decrease in Z_i (i = 1, 2, 3) of the compartment (i) of the aerosol droplets. Since the space–sprayed pesticide initially existed in the aerosol droplets, the decrease of Z_i promoted transference to the air compartment (4). Thus, aerial amount of the pesticide should increase with temperature.

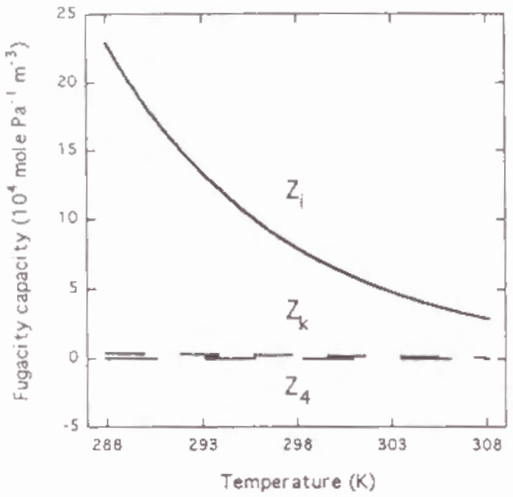

Figure 6–4. Fugacity capacities in each compartment as a function of temperature. Z_i: aerosol droplets (i = 1, 2, 3), Z_4: air (4) and Z_k: floor, wall and ceiling (k = 5, 6, 7).

Figure 6–5 shows the sensitivity to temperature when aerial amounts of the pesticide are sum of the small–sized droplets (3) and air (4). The aerial (3 and 4) and total amounts (6 and 7) on wall and ceiling increased in proportion to temperature, although the amount on floor (5) was almost fixed.

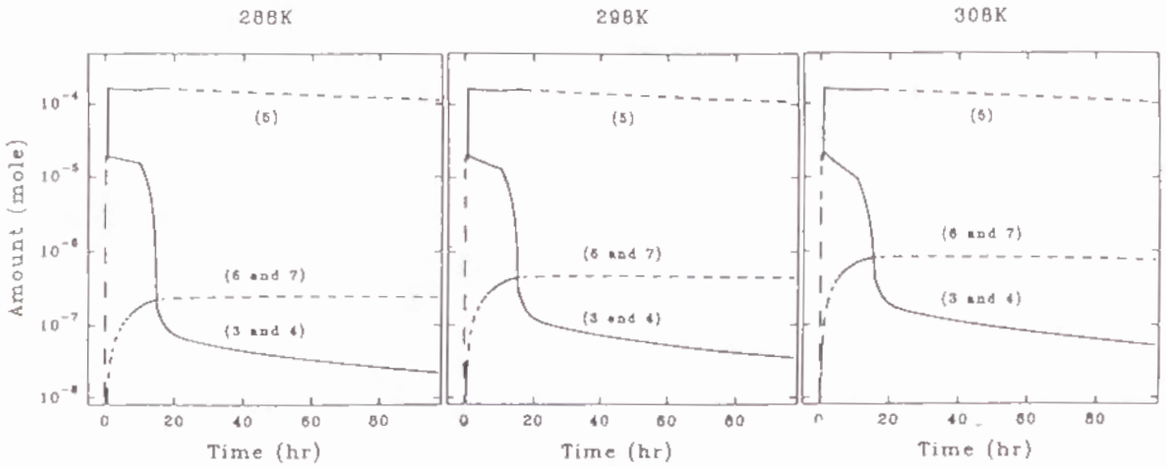

Figure 6–5. Room temperature dependency of pesticide behavior in air (3 and 4), floor (5) and wall and ceiling (6 and 7).

[2] Electric Vaporizer (VAPOR–MOM)

Temperature dependency

The unsteady state behavior of allethrin in air, floor, wall and ceiling was simulated when room temperature was varied. The following table gives relations between fugacity capacity and room temperature.

Table 6–10. Temperature–dependent fugacity capacity (* K_{ow}: $10^{4.78}$)

Temperature	288 K	298 K	308 K
Condensed droplets (i)	7.85×10^{5}	1.52×10^{5}	8.98×10^{4}
Air (j)	4.18×10^{-4}	4.04×10^{-4}	3.90×10^{-4}
Floor, wall and ceiling (k)*	2.49×10^{4}	5.42×10^{4}	3.05×10^{5}

Although fugacity capacities (Z_k) of floor (k = 7), wall (k = 8) and ceiling compartments (k = 9, 10, 11) slightly increased in proportion to temperature, that (Z_i, i = 1, 2, 3) of the condensed droplets compartment (i) largely decreased with temperature (figure 6–6). When Z_i of the condensed droplets compartment (i) became smaller, the pesticide in the droplets (i) should transfer more largely to air compartment (5).

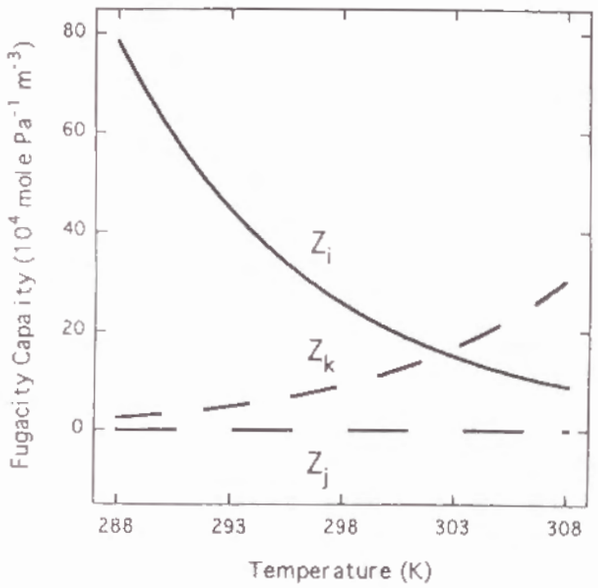

Figure 6–6. Fugacity capacities in each compartment as a function of temperature. Z_i: condensed droplets (i = 1, 2, 3), Z_j: airs (j = 4, 5, 6) and Z_k: floor, wall and ceiling (k = 7, 8, 9, 10, 11).

The predicted time-dependent amount of the pesticide is shown in figure 6-7, where amount of the pesticide in air (4, 5 and 6) was sum of the pesticide in the vapor- (j = 4), droplet-supplying (j = 5) and breathing air compartment (j = 6) and that on ceiling (9, 10 and 11) was sum of the droplets-absorbing (k = 9), droplets-connecting (k = 10) and the third ceiling compartment (k = 11). The amounts in air (4, 5 and 6) and on floor and wall (7 and 8) increased with temperature whereas the amount in ceiling (9, 10 and 11) slightly decreased.

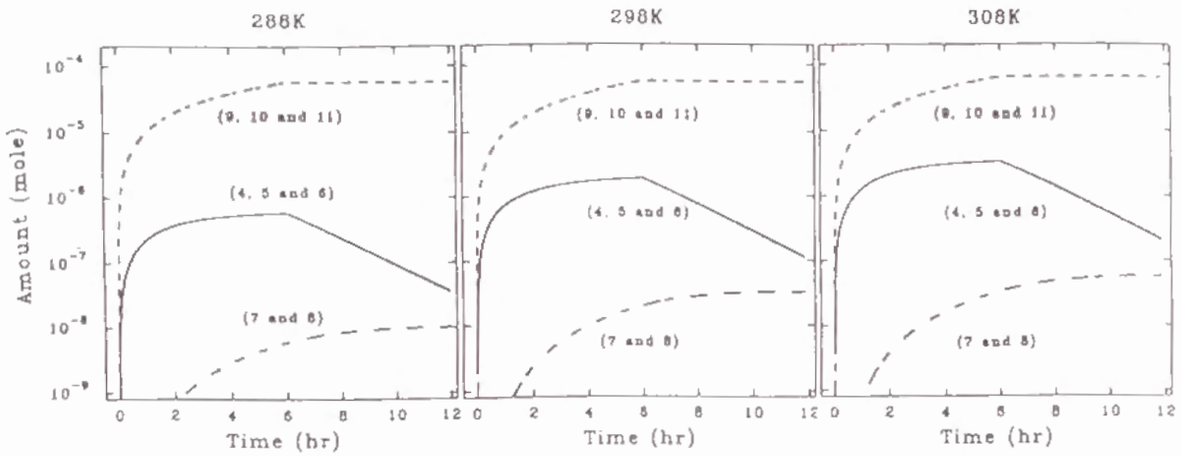

Figure 6-7. Room temperature dependency of pesticide behavior in air (4, 5 and 6), floor and wall (7 and 8) and ceiling (9, 10 and 11).

[3] Broadcast Spraying (CARPET-MOM)

Temperature dependency

Room temperature (T) was varied at a fixed humidity (60% relative humidity). Immediately after broadcast spraying, 60% of the treated chlorpyrifos existed in the water pool compartment (1) and 0.006% was in the flying droplets compartment (3). Thus, the total behavior of the pesticide was regulated by the water pool compartment.

Fugacity capacity (Z_1) of the water pool compartment decreased with time post application (figure 6-8). The decreasing rate of Z_1 at 308 K was larger than that at 288 K since the drying rate (R_d) of the compartment (1) increased with temperature.

A curve of temperature-dependent Z_1 at 2 hr post application shows a remarkable increase with temperature (figure 6-9). Thus, transference of the pesticide from the water pool compartment (1) to floor (5) and air compartment (4) should become smaller under higher temperature. Since the

pesticide in air compartment (4) transferred to the wall and ceiling compartment (6 and 7), the amounts on these compartments (6 and 7) should decrease in proportion to temperature.

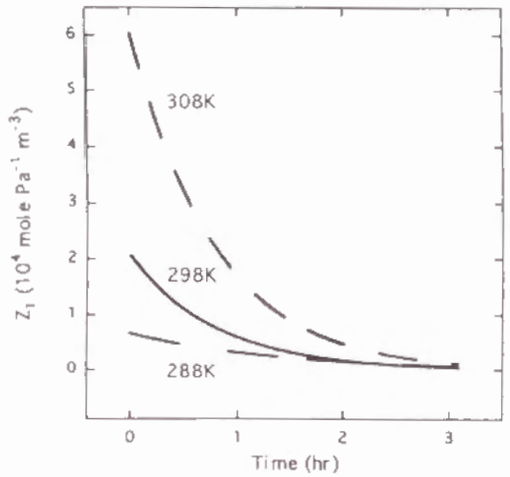

Figure 6-8. Fugacity capacity (Z_1) of the water pool compartment (1) at each temperature as a function of time.
Temperature: 288 K, 298 K and 308 K.

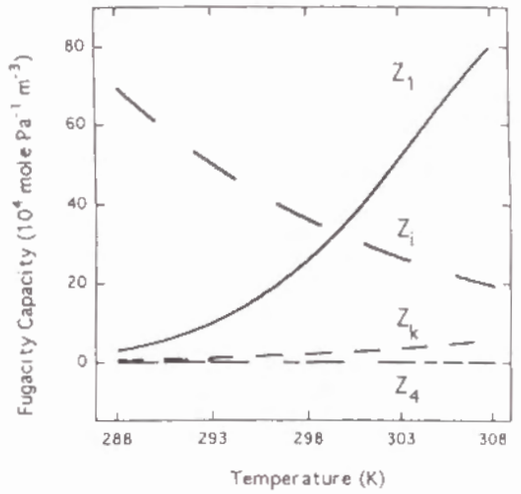

Figure 6-9. Fugacity capacity in each compartment as a function of temperature at 2 hr after application. Z_1: water pool (1), Z_i: flying droplets (i), Z_4: air (4) and Z_k: floor, wall and ceiling (k).

The other fugacity capacities changeable with temperature are summarized in figure 6-9 and following table.

Table 6-11. Temperature-dependent fugacity capacity at 60% relative humidity (* K_{ow}: $10^{5.1}$)

Temperature	288	298	308
Water pool (1)*	($1.26\times10^5\ e^{-at} + 1$) C / P		
a =	2.03×10^{-4}	3.44×10^{-4}	3.53×10^{-4}
C / P =	5.29×10^{-2}	1.64×10^{-1}	4.78×10^{-1}
Flying droplets (i)	6.98×10^5	3.62×10^5	1.95×10^5
Air (j)	4.18×10^{-4}	4.04×10^{-4}	3.90×10^{-4}
Floor, wall and ceiling (k)	6.66×10^3	2.07×10^4	6.01×10^4

Figure 6-10 shows the amounts in air (3 and 4) and on wall and ceiling (6 and 7) decrease with temperature, although the amounts on floor (1 and 5) slightly increase.

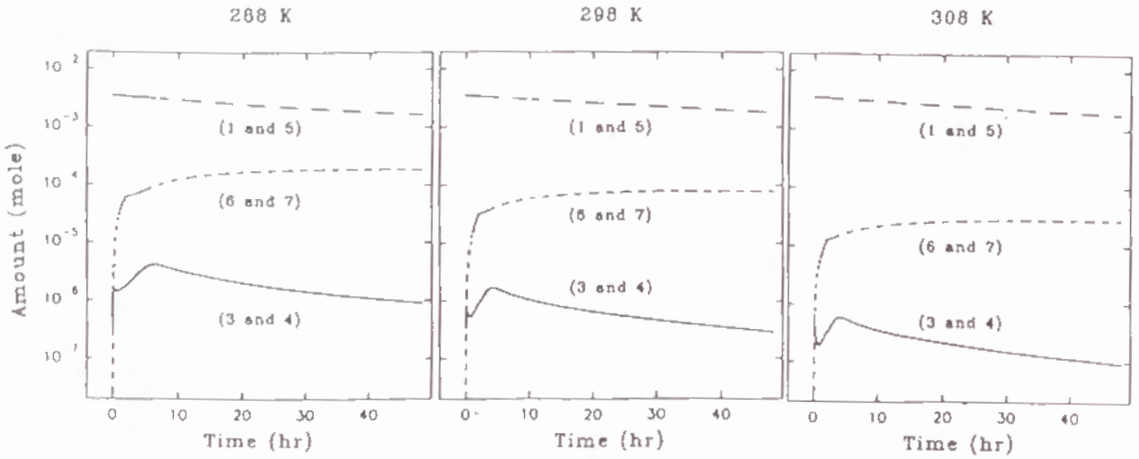

Figure 6–10. Room temperature dependency of pesticide behavior in air (3 and 4), floor (1 and 5) and wall and ceiling (6 and 7).

Humidity dependency

Sensitivity to room humidity (40%, 60% and 80% relative humidity) was analyzed at a fixed temperature (298 K). Although fugacity capacities of the flying droplets (i = 2, 3), air (4) and floor, wall and ceiling compartment (k = 5, 6, 7) kept unaffected values under various humidities, Z_1 of the water pool at a fixed time (2 hr post application) increased in proportion to humidity as shown in figure 6–11 and the following table.

Table 6–12. Humidity–dependent fugacity capacity at 298 K

Relative Humidity	40%	60%	80%
Water pool (1)		$0.164 + 2.07\times10^{4}\ e^{-at}$	
a =	5.33×10^{-4}	3.44×10^{-4}	1.70×10^{-4}

The fugacity capacity (Z_1) of the water pool compartment (1) changed with time and the decreasing rate at 80% relative humidity was milder than that at 40% as shown in figure 6–6–12 due to the lower drying rate (R_d). Thus, the aerial concentration of the pesticide at 80% should slowly increase with time, compared with that at 40%.

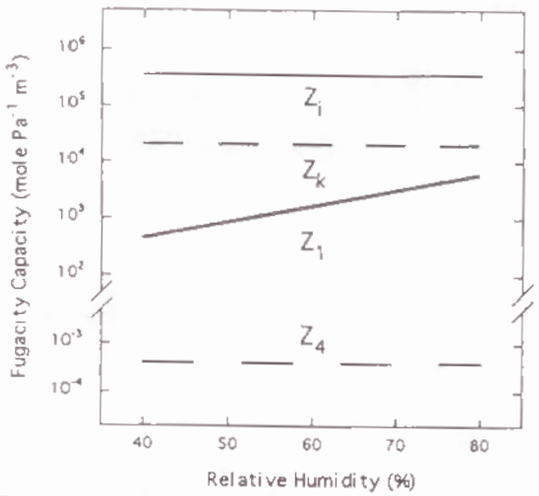

Figure 6–11. Fugacity capacity in each compartment as a function of humidity.
Z_1: water pool (1), Z_i: flying droplets (i), Z_4: air (4) and Z_k: floor, wall and ceiling (k).

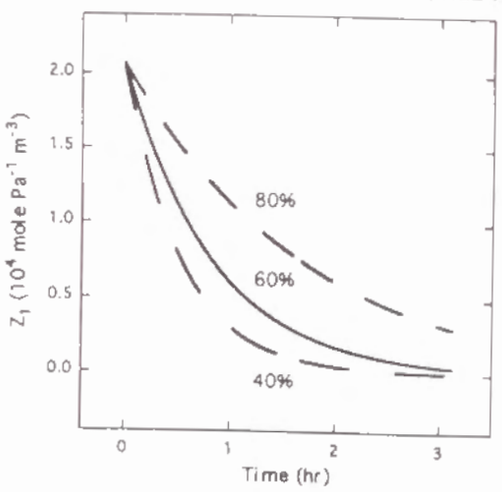

Figure 6–12. Fugacity capacity (Z_1) of the water pool compartment at each humidity as a function of time.
Humidity: 40%, 60% and 80% relative humidity.

The amount (6 and 7) on wall and ceiling slightly decreased in proportion to relative humidity, but no dominant differences were observed in behavior of the pesticide on floor (1 and 5). The increased drying rate (R_d) at 40% relative humidity quickly formed a maximum point of the aerial amount (3 and 4) as shown in figure 6–13.

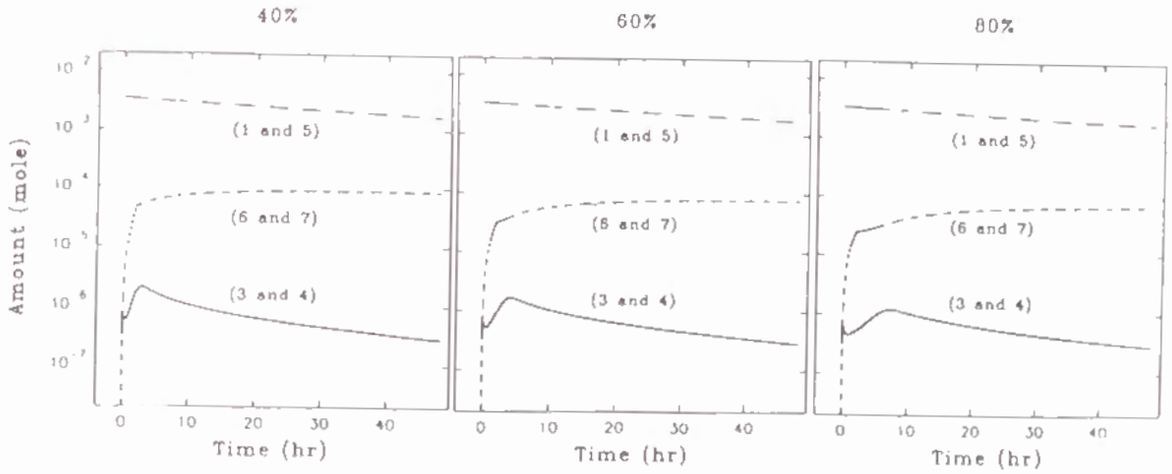

Figure 6–13. Room humidity dependency of pesticide behavior in air (3 and 4), floor (1 and 5) and wall and ceiling (6 and 7).

Conclusion

The established Fugacity models (SPRAY-MOM, VAPOR-MOM and CARPET-MOM) were improved to include room temperature and humidity changes.

Room temperature directly affects the fugacity capacities, changing rates in volume of the droplets, floor, wall and ceiling compartments and transfer parameters for the three models; settling velocities of the droplets for SPRAY-MOM and CARPET-MOM; condensed ratio of the evaporated pesticide for VAPOR-MOM; and the drying rate of the sprayed emulsion for CARPET-MOM. In SPRAY-MOM and VAPOR-MOM, the aerial concentrations of each pesticide increase with temperature and also the amounts on wall and ceiling (SPRAY-MOM) and on floor and wall (VAPOR-MOM) increase. However, CARPET-MOM shows a decrease in the aerial concentration and amounts on wall and ceiling at higher temperature, although the amount on floor is almost fixed.

Room humidity affects the drying rate (R_d) and fugacity capacity of the sprayed emulsion in CARPET-MOM and thus, the aerial concentration varies with humidity. The concentration in air quickly attains a maximum point, and the amounts on wall and ceiling slightly increase at lower humidity.

Thus, the three modified models can now describe accurately the aerial concentrations and amounts of pesticides on floor, wall and ceiling under various room temperature and humidity conditions.

Chapter 7.

CONCLUSION

From a view point of safety assessment for human health against pesticides, three kinds of computer soft (SPRAY-MOM, VAPOR-MOM and CARPET-MOM) were developed for the description of the pesticide behavior in three popular spraying procedures: space spraying, electric vaporizer and broadcast spraying, respectively:

(1) SPRAY-MOM describes the pesticide behavior in a room where pesticide aerosols are sprayed.

(2) VAPOR-MOM analyzes the pesticide behavior when an electric vaporizer, a new delivery system for mosquito control, is used.

(3) CARPET-MOM simulates the pesticide behavior when a broadcast treatment is done on the surface area of a carpet.

An improvement was additionally made to all three softs (1) to (3) against room temperature and humidity changes. The modified models describe the aerial concentrations and amounts of pesticides on floor, wall and ceiling under various conditions including room temperature and humidity changes.

In several simulation experiments, it was turned out that all the modified softs describe the pesticide behavior in good accordance with the measured ones and that they are very useful to supply data needed for the safety assessment of human health without the realization of experiments.

Acknowledgements

The author would like to thank Dr. Masatoshi Matsuo for his valuable discussion and warm support and acknowledge Drs. T. Katoh, J. Ohnishi, Y. Takimoto, F. Kishida and Y. Kakuta for their helpful discussions. The author is also grateful to Research Director H. Yamada of Sumitomo Chemical Co., Ltd. for his continuous support. The author deeply thanks Prof. Dr. Kozi Asada of Kyoto University, who kindly read this article and constructively commented.

REFERENCES

1) Mackay D. and Paterson S. Fugacity revisited, Environ. Sci. Technol., 16, 654A–660A, (1982)
2) Class T. J. and Kintrup J. Pyrethroids as household insecticides: analysis, indoor exposure and persistence, Fresenius J. Anal. Chem., 340, 446–453, (1991)
3) Hinds W. T. "Aerosol Technology", A Wiley Interscience Publ., New York, (1982)
4) Mackay D. and Paterson S. Model Describing the Rates of Transfer Processes of Organic Chemicals between Atmosphere and Water, Environ. Sci. Technol., 20, 810–816, (1986)
5) Mackay D., Paterson S., Cheung B. and Neely W. B. Evaluating the Environmental Behavior of Cemicals with a Level III Fugacity Model, Chemosphere, 14, 335–374, (1985)
6) Lapcik L. and Panak J. Kinetics of swollen Surface Layer Formation in Poly(vinyl chloride)–Solvent System, J. Polym. Sci., 14, 981–988, (1976)
7) Matoba Y. A Private Communication, From the Consumer Section of Tokyo Metropolitan Institute, (1991)
8) Tsuda S., Nisibe I., Shinjyo G. Influence of Droplet Sizes on the Percentage of Airborne Spray Droplets in Oil-based Aerosols, J. Pesticide Sci., 13, 253–260, (1988)
9) Wike C. R. and Lee C. Y. Estimation of Diffusion Coefficients for Gases and Vapors, Ind. Eng. Chem., 47, 1253–57, (1955)
10) Gabel J–P and Wittmann J. C. Food and Packaging Interactions: Penetration of Fatty Food Simulants Into Rigid Poly(vinyl chloride), J. Agric. Food Chem., 39, 1927–1932, (1991)
11) Hirai O., Akiyama S., Ono K. and Kawakatsu H. Manufacturing Trial of Art and Packing Paper Utilized the odds and ends of "Igusa", Report of the Fukushima Industrial Research Institute of Fukushima Prefecture, 1983, 49–53, (1984)
12) Small P. A. Some Factor Affecting the Solubility of Polymers, J. Appl. Chem., 3, 71–80, (1953)
13) Jassen J. E. Ventilation for Acceptable Indoor Air Quality, ASHRAE Journal, October, (1989)
14) Matoba Y., Hirota T., Ohnishi J., Murai N. and Matsuo M., An Indoor Simulation of the

Behavior of Insecticides Supplied by an Electric Vaporizer, Chemosphere, 28, 435–451, (1994)

15) Matoba Y., Ohnishi J. and Matsuo M., A Simulation of Insecticides in Indoor Aerosol Space Spraying, Chemosphere, 26, 1167–1186, (1993)

16) Hartley G. S., Evaporation of Pesticides, Pesticide Formulations Research: Physical and Colloidal Chemical Aspects, American Chemical Society, Washington D. C., (1969)

17) Dureja P, Casida J. E. and Ruzo L. O., Dinitroanilines as Photostabilizers for Pyrethroids, J. Agric. Food Chem., 32, 246–250, (1984)

18) Vaccaro J. R., Nolan R. J., Hugo J. M., Pillepich J. L., Murphy P. G. and Bartels M. J., Evaluation of Dislodgable Residue and Absorbed Doses of Chlorpyrifos to Crawling Infants Following Indoor Broadcast Applications of a Chlorpyrifos Based Emulsifiable Concentrate, The Dow Chemical Company, Midland, August 28, (1991)

19) Matoba Y., Ohnishi J. and Matsuo M., Indoor Simulation of Insecticides Supplied with an Electric Vaporizer by the Fugacity Model, Chemosphere, 28, 767–786, (1994)

20) Lewis W. K., Mech. Eng., 44, 445, (1922)

21) McAdams W. H., "Heat Transmission", 3rd Ed., McGraw–Hill Book Co., (1954)

22) Lyman W. J., Reehl W. F. and Rosenblatt D. H., "Handbook of Chemical Property Estimation Methods", McGraw–Hill Book Company, (1982)

23) Chen Z. M., Zabik M. J. and Leavitt R. A., Comparative Study of Thin Film Photodegradative Rates for 36 Pesticides, Ind. Eng. Chem. Prod. Res. Dev., 23, 5–11, (1984)

24) Matoba Y., Ohnishi J. and Matsuo M., Indoor Simulation of Insecticides in Broadcast Spraying, Chemosphere, 30, 345–365, (1994)

25) Matoba Y., Ohnishi J. and Masatoshi Matsuo, Temperature– and humidity–dependency of pesticide behavior in indoor simulation, Chemosphere, (in press, 1995)

APPENDIX

1. Fugacity model

Fugacity, which means escaping or fleering tendency, has an unit of pressure (Pa) and can be viewed as the partial pressure which a chemical exerts when it attempts to escape from one media called compartment and migrate to another.

When a chemical achieves an equilibrium between air and floor compartments, the fugacity of the chemical in floor is equal to that in air, but these common fugacities correspond to different concentrations. If the fugacity in floor exceeds that in air, the chemical will evaporate until a new equilibrium is established.

The use of fugacity instead of concentration thus immediately reveals the equilibrium status of compartments and the likely direction of diffusive transfer. Further, the magnitude of fugacity difference controls the rate of transfer.

The relationship between fugacity (f, Pa) and concentration (C, mole m^{-3}) is simply stated as:

$$C = Z f$$

where Z is "fugacity capacity" with an unit of mole m^{-3} Pa^{-1} and quantifies the capacity of the compartment for fugacity.

In the treated room, chemicals are subject to degrading reactions such as photolysis and oxidations and their lifetime or persistence is limited. For the reactions, a single first order kinetics is assumed with a half–life τ (s) and thus, the rate constant K (s^{-1}) and the reaction rate N (mole s^{-1}) can be calculated as:

$$N = V K C = ln2\ V C / \tau$$

A second loss mechanism is by air exchange. The rate of loss N (mole s^{-1}) is then:

$$N = G\ C$$

where G is the air exchange rate ($m^3\ s^{-1}$) and C is the aerial concentration in a flowing compartment.

A diffusive transfer rate of a chemical between compartment x and y can be written as:

$$N = D_{x,y}\ (f_x - f_y)$$

where $D_{x,y}$ is a transfer parameter with an unit of mole $s^{-1}\ Pa^{-1}$ and f_x and f_y are the fugacities of the chemical in the compartment x and y.

Thus, the general differential equation of the chemical in the compartment x is expressed as:

$$V_x\ Z_x\ \frac{d\ f_x}{d\ t} = E_x + G_x\ (\ C_{Bx} - Z_x\ f_x\ ) - D_{x,y}\ (\ f_x - f_y\ ) - V_x\ Z_x\ f_x\ K_x$$

where E_x represents emission, G_x flow rate and C_{Bx} inflow concentration. The simulation of the chemical behavior is done with all compartments such as air, floor, wall and ceiling. Each compartment has each linear algebraic equation in terms of the chemical which can be solved by a computer with a BASIC program.

2. Definition of Symbols

Definition of symbols

Symbols	Dimension	Definition
A	m^2	surface area of compartment
A_1		air–faced surface area ratio of compartment 1 to the floor
A_5		air–faced surface area ratio of compartment 5 to the floor
A_{15}		ratio of a contacting surface area formed between compartment 5 and 1 to the floor
A_{a5}		contacting area ratio of compartment 5 to the floor
A_{inlet}	m^2	inlet area
A_{room}	m^2	cross–sectional area of the room
A_{wick}	m^2	cross–sectional area of the wick
a_c		constant for water solubility
a_p		constant for vapor pressure
b_c		constant for water solubility
b_p		constant for vapor pressure
C	mole m^{-3}	solubility in water
C_H	kcal(K kg–dry air)$^{-1}$	humid heat
C_r		condensed ratio to the evaporated pesticide
D	mole $s^{-1}\ Pa^{-1}$	transfer parameter
D_{air}	$m^2\ s^{-1}$	diffusion coefficient in air
D_k	$m^2\ s^{-1}$	diffusion coefficient in compartment k
d	m	droplet diameter
E_T	g s^{-1}	total evaporation rate of the pesticide
E_v	mole s^{-1}	evaporating amount of complete vapor of the pesticide per second
e	m	diffusion depth of the pesticide in a polymer
f	Pa	fugacity
f_a	Pa	fugacity added to ceiling compartment by every droplet–absorption
f_{ia}	Pa	fugacity of compartment i just before absorption
G	s^{-1}	air exchange rate

g	$m\ s^{-2}$	gravity acceleration
H	kg–H_2O / kg–dry air	room humidity
$H_{[i]}$	m	thickness of droplet zone [i]
H_w	kg–H_2O / kg–dry air	humidity at T_w
h	kcal s^{-1} m^{-2} K^{-1}	film coefficient of heat transfer
h_b	m	height of the bottom of spray zone from the floor at time 0
h_h	m	height of the head of spray zone from the floor at time 0
K	s^{-1}	photo–degradation and oxidation rate
K_{ow}		octanol/water partition coefficient
k	$m\ s^{-1}$	pesticide velocity in the compartment
L_d	m	room length
M	g $mole^{-1}$	molecular weight
M_{air}	g $mole^{-1}$	molecular weight of air
MF_s		upper limit of vaporous pesticide in the cell
m_{cell}	g s^{-1}	mass flow rate of the indoor air into the cell
N	mole	chemical mass
n_i		number of droplets (i)
n_T		total number of droplets
P	Pa	vapor pressure
P^s_{cell}	Pa	saturated vapor pressure of the pesticide at T_{cell}
P_d	Pa	partial pressure on the droplet surface
P_f		polymer/water partition coefficient for the floor
P_L	Pa	sub–cooled liquid vapor pressure
P_{room}	Pa	room pressure
P_w	Pa	partial pressure of water vapor on the droplet surface
P_∞	Pa	partial pressure well away from the droplets
p_s	Pa	saturated vapor pressure of water
R	Pa m^3 K^{-1} $mole^{-1}$	gas constant
R_a		volume ratio of the pesticide droplets at time 0
R_d	kg–H_2O s^{-1} m^{-2}	constant rate of drying of sprayed emulsion
S		slip correction factor

T	K	room temperature
T_{cell}	K	cell temperature above the electric vaporizer
T_d	K	droplet temperature
T_M	K	melting point
T_w	K	web–bulb temperature
T_{wick}	K	heating temperature around the wick
T_∞	K	temperature well away from the droplet
t	s	time after application
t_i	s	time after generation of droplets (i)
t_ℓ	s	life time of the droplets from generation to absorption
t_x	h	time required for droplet zone [i] to reach the floor
t_y	h	time required for droplet zone [i] to be completely absorbed in the floor
t_z	s	time until the droplet solvent evaporates completely
V	m^3	compartment volume
$V_{[i]}$	m^3	volume of spray zone [i]
V_{ia}	m^3	droplet volume just before absorption
V_{room}	m^3	room volume
v_A	$m\ s^{-1}$	inflow velocity of complete vapor of the pesticide into the room
v_f	$m\ s^{-1}$	velocity of the fluid movement caused by the air exchange
v_i	$m\ s^{-1}$	droplet settling velocity
v_{inlet}	$m\ s^{-1}$	air velocity at the air inlet
v_T	$m\ s^{-1}$	inflow velocity of the pesticide into the room
Z	mole Pa^{-1} m^{-3}	fugacity capacity
α	$m^2\ s^{-1}$	diameter coefficient
β	$m^{-1}\ s^{-1}$	velocity coefficient
δ	$cal^{0.5}\ cm^{-1.5}$	solubility parameter
η	g m^{-1} s^{-1}	air viscosity
ρ	g m^{-3}	pesticide density
ρ_d	g m^{-3}	droplet density
τ	s	half–life time of photo–degradation and oxidation

τ_{jk}	h	half-life time of transference between j and k compartments
φ	%	relative humidity

Definition of subscripts

Subscripts	Definition
i	droplets
j	air
k	floor, wall and ceiling

3. Publication List

1) Yoshihide Matoba, Jun-ichi Ohnishi and Masatoshi Matsuo, A simulation of insecticides in indoor aerosol space spraying, Chemosphere, 26, 1167-1186, (1993)

2) Yoshihide Matoba, Tomoo Hirota, Jun-ichi Ohnishi, Norio Murai and Masatoshi Matsuo, An indoor simulation of the behavior of insecticides supplied by an electric vaporizer, Chemosphere, 28, 435-451, (1994)

3) Yoshihide Matoba, Jun-ichi Ohnishi and Masatoshi Matsuo, Indoor simulation of insecticides supplied with an electric vaporizer by the fugacity model, Chemosphere, 28, 767-786, (1994)

4) Yoshihide Matoba, Jun-ichi Ohnishi and Masatoshi Matsuo, Indoor simulation of insecticides in broadcast spraying, Chemosphere, 30, 345-365, (1995)

5) Yoshihide Matoba, Jun-ichi Ohnishi and Masatoshi Matsuo, Temperature- and humidity-dependency of pesticide behavior in indoor simulation, Chemosphere, (in press, 1995)